UNIVERSITA' VITA-SALUTE SAN RAFFAELE

CORSO DI DOTTORATO DI RICERCA INTERNAZIONALE IN MEDICINA MOLECOLARE

Curriculum in Terapia Genica e Cellulare

"DISSECTING THE NON-CELL AUTONOMOUS EFFECTS OF ONCOGENE ACTIVATION ON HEMATOPOIESIS"

DoS: Dr. Eugenio Montini

Second Supervisor: Prof. Clemens Schmitt

Tesi di DOTTORATO DI RICERCA di Cristina Colleoni

Matr. 015477

Ciclo di Dottorato XXXV°

SSD BIO/13

Anno Accademico 2021/2022

UNIVERSITA' VITA-SALUTE SAN RAFFAELE

CORSO DI DOTTORATO DI RICERCA INTERNAZIONALE IN MEDICINA MOLECOLARE

Curriculum in Terapia Genica e Cellulare

"DISSECTING THE NON-CELL AUTONOMOUS EFFECTS OF ONCOGENE ACTIVATION ON HEMATOPOIESIS"

DoS: Dr. Eugenio Montini

Second Supervisor: Prof. Clemens Schmitt

Tesi di DOTTORATO DI RICERCA di Cristina Colleoni

Matr. 015477

Ciclo di Dottorato XXXV°

SSD BIO/13

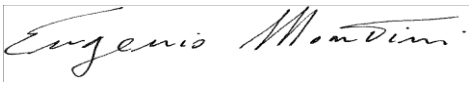

Anno Accademico 2021/2022 Signature of the DoS

CONSULTAZIONE TESI DI DOTTORATO DI RICERCA

La sottoscritta	Cristina Colleoni
Matricola / *registration number*	015477
nata a/ *born at*	Seriate, BG
il/*on*	08/06/1994

autore della tesi di Dottorato di ricerca dal titolo / author of the PhD Thesis entitled

"Dissecting the non-cell autonomous effects of oncogene activation on hematopoiesis"

x AUTORIZZA la Consultazione della tesi / AUTHORIZES *the Consultation of the thesis*

□ NON AUTORIZZA la Consultazione della tesi per …… mesi /NOT AUTHORIZES *the Consultation of the thesis for …… months*

a partire dalla data di conseguimento del titolo e precisamente */ from the PhD thesis date, specifically*
Dal / *from* ……/……/…… Al / *to* ……/……/……

Poiché /*because*:

□ l'intera ricerca o parti di essa sono potenzialmente soggette a brevettabilità/ *The whole project or part of it might be subject to patentability;*

□ ci sono parti di tesi che sono già state sottoposte a un editore o sono in attesa di pubblicazione/ *Parts of the thesis have already been submitted to a publisher or are in press;*

□ la tesi è finanziata da enti esterni che vantano dei diritti su di esse e sulla loro pubblicazione/ *the thesis project is financed by external bodies that have rights over it and on its publication.*

E' fatto divieto di riprodurre, in tutto o in parte, quanto in essa contenuto / *It is not allowed to copy, in whole or in part, the data and the contents of the thesis*

Data /Date 11/11/2022 Firma /Signature 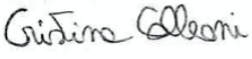

DECLARATION

This thesis has been:

- composed by myself and has not been used in any previous application for a degree. Throughout the text I use both 'I' and 'We' interchangeably.
- has been written according to the editing guidelines approved by the University.

Permission to use images and other material covered by copyright has been sought and obtained.

All the results presented here were obtained by myself, except for:

1) Luminex assays on plasma samples (Results, Chapter 3.4 and 3.5, Figures 3.6a and Figure 3.7g) were performed by Bioclarma.
2) Cell sorting for gene expression experiments (Results, Chapter 3.6, Figure 3.7) was performed by Flow cytometry Resource, Advanced Cytometry Technical Applications Laboratory (FRACTAL) at IRCCS Ospedale San Raffaele.
3) Sequencing of the cDNA libraries (Results, Chapter 3.7) were performed by Center for Omics Sciences (COSR) at the IRCCS Ospedale San Raffaele
4) Gene expression analysis (Results, chapter 3.6, Figures from 3.7 to 3.13), were performed in collaboration with Dr. Ivan Merelli, Facility Manager of the Bioinformatics Core at San Raffaele Telethon Institute for Gene Therapy
5) Some of the figures (Introduction, Chapter 1, Figure 1.2b, Figure 1.3, 1.4, 1.5 and Discussion, Chapter 4, Figure 4.1) were created with BioRender, under regular license.

All sources of information are acknowledged by means of reference.

Acknowledgements

First of all, I would like to thank my DoS, Eugenio Montini, for giving me the chance to work on this very exciting project despite my inexperience when I started, and for supervising my work during these years.

Secondly, a huge thank you to Daniela Cesana, who helped me theoretically and practically in all of my experiments, as well as personally supporting and rooting for me during this time.

I also want to acknowledge Pierangela Gallina for her help in the animal experiments, Laura Rudilosso for her support in the generation of the RNA-sequencing libraries, Fabrizio Benedicenti for the sequencing, and all of my lab members in general.

I also want to thank my collaborator for this project in all the gene expression data, Ivan Merelli, from the Bioinformatics Core at SR-TIGET, for his expertise and ability in RNA-sequencing analysis.

Moreover, thanks to Monica Romano, Emanuele Canonico, and Simona di Terlizzi at FRACTAL for their expertise in cell sorting, and Dejan Lazarevic from COSR for the sequencing process.

Dedications

"*Where you invest your love, you invest your life*" – (Awake My Soul, Mumford & Sons)

This PhD Thesis is dedicated to:

my parents and my sister Marta

my grandmas Minica and Elisa

my friends, especially Jasmine, Sara, Giulia, Paola, and Greta

my best friend in heaven, Nakky

and all of my colleagues, especially Daniela, Carlo, and Francesco.

Thank you for your love and support throughout these three years.

Abstract

In hematopoietic stem and progenitor cell (HSPC) gene therapy (GT), insertional mutagenesis may result in oncogene activation, increasing the risk of leukemia in patients. Moreover, hBRAFV600E-expressing human HSPCs transplanted into immune-deficient (NSG) mice, even in small numbers, induce lethal bone marrow (BM) failure. This aggressive phenotype is due to the engagement of senescence, characterized by cell cycle blockade and a senescence-associated secretory phenotype, affecting also non-mutated bystander cells. Thus, it is fundamental to describe oncogene activation in HSPCs, since it poses risks before the malignant transformation. To investigate the fate of senescent cells in the presence or absence of an active immune system, we transplanted NSG or immune-competent (WT) mice with mouse (m) HSPCs transduced with lentiviral vectors expressing mBrafV600E, an N-truncated version (mBraf trunc), or GFP as control.

In NSG recipients, mBraf-trunc and mBrafV600E expression caused dose-dependent lethality and reduced cellularity, the latter resulting in a more aggressive phenotype. As opposed to the humanized model, only mBrafV600E-lymphoid cells were impaired, but not bystander cells. Transcriptional profiling showed upregulated cell cycle inhibitor genes Cdkn2d and Cdk2ap2, not Cdkn2a or Cdkn1a. Hallmarks upregulated were TNFα signaling, oxidative stress pathways, and apoptosis. Downregulated processes were ribosome biogenesis, interferon signaling, and innate and adaptive immune response (MHC class II and B and T cell development). Instead, in WT recipients, we observed reduced lethality (only 60%) and complete clearance of oncogene-expressing cells in the surviving mBrafV600E mice, suggesting that the immunological competence of recipients promotes a more efficient clearance of senescent cells. Transcriptional analysis showed similar immune suppression to NSG, but upregulated hallmarks were related to cell cycle, G2/M checkpoint, E2F targets, DNA replication, and repair processes in B cells, while apoptosis was downregulated. This suggests that B cells are potentially escaping senescence and returning to the cell cycle. This study aspires to identify species-specific or universal biomarkers for pre-clinical and clinical GT studies and to recognize factors determining the resilience/clearance of senescent cells, suggesting strategies for their elimination.

Table of Contents

Acronyms and Abbreviations

HSCs = Hematopoietic Stem Cells

HSPCs = Hematopoietic Stem and Progenitor Cells

GT = Gene Therapy

mBraf or hBRAF = Mouse Braf or Human BRAF

γ-RV = Gamma Retroviral Vector

LV = Lentiviral Vector

SIN = Self-Inactivating

LTR = Long Terminal Repeat

CIS = Common Integration Site

RTK = Receptor Tyrosine Kinase

WT = Wild-Type

OIS = Oncogene-Induced Senescence

DDR = DNA damage response

Rb = Retinoblastoma

SASP = Senescence-Associated Secretory Phenotype

NFκB = Nuclear Factor κB

AML = Acute Myeloid Leukemia

MDS = Myelodysplastic Syndrome

HCL = Hairy Cell Leukemia

LCH = Langerhans Cell Histiocytosis

ECD = Erdheim-Chester Disease

ECM = Extracellular matrix

MMPs = Matrix metalloproteinases

IL = Interleukin

CCL = Chemokine (C-C motif) Ligand

TNFα = Tumor Necrosis Factor Alpha

IFNα, IFNγ = Interferon Alpha or Gamma

uPAR = Urokinase Receptor

ROS = Reactive Oxygen Species

NK = Natural Killer

CR = Conserved domain

BM = Bone Marrow

PB = Peripheral Blood

NSG = Immune-Deficient, NOD.Cg-*Prkdc*^{scid} *Il2rg*^{tm1Wjl}/SzJ mice

C57 = Immune-Competent, C57BL/6 mice

CSH = Crystal-Storing Histiocytosis

List of Figures and Tables

1. Introduction

In hematopoietic stem cell gene therapy (GT), patients' hematopoietic stem and progenitor cells (HSPCs) are genetically modified *ex vivo* with integrating vectors and reinfused to reconstitute the hematopoietic system and provide therapeutic benefits. This strategy has recently gained substantial success by progressing from early-stage clinical trials to the first Advanced Therapy Medicinal Products (ATMP) approved for the EU market (*Ferrari et al., 2020*). Part of the attainments of HSPC GT is due to the great advantage of transplanting autologous, patient-derived, genetically engineered cells, as opposed to an allogeneic transplant. Indeed, autologous transplant overcomes both risks of graft-versus-host disease and difficulties in finding a properly matched HLA donor for each patient; moreover, it partially reduces the risk of engraftment failure. Therefore, HSPCs GT may become a new pillar of treatment for several inherited monogenic affections *(Naldini et al., 2022*). Despite these exciting prospects, the genetic alterations caused by the vector integration in semi random positions of the host cell genome have been linked aberrant clonal expansions and oncogenic transformation in patients from different gamma retroviral and lentiviral vector based clinical trials (*Hacein-Bey-Abina, von Kalle, et al., Science, 2003; Hacein-Bey-Abina, Garrigue, et al., 2008; Howe, Mansour, et al., 2008; Ott, Schmidt, et al., 2006; Stein, Ott, et al., 2010; Cavazzana-Calvo et al., 2010; Fraietta et al., 2018; Cesana et al., 2021; Cicalese et al., 2021, Williams et al., 2022).* Moreover, it has been recently showed that NSG immune-deficient mice transplanted with human HSPCs expressing the activated $BRAF^{V600E}$ oncogene, even at low numbers, develop multi-organ mixed histiocytosis and succumb by bone marrow failure. At the base of this aggressive phenotype is the pro-inflammatory Senescence-Associated Secretory Phenotype (SASP) of human cells consequent to the activation of the Oncogene Induced Senescence (OIS) program which affects also non-mutated bystander cells (*Biavasco, Lettera et al., 2021*). Therefore, oncogene activation in HSCPs leads to the accumulation of senescent cells which, besides the inherent risk of cell transformation, is highly detrimental for the tissues where they reside for prolonged time.

These recent findings prompted us to further deepen our knowledge on the mechanisms of SASP induction and its modulation in HSPCs in an ex vivo GT context as well as on the interactions between senescent cells and the immune system. Altogether, we aim to develop novel strategies to minimize the potential side effects of HSPC GT.

1.1 The safety of gene therapy

1.1.1 Integrating vectors and the risk of insertional mutagenesis

Gene therapy (GT) uses different viral and non -viral vectors to deliver genes or edit genetic sequences organs at high efficiency in cells ex-vivo or even entire organs in vivo, and is used for the therapy of several genetic and acquired diseases. Nevertheless, the deliberated or inadvertent integration of vector sequences into the host cellular genome significantly increases the risk of deregulation of cancer-related genes and potentially trigger malignant transformation in GT patients. Notably, with gamma-retroviral vectors (γ-RV) and lentiviral vectors (LV), the preferred vectors in HSPCs-GT and cancer immunotherapy applications, aberrant clonal expansions and oncogenic transformation of genetically modified cells have occurred in several patients in multiple clinical trials and preclinical models as the result of insertional mutagenesis (*Hacein-Bey-Abina, von Kalle, et al., Science, 2003*; *Hacein-Bey-Abina, Garrigue, et al., 2008; Howe, Mansour, et al., 2008; Ott, Schmidt, et al., 2006; Stein, Ott, et al., 2010; Cavazzana-Calvo et al., 2010; Fraietta et al., 2018; Cesana et al., 2012; Moiani et al., 2012).* While the ability of γ-RVs and LV to integrate in semi-random positions of the host cell genome is beneficial because ensures the stable expression of the therapeutic transgene to the marked cell and its progeny, it an also result in the alteration of the expression levels or mRNA structure of genes targeted by or nearby the vector insertion. When insertions trigger the aberrant activation of a proto-oncogene or inactivation of a tumor suppressor gene, they could potentially cause clonal expansion or even oncogenic transformation of individual cell clones.

Historically, retroviruses were discovered in the 20th century in animal studies, for their association with tumor development as the result of insertional mutagenesis (*Ellerman and Bang 1908; Rous 1911; Gross 1951; Weiss et al., 1982*). At first, the risk of oncogenic transformation by the use of vectors derived from gamma-retroviruses was considered low, since the viral genome has been modified to lack the capability to replicate. Indeed, the use of replication-defective vectors reduces the burden of insertions in the target cells compared to replicating parental virus. Moreover, even in the case of proto-oncogene activation, malignant transformation would occur upon the acquisition of additional mutations on genes that specifically synergize with the initial genetic lesion caused by the vector insertion. Unfortunately, these optimistic beliefs changed radically after the onset of leukemia in patients from different HSPC-GT clinical trials with γ-RVs. In two of the first HSPCs GT clinical trials conducted in France and United Kindom, patients with X-linked SCID were transplanted with autologous HSPCs, transduced with a γ-RV coding for the missing IL-2 receptor gamma (IL2RG) gene. Indeed, despite the initial success of the treatment, 6 patients developed T cell leukemia even 15 years after gene therapy. Integration site analysis of the patient's leukemic cells showed vector insertions upstream of the *LMO2* and, to a lesser extent, *CCND2* and *BMI1* proto-oncogenes (*Cavazzana-Calvo et al., 2000; Hacein-Bey-Abina et al., 2002; Schwarzwaelder et al., 2007; Deichmann et al., 2007; Hacein-Bey-Abina et al., 2008. Six et al., 2017; Cesana et al., 2021*). Other patients, enrolled in the γ-RV-based HSPC-GT clinical trials for Chronic Granulomatous Disease, Wiskott-Aldrich Syndrome, and Adenosine Deaminase Deficiency, developed myelodysplastic syndrome (MDS) as the result of the activation of *MECOM*, *PRDM16* or *SETBP1* genes, or T-cell leukemia resulting from the activation of *LMO2* gene (*Ott, Schmidt, et al., 2006; Botzug et al., 2006; ; Cicalese et al., 2021*). Moreover, many more patients from these γ-RV-based HSPC-GT clinical trials, even in absence of malignant transformation, showed also clonal expansions of myeloid or T-cell clones with integrations targeting the same oncogenes caused by vector insertions are events defined as vector-mediated genotoxicity (*Baum et al., 2006*).

To overcome the risks of insertional mutagenesis, past and ongoing efforts to develop safer vectors have been made. One of the main improvements involved replacing the initial use of

γ-RVs, derived from the Moloney Murine Leukemia Virus (MLV) with LVs originating from the Human Immunodeficiency Virus 1 (HIV-1) virus; this solution had the advantage of reducing the integration bias in cancer genes. The generation of self-inactivating lentiviral vectors (SIN.LV) (*Zufferey et al., 1998*), where a portion of the 3' long terminal repeat (LTR) had been deleted, inhibited the LTR promoter activity without losing the vector's efficacy in integration or titration.

All retroviruses integrate semi-randomly into the genome. The process of integration does not occur indiscriminately for multiple reasons. Common insertion sites (CIS), which are genes that are more recurrently targeted by integrating vectors, are the consequence of two aspects. On one hand the preference of the vector to integrate in certain regions of the genomes is dictated by accessible portions of the same, on the other certain integrations may give selective advantage to certain clones. Regarding the first aspect, the interaction of the integrating vector with host proteins can favor or obstruct the access to DNA. In particular, there are proteins that favor the integration process: in the case of LVs, the protein LEDGF/p75 binds the HIV integrase, promoting the tethering of the HIV pre-integration complex to the chromatin. In the case of γ-RV, previous literature reports bromo-and extraterminal domain (BET) proteins as the functional equivalent of LEDGF/p75 for MLV, thus promoting the tethering of the pre-integration complex to chromatin (*Debyser et al., 2014*). On the other hand, the binding of nucleosomes to the DNA shapes its tridimensional structure in such a way that some DNA portions are sterically less accessible for integration to occur (*Pruss, Bushman et al., 1994; Pruss, Reeves et al., 1994*). Moreover, the architecture of the nucleus itself dictates whether the integration can happen, as HIV integration cluster more preferentially near the nuclear pore. Indeed, the region of the nuclear pore contains active transcription chromatin marks, easily accessible by integrating vectors (*Marini et al., 2015*). The second aspect concerns the selective advantage of clones harboring a certain integration. Regarding this, each retrovirus shows different target preferences. Although both MLV and HIV show a preference of integrating within the transcriptional unit, up to 20% of MLV integrations occur upstream or downstream of the transcription start site (TSS), thus showing a preference for promoter regions. In addition MLV insertion sites were also

enriched nearby CpG islands, genomic regions associated with the TSS in the genomes of vertebrates. (*Schroder et al., 2002; Wu et al., 2003; Mitchell et al., 2004*). These findings confirm that γ-RV, since they origin from MLV, are more prone to integrate nearby promoter sequences, thus favoring the alteration of the expression of genes to a greater extent compared to LV, derived from HIV. This alteration of gene expression after integration may provide a selective advantage of certain clones compared to others, affecting the distribution of CIS. In particular, the integration nearby oncogenes, promoting their activation, provides a higher proliferative capacity of clones harboring that integration, thus resulting in oncogenes being the most frequent CIS after the use of genotoxic vectors.

The superior safety profile of SIN.LV has been demonstrated in a tumor-prone mouse model such as *Cdkn2a*$^{-/-}$ mice, which lack two important regulators of cell cycle (p16^{INK4a} and p19^{Arf}) and cellular senescence against aberrant proto-oncogene activation (*Lund et al., 2002; Serrano et al., 1996*). This in vivo genotoxicity assay employed mouse HSPCs, collected from the BM of *Cdkn2a*$^{-/-}$ mice, transduced with different LV designs, and transplanted into recipient mice. SIN.LV, as opposed to γ-RV, showed a promising safety profile (*Montini et al., 2006*; *Montini et al., 2009, Cesana, Ranzani et al. 2014*). Moreover, it required significantly greater LV integration loads to reach the same oncogenic risk and acceleration of tumor development than γ-RV. Additionally, the whole transcriptome analysis of chimeric LV-cellular genome fusion transcripts showed that SIN LV has a sharply reduced tendency to engage in aberrant splicing compared with vectors carrying active LTRs (*Cesana et al., 2012; Moiani et al., 2021*). Other safety in vivo studies have been carried out and confirmed the safety of SIN LVs (*Modlich et al., 2009; Arumugam et al. 2009; Zychlinski et al., 2008*). Thus, the use of SIN LVs reduces the risk of insertional mutagenesis when compared to the use of vectors with active LTRs.

Over time, multiple vector designs have been developed to further reduce potential insertional mutagenesis. One of these developments was the addition of chromatin insulators, regulatory elements which prevent the portion they delimit from acting as an enhancer/promoter to proto-oncogenes (*Emery et al., 2011*). However, in a clinical trial using an LV to treat β-thalassemia, vector integration appeared to cause clonal dominance in one

of the patients (*Cavazzana-Calvo et al., 2010*). The integration occurred within the HMGA2 gene, inducing the formation of an aberrantly spliced mRNA form. Sequencing of the HGMA2 spliced mRNA form showed truncation by alternative splicing of the third intron with a cryptic 3′ splice signal (GTAT(C)6AG), located within the cHS4 insulator core and cleavage/polyadenylation within the adjacent R region of the 5' LTR. Yet, this clonal expansion did not result in overt leukemia.

With the increasing number of patients treated by gene therapy, the emergence of rare genotoxic effects is now apparent also for SIN.LVs. Indeed, events of LV-mediated genotoxicity were reported in clinical trials, as dominant clones with LV integrations targeting HMGA2 and other cancer-related genes were observed in other HSPC-GT clinical trials for X-linked severe immunodeficiency (*De Ravin et al., 2016*), adrenoleukodystrophy (*Eichler et al., 2017*), and in two different CAR-T cancer immunotherapy trials (*Fraietta et al., 2018; Shah et al., 2019*). More recently, 3 patients enrolled in the clinical trial of Adrenoleukodystrophy developed MDS as the result of insertional activation of the MECOM oncogene (*Bluebird-bio clinical trial; Williams et al., 2022*)

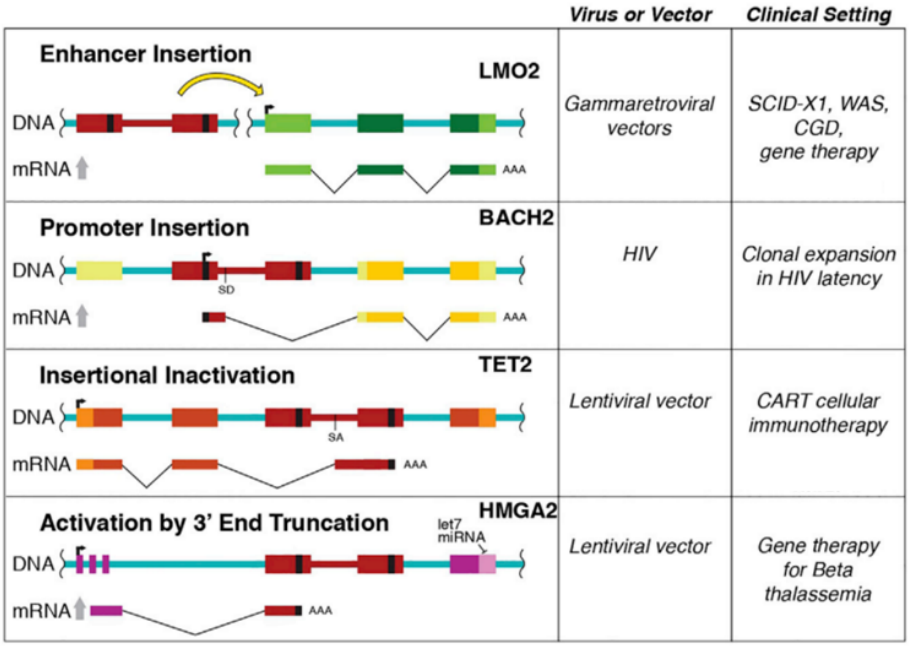

Figure 1.1. Mechanisms of insertional mutagenesis through retrovirus integration *characterized in gene therapy and HIV fields (from Bushman 2020).*

To summarize, four different mechanisms of retroviral insertional mutagenesis have been characterized thus far (**Figure 1.1**): gene activation by integration of an enhancer sequence encoded in a retroviral vector, defined as enhancer insertion (*Hacein-Bey-Abina et al., 2008*), gene activation by promoter insertion (*Cesana et al., 2017*), gene inactivation by insertional disruption (*Fraietta et al., 2018*), and gene activation by mRNA 3' end substitution (*Cavazzana-Calvo et al., 2010*). Each of these integration mechanisms resulted in clonal expansion or transformation in patients.

1.1.2 In vivo safety studies and oncogenes as common insertion sites

Further studies on the safety of LV and their different designs have been carried out. Through the use of Cdkn2a$^{-/-}$ mutant mice, acceleration of their spontaneous oncogenesis was observed after treatment to assess oncogenic risk (*Cesana et al., 2014*). The tested vectors were the following: (i) vector with active LTRs and strong SF promoter; (ii) vector with SIN LTRs and strong SF promoter; (iii) vector with SIN LTRs, strong SF promoter and 3′-truncated open reading frame (ORF) of the Woodchuck posttranscriptional regulatory element (PRE); (iv) vector with SIN LTRs, weak PGK promoter, and PRE; (v) vector with SIN LTRs, strong SF promoter, chromatin insulators, and PRE. A group of mice was also mock-treated as a control.

Overall, a ranking of the genotoxic potential of the different vector designs have been carried out (**Figure 1.2a**): with vectors (i) and (ii) being the most genotoxic, given that integration of those type of vectors led to the insertion of a promoter sequence (active LTRs in (i) and strong promoter in the case of (ii)). Vector design (iii) was still strongly genotoxic, because of the insertion of a strong SF promoter acting as an enhancer, despite the use of SIN LTRs and the mutated PRE. Vector design (iv) showed less genotoxicity, given that the PGK promoter is weaker than the SF, but still a significantly faster lethality and tumor progression were observed when compared to mock treatment. Finally, vector design (v) was the least

genotoxic of all, with insulators functioning as inhibitors of the enhancer activity possessed by the SF promoter.

All the tumors developed by mice contained integrations of the different vectors, with the most genotoxic design integrating more often in the proximity of oncogenes, while the least genotoxic designs showed more frequency in targeting tumor-suppressor genes. The proto-oncogene Braf was the highest-ranking CIS gene in Cdkn2a$^{-/-}$ tumors induced by vectors (i) and (ii). Integration was predominantly in the same orientation as Braf, between intron 11 and intron 12, and therefore comparable to transposon integration in sarcomas of Cdkn2a$^{-/-}$ mice in a previous study (*Collier et al., 2005*). LV integration generated a truncated, constitutively active form of mouse Braf (**Figure 1.2b**), only containing the catalytic portion of the protein.

Another CIS gene in lesser genotoxic vector designs than (iii, iv, and v) was the proto-oncogene Map3k8, in which LVs integration was analogous to γ-retroviral integrations in mouse lymphomas (*Patriotis et al., 1993; Patriotis et al., 1994; Lund et al., 2002*). The most common CIS gene found in Cdkn2a$^{-/-}$ tumors and induced by vectors (iv) and (v) was the tumor-suppressor gene Pten, followed by another tumor suppressor, such as Rasa1.

By performing gene ontology analysis, over-represented gene classes in the CIS were regulation of protein kinase cascade, guanosine tri-phosphatase regulator activity, and mitogen-activated protein kinase signaling pathway. Overall, all these belong to the receptor tyrosine kinase (RTK) pathway (**Figure 1.2c**), aberrantly activated in a vast range of human and murine tumors. The LV integration in genes belonging to the RTK pathway may collaborate with the genetic lesion of the Cdkn2a$^{-/-}$ mice to induce tumorigenesis. Interestingly, when vectors were tested on WT mice, Braf activation was not able to induce cancers, suggesting that when the product of the Cdkn2a gene (p16^{Ink4a}), a cell cycle inhibitor, is fully produced, it can inhibit aberrant cell proliferation with the induction of senescence/apoptosis instead (*Kang et al, 2011; Michaloglou et al., 2005*).

And finally, on the topic of tumor suppression, it is worth mentioning that, throughout the evolutionary process, humans have developed protective mechanisms to avoid potential tumorigenesis. Two of the most significant ones are the immune system and oncogene-induced senescence.

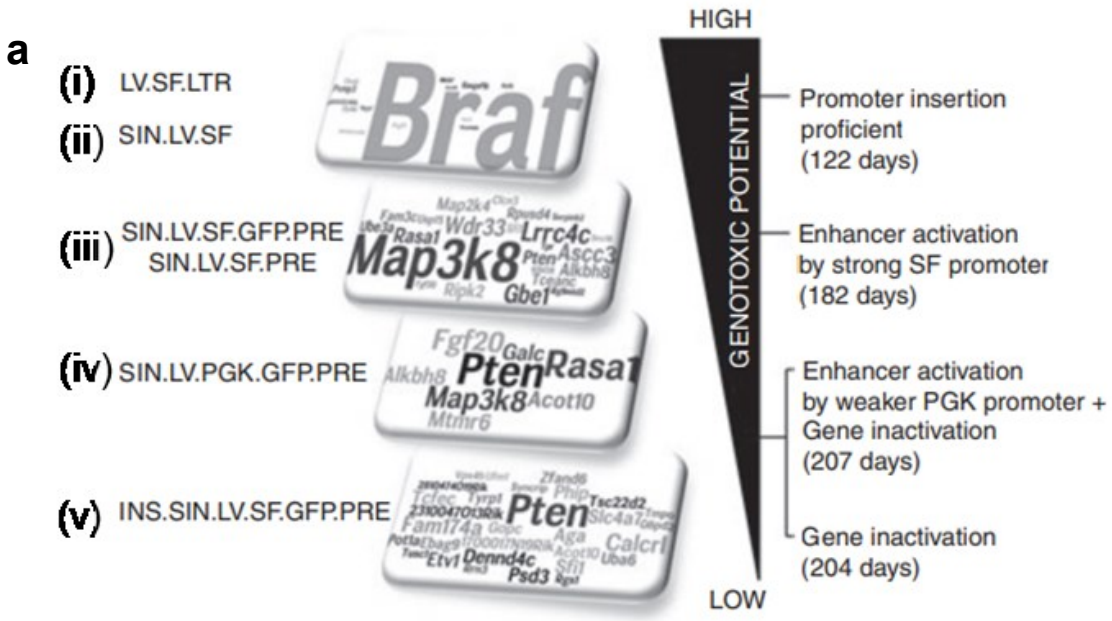

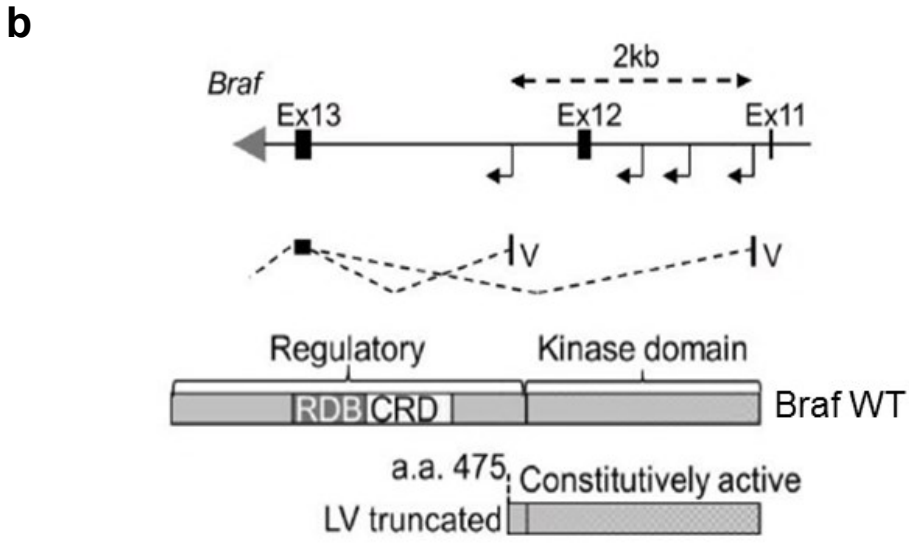

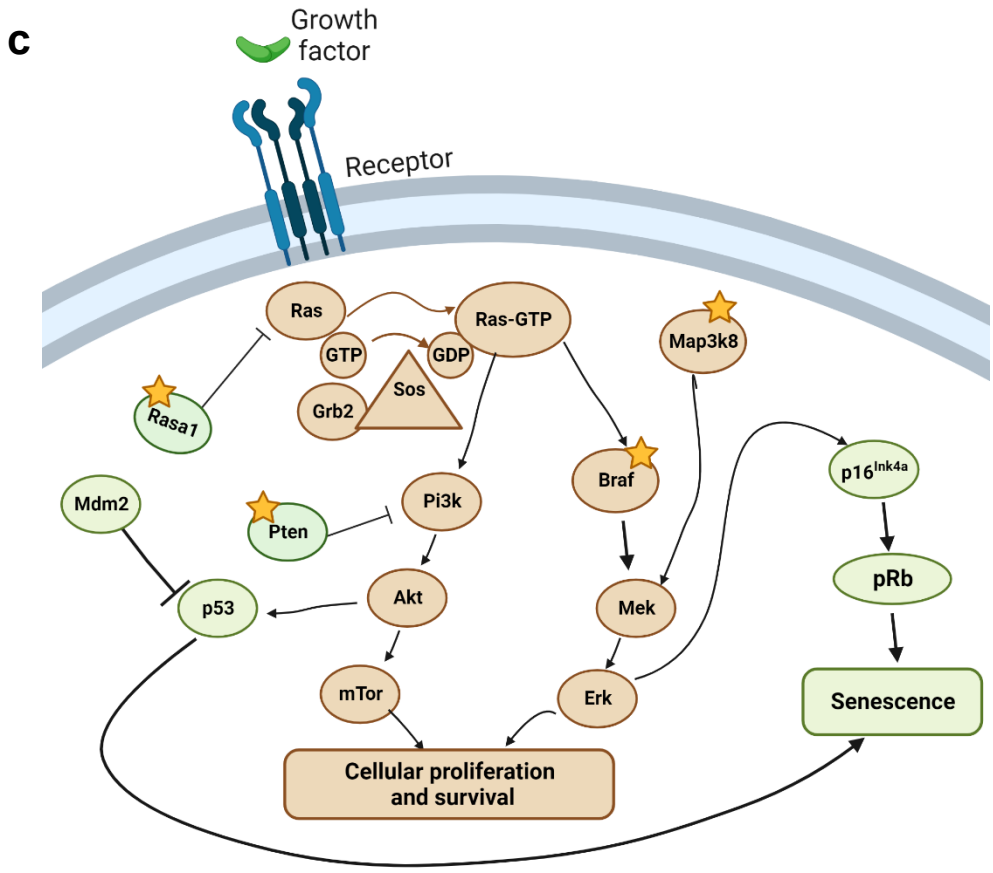

Figure 1.2. LV designs and their targeting of the RTK pathway. *(a) Summary scheme of the genotoxic potential of different vector design and their CIS (from Cesana et al., 2014). (b) Generation of a truncated form of Braf by insertion of a genotoxic LV vector in Cdkn2a$^{-/-}$ mice. (c) The activation of the RTK pathway by insertional mutagenesis. CIS are identified by the star symbol. Cdkn2a$^{-/-}$ mice lack the production of the cell cycle inhibitor p16^{Ink4a}, thus the senescence mechanism on the right can be activated only in WT mice. Image created with BioRender.*

1.2 Cellular senescence

1.2.1 Senescence, DNA damage, and cell cycle arrest

Oncogene-induced senescence (OIS) is a complex cellular process that prevents cancer progression by halting the proliferation of differentiated oncogene-expressing cells (*Yaswen and Campisi, 2007*). OIS is one of the possible routes taking part in the broader process

known as cellular senescence, first discovered as an exit from the cell cycle after exhaustion of the proliferative capacity of human fibroblast kept in culture (*Hayflick and Moorhead, 1961*). Over time, that definition has been attributed to replicative senescence, while it has been revealed that cellular senescence can be induced by different types of stimuli. Senescence can be explained as a stable, most of the time permanent state of cell cycle arrest, triggered in response to endogenous and exogenous stresses (**Figure 1.3**), such as telomere shortening (*Hayflick et and Moorhead, 1961; Bodnar et al., 1998*), aberrant DNA replication and DNA damage accumulation (*Di Micco et al., 2006; Bartkova et al., 2006*), ROS accumulation, loss of tumor suppression or oncogene overexpression (*Serrano et al., 1997*), embryonic development (*Rajagopalan et al., 2012*), wound healing (*Jun et al., 2010*), tissue repair (*Krizhanovsky et al., 2008*), and physiological aging (*Baker et al., 2008; Baker et al., 2011*). In summary, cells undergo senescence after being subjected to a certain level of damage or stress that reaches the point of no return. As senescence occurs with cell cycle arrest, its most common mechanism is the induction of the expression of cell cycle inhibitors, such as p53, $p16^{Ink4a}$, or both. When cells undergo severe DNA damage, a response defined as DNA damage response (DDR) occurs. One of the first activated proteins is ATM (ataxia telangiectasia mutated), which in turn phosphorylates the nucleosomal histone H2AX and the p53-binding protein 53BP1. These two proteins form a tridimensional structure, typical of senescence, known as heterochromatin foci (*Campisi and D'Adda di Fagagna, 2007).* ATM also phosphorylates the Chk1/2 proteins that activate p53 (*Wahl and Carr, 2001*), a cell cycle inhibitor and tumor suppressor. p53 in turn stimulates p21, inducing cell-cycle arrest through inhibition of cyclin E–Cdk2 (*von Zglinicki 2002; Sedelnikova et al., 2004; Passos et al., 2010*).

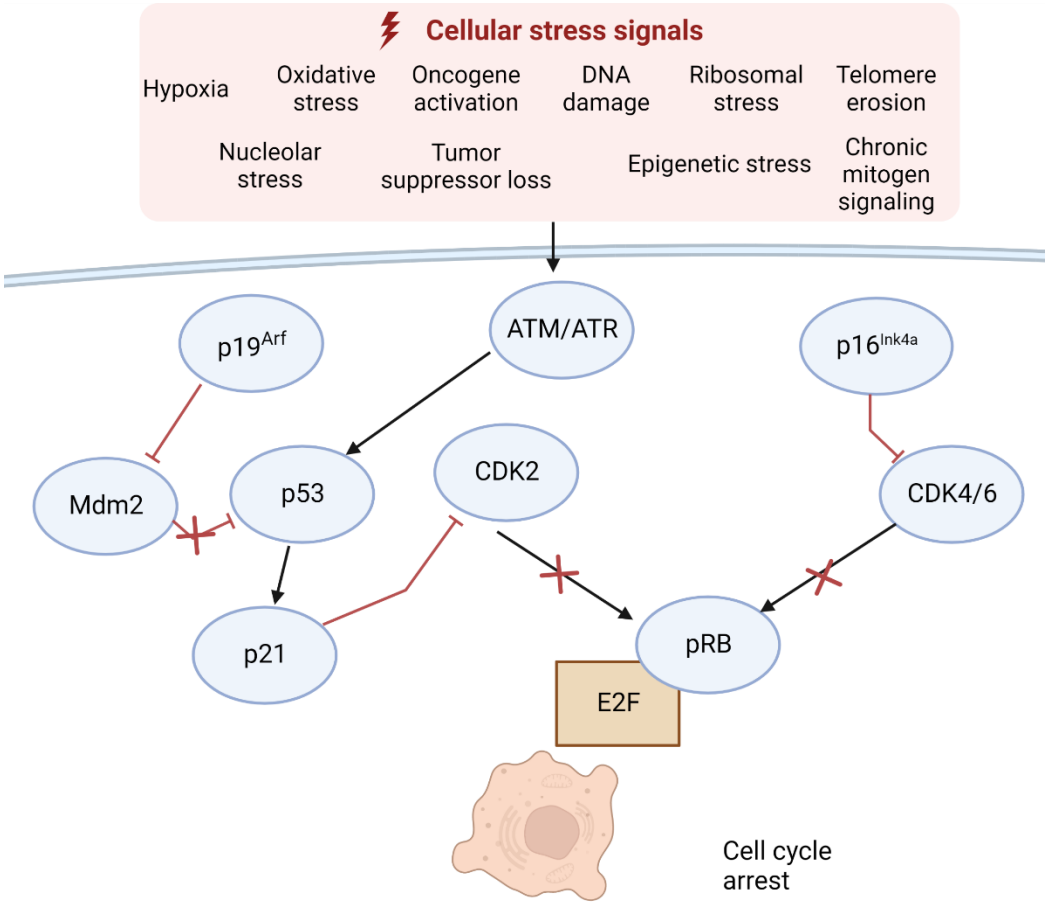

Figure 1.3. Senescence-inducing stimuli and main effector pathways. *Cellular signaling cascades that can activate p53, $p^{16Ink4a}$, or both. Image created with BioRender.*

In the other case, when $p16^{Ink4a}$ is stimulated, it inhibits cell-cycle progression but through inhibition of cyclin D–Cdk4 and cyclin D–Cdk6. $p16^{Ink4a}$ belongs to the Ink4 protein family, which comprises also of $p15^{Ink4b}$, $p18^{Ink4c}$, and $p19^{Ink4d}$. The Ink4 family members were named after their inhibitory function against Cdk4 (and Cdk6) (*Cánepa et al., 2007*). $p16^{Ink4a}$ is a particularly common tumor suppressor in human cancers (*Rocco and Sidransky, 2001*), and its expression is a senescence hallmark in human cells (*Buj et al., 2021*). Both p53 and $p16^{Ink4a}$, by inhibiting Cdk2/4/6, leave Rb in its active, hypo-phosphorylated form. Rb, in turn, can inhibit the E2F transcription factor, which is responsible for the G1/S cell cycle progression. Mild damage may lead to a temporary cell-cycle blockade, which can be

repaired. Even so, chronic or permanent damage provokes permanent arrest in proliferation, thus causing senescence.

Another pathway that can induce p53 involves $p19^{ARF}$, encoded in the INK4a locus, the same locus as $p16^{Ink4a}$ (*Haber, 1997*). $p19^{ARF}$ can activate p53 by sequestering Mdm2, thus preventing Mdm2-mediated degradation of p53 (*Tao and Levine, 1999*). Like p16, $p19^{ARF}$ is induced after stresses such as irradiation (*Khan et al., 2000; Qi et al., 2004*) or oncogene overexpression (*Lowe and Sherr, 2003*). Yet, it has proven to be a more common tumor suppressor in mice than p16. $p19^{ARF}$ inactivation in mouse germinal cells induces tumors in a widespread fashion (*Kamijo et al., 1997*), in a similar manner to what happens when p53 is inhibited in human cells (*Joerger and Fersht, 2016*). Inhibition of $p16^{Ink4a}$, on the other hand, generates only a specific set of tumors (*Krimpenfort et al., 2001; Sharpless et al., 2001*). This suggests that there may be species-specific routes to cell cycle arrest. Moreover, past studies have reported the possible existence of a pathway that connects $p16^{Ink4a}$ and DDR, occurring in replicative senescence induced by telomere dysfunction. When TRF2 is inhibited to uncap telomeres, $p16^{Ink4a}$ is induced without the activation of p53 (*Smogorzewska & de Lange, 2002*). The authors, however, found that this specific signaling was human-specific and did not occur in mouse cells, where only p53 signaling was activated, but when abrogated, it was not compensated by $p16^{Ink4a}$ action.

Regarding the rest of the Ink4 family, it has been demonstrated that inactivated $p15^{Ink4b}$ and $p18^{Ink4c}$ can be found in a variety of tumors. Epigenetic silencing of $p15^{Ink4b}$ was reported in rare glial tumors, leukemia, and myelodysplasia, without the silencing of $p16^{Ink4a}$ (*Esteller et al., 2001*). Given the overlap in the function of Ink4 proteins, loss of function of more than one of these genes might be more tumorigenic, as in some tumors, such as T-cell acute lymphoblastic leukemia, deletion of the entire 9p21 portion encoding for all Ink4 genes is frequently found (*Cánepa et al., 2007*). Although the loss of function of $p18^{Ink4c}$ is rare in human tumors, it has been reported to be a haplo-insufficient tumor suppressor in mice (*Bai et al., 2003*). Curiously, despite its cell cycle inhibitor role, there is no evidence of $p19^{Ink4d}$ being a tumor suppressor (*Ortega et al., 2002*). On the other hand, studies have shown that $p19^{Ink4d}$ regulates genomic stability and cell vitality after DNA damage during genotoxic

stress in neuroblastoma cells and fibroblasts. Cells overexpressing or null of $p19^{Ink4d}$ were subjected to UV irradiation: when overexpressed, this cell cycle inhibitor increased the cells' capacity for DNA repair. $p19^{Ink4d}$, on the other hand, showed the opposite phenotype (*Ceruti et al., 2005; Scassa et al., 2007*). Knockdown of $p19^{Ink4d}$ also rendered cells sensitive to apoptosis and autophagy (*Tavera-Mendoza et al., 2006*). Finally, $p19^{Ink4d}$ was shown as specific in hematopoietic cells, regulating the quiescence of hematopoietic stem cells (HSCs) by inhibiting the passage from G_0 to G_1 and preventing the accumulation of DNA damage under genotoxic conditions (*Hilpert et al., 2014*).

Finally, the murine and the human capability of undergoing senescence also depend on the telomere itself. Telomeres of laboratory mice are 5-10 times longer than human telomeres (*Hemann and Greider, 2000*). Additionally, in their lifetime, humans undergo 105 more cell divisions compared to mice (*Rangarajan and Weinberg, 2003*), thus reaching cellular senescence faster. Moreover, mice with longer telomeres develop less DNA damage, have better metabolic and neurocognitive parameters, and have less spontaneous tumor incidence in aging (*Muñoz-Lorente et al., 2019*). Mechanistically speaking, humans and mice have the same incidence of cancer (30%) but develop different tumor spectrums. However, telomerase-deficient mice (after 5/6 generations) do develop epithelial cancers that are common in humans, not the ones usually observed in mice (*Artandi et al., Nature 2000*).

Proliferation arrest in senescent cells does not arrest their metabolic processes altogether, on the contrary, they are still metabolically active. After all, another common feature of senescence is the secretion of pro-inflammatory factors, namely cytokines, chemokines, growth factors, proteases, and extracellular matrix (ECM) remodeling factors, together named senescence-associated secretory phenotype (SASP). SASP released by senescent cells affects neighboring cells, in two ways: on one hand, it recruits the immune system for their clearance, on the other, it turns neighboring cells into senescent cells, with a phenomenon called paracrine senescence (*van Deursen 2014*).

In 2008, Coppé et al. demonstrated that genotoxic stress is accompanied by the secretion of a significant number of pro-inflammatory factors in cultured human epithelial cells,

especially when the RAS oncogene is over-expressed. SASP-induced epithelial-mesenchymal transition and invasiveness through paracrine signaling depend on two main interleukins: interleukin-6 (IL-6) and IL-8. More recently, persistent DNA damage and DDR signaling in senescent cells have been demonstrated to be the actual cause of SASP. Chromatin lesions initiated SASP after DNA double-strand breaks and after the activation of ATM and Chk2, specifically the secretion of IL-6, the most common SASP factor, independently of p53. IL-6 secretion can influence paracrine senescence by affecting bystander cells that express the IL-6 receptor and the gp130 signaling process, thus targeting epithelial and endothelial cells of different organs (*Rodier et al., 2009*).

DDR signaling is the main driver of SASP, and it proceeds without being dependent on cell-cycle inhibitors. Indeed, ectopic expression of $p16^{Ink4a}$ promoted cell cycle blockade and induced senescence, but without the production of SASP in human fibroblasts. On the other hand, radiation-induced or OIS (RAS activation) generated a prominent SASP in the same fibroblasts (*Coppé et al., 2011*). Nevertheless, $p16^{Ink4a}$ may have a more indirect effect on SASP, by protecting cells from cumulative DNA damage, hence limiting inflammation and pro-inflammatory factors secretion. Other than persistent DNA damage, activated oncogene (BRAFV600E) expression can induce SASP without telomere erosion, as the expression of hTERT protected the telomeres while maintaining the aberrant OIS (*Kuilman et al., 2008*).

Other than DDR signaling, cytoplasmic DNA, such as DNA that is aberrantly outside of the nucleus and/or mitochondria due to genotoxic stress, also triggers a downstream response by functioning as a danger-associated molecular pattern (DAMP). The cGAS–STING axis that follows is associated with auto-inflammatory diseases, senescence, and cancer. An enzyme, called cyclic guanosine monophosphate (GMP)-adenosine monophosphate (AMP) synthase (cGAS) binds cytoplasmic DNA in a sequence-independent fashion. cGAS undergoes a conformational change in the catalytic portion of the enzyme for the conversion of GTP and ATP nucleotides into cyclic GMP-AMP (cGAMP) (*Sun et al., 2013; Wu et al., 2013*). In turn, cGAMP serves as a second messenger and as a ligand for the adaptor protein Stimulator of IFN Gene (STING) (*Ishikawa and Barber, 2008; Jin et al., 2008; Zhong et al., 2008; Sun et al., 2009*). STING also undergoes conformational change after binding to cGAMP (*Gao*

et al., 2013b; Zhang et al., 2013), and translocates from the ER to the Golgi apparatus (*Ishikawa and Barber, 2008; Saitoh et al., 2009*). Afterward, STING phosphorylates and thus activates two proteins through its C-terminal portion: TANK-binding kinase 1 (TBK1) and IFN regulatory factor 3 (IRF3). Moreover, STING activates NF-κB, which functions together with IRF3 to activate the transcription of different cytokines, including Interferon 1 (*Tanaka and Chen, 2012; Liu et al., 2015*). The cGAS-cGAMP-STING pathway can be induced by different stimuli, i.e. mitogenic stress, oxidation, radiation, or chemotherapy, and results in the secretion of cytokines or chemokines, mainly IFN-β, IL-1β, IL-6, and IL-8 (*Dou et al., 2017; Glück et al., 2017; Yang et al., 2017*).

Although both cell cycle arrest signaling and cytokine production signaling derive from the DDR response, they act separately. This hypothesis is further supported by the notion that pharmacological inhibition of cell cycle kinases CDK4/6 promotes senescence both in vitro on primary fibroblast and in vivo as a tumor-suppressive mechanism in a breast cancer mouse model. (*Wang et al*., 2022). This inhibition is nevertheless associated with a p53-associated secretory phenotype but lacks the activation of the main player controlling SASP, such as the transcription factor NF-κB.

1.2.2 The NFκB pathway signaling

The nuclear factor κB (NF-κB) was first discovered as a DNA-binding protein targeting the kappa immunoglobulin light chain enhancer in B cells (*Sen and Baltimore, 1986*). This family of transcription factors consists of five subunits: p65 (RelA), c-Rel, RelB, and the p105 and p100 precursors, which undergo post-translational cleavage and turn into p50 and p52, respectively. NF-κB has two subunits that can form homo or heterodimers. Both subunits have a DNA binding domain and a regulatory domain by which they interact with their inhibitor, IκB. In unstimulated cells, NF-κB is found in the cytoplasm, interacting with IκB (*Ghosh et al., 1998*). NF-κB activation stimulates its translocation into the nucleus, where the transcription factor binds to promoters and enhancers of its target genes. Besides the cleavage of p105 and p100 into their activated subunits, another activating modification

is the phosphorylation, acetylation, and methylation of p65 (*Perkins et al., 2006*). The NF-κB transcription factor complex is activated after various stimuli and regulates the expression of numerous target genes involved in processes such as cell migration, cell proliferation, apoptosis, inflammation, and innate and adaptive immunity.

NF-κB activation follows the activation of IKK, a kinase complex that releases the inhibitor from the subunits through phosphorylation, followed by proteasomal degradation of IκB. IKK has three subunits: IKKα, IKKβ, and IKKγ or NEMO. In the classical pathway, IKKβ directly phosphorylates IκBα, leading to its degradation and the p65/p50 heterodimer's activation. In the alternative pathway, a dimer consisting of two subunits of IKKα is phosphorylated by the NF-κB inducing kinase (NIK). The IKKα homodimer then activates p100 into its active form, p52, ensuring the generation of p52-RelB dimers. In both cases, the activated dimers translocate into the nucleus to induce the transcription of the target genes (*Liu et al., 2017*).

The activation of the NF-κB system is most commonly due to pattern recognition receptor pathways such as TLRs and inflammasome (*Vallabhapurapu and Karin, 2009*). In the context of senescence, NF-κB gets activated by DNA damage through ATM-dependent IKK activation (*Lee et al., 1998).* Instead of the canonical cascade through membrane-bound receptors, a genotoxic signaling cascade activates NF-κB. ATM bridges the DDR with the activation of the NF-κB signaling cascade. Moreover, the NEMO subunit has proved indispensable, as a NEMO-deficient cell line of mouse embryonic cells fails to induce the transcription factor after DNA damage (*Hwang et al., 2015*). After NEMO expression is re-established, NF-κB signaling is activated again. In particular, the authors observed that NEMO's C-terminal zinc finger (ZF) domain was the main contributor to this signaling as a regulatory domain of the IKK complex in the cytoplasm. NEMO's function is also regulated by post-translational modifications, most notably by the SUMOylation (small ubiquitin-like modifier) of residues 277 and 309 and the ATM-dependent phosphorylation of residue 85 (*Wu et al., 2006*). NEMO has shown to be a specific regulator of NF-κB activation after genotoxic damage. NEMO's correct function, with the appropriate post-translational

modification, is necessary for NF-κB activation in response to DNA-damaging agents (*Wu et al., 2008*).

In the context of disease, ATM-NEMO-NF-κB signaling is constitutively activated in acute myeloid leukemia (AML) and its primary form, MDS. In MDS and AML patient samples, NEMO and the ATM-NEMO complex are constitutively in the nucleus (*Grosjean-Raillard et al., 2009*). Additionally, human HSPCs collected from high-risk MDS or AML patients are positive for pS1981-ATIM antibody staining, which indicates constitutively active ATM. Inhibition of ATM in these cells reduces this process, inducing the death of leukemic cells. Thus, it is very likely that nuclear ATM-NEMO signaling might be fundamental for the constitutive NF-κB activity found in different human malignancies, in addition to high-risk MDS and AML.

Among the many cellular processes that the NF-κB signaling transcriptionally regulates, the production of SASP is one of them. In an oncogene (H-Ras) induced senescence model, the p65 subunit was significantly enriched in the chromatin of skin fibroblasts undergoing senescence; comparatively, this enrichment did not occur in younger fibroblasts. Specifically, p65 in its activated form accumulated in the senescence-associated heterochromatin foci (SAHF), and its levels directly correlated with increased levels of secreted pro-inflammatory factors (*Chien et al., 2011*). In another study of the same year, activation of the p53-p21 pathway induced senescence in human fibroblasts, characterized by cell cycle arrest and significant production of SASP factors, such as IL-1α and IL-1β. Interestingly, they observed that the senescence phenotype could be reverted with the inhibition of NF-κB signaling, suggesting that it was the cause of the induction of SASP all along (*Rovillain et al., 2011*). More recently, it has been shown that the NF-κB signaling can be triggered by the p38-MAPK kinase, which explains how OIS can activate and trigger SASP. When proto-oncogenes of the RTK pathway are activated, they can phosphorylate p38-MAPK, thereby activating NF-κB downstream in a DDR-independent manner (*Freund et al., 2011*).

1.3 The senescence-associated secretory phenotype (SASP) and the role of senescent cells in shaping the microenvironment

1.3.1 The composition of SASP

The secretion of pro-inflammatory factors in senescence first arose as a hypothesis when it was discovered that senescent cells could turn neighboring cells into tumor cells, suggesting a possible paracrine effect (*Krtolica et al., 2001*). A few years later, another set of experiments observed the abundant secretion of pro-inflammatory molecules in the tissue microenvironment, collectively named senescence-associated secretory phenotype (SASP) (*Coppé et al., 2008*) (**Figure 1.4**).

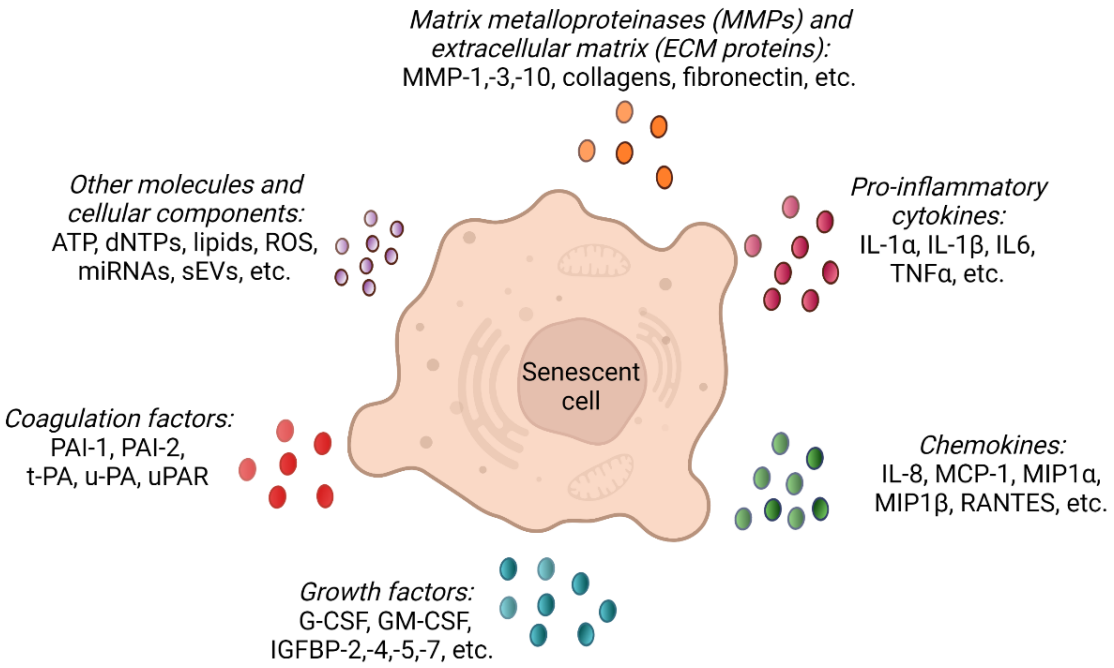

Figure 1.4. The composition of the SASP. *Image created with BioRender.*

The SASP includes different kinds of soluble and insoluble factors, such as cytokines (IL-6, IL-1α, IL-1β, IL-13, IL-15), chemokines (IL-8, GRO-a, MCP-1, MCP-2, MCP-4, MIP-1a, MIP-3a, HCC-4), other inflammatory factors (IFN-γ, GM-CSF, G-CSF) growth factors

(EGH, HGF, SCF, the IGFBP family, etc.), ECM proteins, such as matrix metalloproteinases (MMPs), coagulation factors and receptors (PAI-1, u-PA, t-PA, uPAR) (*Coppé et al., 2010*).

The composition of the SASP can vary in senescent cells, depending on the cell type and the kind of stress stimulus. For example, it is known that oncogene (Ras) induced senescence leads to higher levels of cytokines such as IL-6 and IL-1β, compared to other stimuli like irradiation or proliferative exhaustion. Simple overexpression of cell-cycle inhibitors such as $p16^{Ink4a}$ is not able to induce SASP. Furthermore, the tissue origin of senescent cells has an impact on their transcriptional output, causing variations in the expression of pro-inflammatory factors (*Coppé et al., 2008; Coppé et al., 2011; Hernandez-Segura et al., 2017*). SASP production between human and mouse cells shows some divergences, which in part seem to be influenced by the oxygen levels. Physiological oxygen levels of 3% instead of 21% do effectively induce a more human-like SASP in mouse senescent cells (*Coppé et al., 2010*).

Not all SASP factor production is regulated by NF-κB, since an IL-1 pathway upstream of NF-κB is known to induce SASP production (*Acosta et al., 2013*), while RelA deficiency results in the inhibition of almost all SASP factors except IL-1α (*Kang et al., 2015*). Mature IL-1α is produced by the inflammasome, in human cells after the cleavage by caspase 5, and in mouse cells by the cleavage of caspase 11, suggesting that the activation of the inflammasome may induce IL-1α-driven SASP upstream NF-κB (*Wiggins et al., 2019*). In human foreskin fibroblasts, IL-1α at the cell surface, but not secreted, proved to be pivotal for the secretion of two of the major pro-inflammatory factors in the SASP: IL-6 and IL-8. The same study reported that IL-1α depletion reduces the DNA binding activity of NF-κB, thus impacting the transcription of IL-6 and IL-8 (*Orjalo et al., 2009*).

The secretome of senescent cells can also vary over time and phases of senescence: it has been observed in human fibroblasts that Notch 1 is the main regulator of paracrine senescence and a mediator of a SASP switch between early and late senescence, the latter being IL-1 dependent (*Hoare et al., 2016; Teo et al., 2019*). In particular, the intracellular domain of Notch1 and its target HES1, after overexpression in early senescence, returns to basal levels

in the late phase. Consequently, the early secretome contains mainly TGF-β ligands, while IL-1-dependent SASP correlated with N1CD and HES1 transcription expression. These types of findings have been investigated mainly in human cells.

It is still partially unclear how the IL-1 pathway is activated upstream of NF-κB signaling, and so far, it has been investigated mostly in human cells, not mouse cells. *Lau and David* support the hypothesis that the cGAS-STING pathway may be implicated. In practice, cytoplasmic chromatin fragments in senescent human IMR90 fibroblasts accumulate outside the nucleus and contribute to SASP initiation (*Ivanov et al., 2013*). Moreover, these fragments are known to be sensed by cGAS-STING (*Dou et al., 2017*), which activation for some authors is responsible for senescence initiation, and for others, despite not activating senescence, still influences SASP production (*Yang et al., 2017; Gluck et al., 2017*). Finally, it is also known that chromatin fragments trigger a type 1 interferon (IFN) response, damage-associated molecular patterns, as well as the inflammasome (*Acosta et al., 2013, Davalos et al., 2013, Li and Chen, 2018*). Regarding the latter, the activation of the inflammasome triggers IL-1 production, which could further support *Lau and David*'s hypothesis. This may be one possible explanation for why IL-1 production occurs independently of NF-κB activation.

Regarding other cytokines, IL-6 is one of the most prominent ones in the SASP. It is secreted after genotoxic stress-induced or oncogenic-induced senescence in a variety of mouse and human cell types, such as epithelial cells, fibroblasts, melanocytes, keratinocytes, and monocytes (*Sarkar et al., 2004; Lu et al., 2006; Coppé et al., 2008; Kuilman et al., 2008*). As mentioned before, both NF-κB signaling and IL-1 signaling can induce its transcription. IL-6 regulates different cellular processes, such as proliferation, differentiation, survival, and function of multiple cell lineages. High levels of this cytokine are correlated with chronic inflammation, immune pathologies, and cell/tissue aging (*Gabay 2006; Ishihara and Irano, 2002; Maggio et al., 2009*).

Tumor Necrosis Factor-alpha (TNFα) is also a common cytokine in the SASP. It is one of the key molecules for inflammation, first discovered to be produced by monocytes and

macrophages, albeit other cell types can produce it in particular circumstances, such as lymphocytes, natural killer cells, neutrophils, and fibroblasts (*Grivennikov et al., 2005*). TNFα by itself is a transmembrane protein termed mTNF, while ADAM17 is responsible for the cleavage and production of soluble TNF named sTNF, which is released in the blood plasma (*Black et al., 1997*). The two TNF forms perform different cellular functions: sTNF binds its receptor TNFR1, which is mostly present in immune cells, while mTNF binds TNFR2, expressed in all human tissues, and induces a potent cell signaling cascade (*Eissner et al., 2004*). Both signals can activate NF-κB downstream (*Pimentel-Muiños and Seed, 1999*). Although TNF is a pivotal molecule in different immune responses against bacterial or viral pathogens (*Luo et al., 1993; Herbein and Brien, 2000*), its upregulation is also involved in many inflammatory pathologies, such as sepsis induced by LPS, auto-immune diseases, and neurodegenerative diseases (*Jang et al., 2021; Frankola et al., 2011*). The name Tumor Necrosis Factor was given because of the molecule's ability to exercise anti-tumoral activity in a previous mouse model of sarcoma (*Carswell et al., 1975*). At the same time, there is increasing evidence of TNFα exercising a pro-tumoral and pro-metastatic role in different types of cancers (*Mercogliano et al., 2020*). TNFα signaling plays a pivotal role in senescence since its pathway is upregulated after DDR activation in senescent cells (*Rodier et al., 2009*). More recently, TNF proved to be a key molecule for paracrine senescence in an OIS (BRAFV600E) model of hematopoietic stem cell transplantation *(Biavasco, Lettera, et al., 2021*). The treatment of mice with infliximab, a monoclonal antibody against TNFα admittedly reduced SASP production and ameliorated inflammation, further confirming the key role of this cytokine in SASP after OIS induction.

Another family of pro-inflammatory factors present in the SASP is chemokines. The most frequent ones are IL-8 (CXCL8), GROα, and GROβ (CXCL-1,-2) (*Reinhard et al., 2020; Castro et al., 2003; Bode-Böger et al., 2005*). Other chemokines often upregulated in senescence are part of the CCL family, such as MCP-1 (CCL2), and macrophage inflammatory proteins MIP3α and -1α (*Coppé et al., 2010*)

The interaction between senescent cells and the tissue microenvironment is also regulated by growth factor signaling. The insulin-like growth factor binding proteins, such as IGFBP-2,-3-4,-5,-6,-7, are often upregulated in senescent fibroblasts, epithelial or endothelial cells (*Coppé et al., 2008; Wang et al., 1996; Grillari et al., 2000*). When IGFBPs are secreted, they stimulate paracrine senescence in neighboring cells (*Wajapeyee et al., 2008*). Furthermore, colony-stimulating factors, such as GM-CSF and G-CSF are overexpressed and secreted by senescent fibroblasts (*Coppé et al., 2008*). Regarding the increased secretion of interferon, literature shows that cytoplasmic DNA signaling activated after senescence stimuli is able to induce the production and secretion of IFN type I (*Yang et al., 2017*). Secondly, a recent study reports that during cellular senescence, a retro-transposable element such as LINE-1, is de-repressed at the transcriptional level. Consequently, the retrotranscribed cDNA encoding for LINE-1 triggers a type I IFN response (*De Cecco et al., 2019*).

ECM proteins and extracellular proteases form a highly enriched subset of the SASP. SASP proteases perform degradation of ECM and cleavage of transmembrane proteins (for example, TNFα) which turns them into soluble factors. These functions can mold and change the microenvironment around senescent cells, thus contributing to either the clearance of senescent cells or the persistence of chronic inflammation. Some of the ECM proteases are MMPs. MMP-1, -3, and -10 are often upregulated in both mouse and human fibroblasts (*Liu and Hornsby 2003; Hornebeck and Maquart, 2003*). MMPs are responsible for the cleavage of different chemokines of the CXCL and CCL family (*Van Den Steen et al., 2003*), rendering them soluble factors and active parts of the SASP for paracrine senescence. Another implied family of proteases is collagenases, responsible for the breakdown of collagen present in the ECM. In the recent past, many ECM proteins, such as collagens I, III, IV, fibronectin, tenascins, and MMPs have been reported to be strongly downregulated in resistant retinoblastoma human cell lines (*Reinhard et al., 2020*), suggesting a positive role of the tumor suppressor Rb in the regulation of the signaling for their transcription.

Other proteases present in the SASP include serine proteases and proteins involved in coagulation, such as urokinase (uPA), tissue-type plasminogen activator (tPA), urokinase

receptor (uPAR) and their inhibitors, such as PAI-1 and PAI-2 (*Blasi and Carmeliet, 2002*). PAI-1 is a common SASP protein upregulated in aged donors too (*Mu et al., 1995; Mu et al., 1998; Martens et al., 2003*). uPAR is a cell surface receptor induced in different models of senescence that has recently become a potential candidate for the development of universal senolytics, namely because CAR-T cells against uPAR have been able to eliminate senescent cells specifically in different models of senescence-associated diseases, such as adenocarcinoma and liver fibrosis (*Amor et al., 2020*). Contrary to the previously held belief that the only function of uPAR was regulating plasmin in coagulation, uPAR is indeed involved in different cellular processes related to cancer, such as cell cycle regulation, cell adhesion, and cell migration. Thereby, uPAR effectively controls the shift from tumor dormancy to the second wave of tumor proliferation that commonly triggers the development of metastases by cross-talking with tyrosine kinase receptors. Interestingly, there is a direct correlation between the mutational burden in the Ras pathway and the overexpression of uPAR in non-small cell lung cancer and colorectal cancer patients (*Mauro et al., 2017*).

The cited molecules are not the only ones contributing to SASP: there is growing evidence on the importance of other molecules and cellular components, such as ATP (*Pini et al., 2021*), nucleotides and their metabolism (*Delfarah et al., 2019*), lipids (*Hamsanathan and Gurkar, 2022*), ROS (*Nelson et al., 2018*), micro RNAs (miRNAs) (*Panda et al., 2018*), small extracellular vesicles (sEVs) (*Borghesan et al., 2019*), mitochondria (*Martini and Passos, 2022*), and ribosome biogenesis (*Lessard et al., 2018*) in paracrine senescence.

1.3.2 The biological function and role of SASP

In literature, SASP has shown opposite roles: on one hand, it contains many factors that can attract the innate and adaptive immune system (*Hoare et al., 2016; Toso et al., 2014; Xue et al., 2007*), favoring the clearance of senescent cells. On the other hand, the double role that many SASP factors have in both inducing senescence but also inflammation correlated to tumors shows the detrimental side of the SASP.

From a biological standpoint, the actual function of senescent cells and the SASP has been debated for many years. As we already know, senescent cells are present during embryogenesis, and they also play a fundamental role in the correct human development before birth (*Storer et al., 2013*). Embryos of different species, such as mice, humans, birds, amphibians, and fish were observed to express a considerable amount of senescence markers (*Da Silva-Alvarez et al., 2019*). Besides, the process of senescence is also implicated in tissue regeneration, such as musculoskeletal, limb, heart, and liver regeneration (*Antelo-Iglesias et al., 2021*) and wound healing (*Demaria et al., 2014*). These functions are due to the interaction of senescent cells with their environment through SASP factors secretion since they both impair the proliferation of the damaged cells in the tissue while also inducing neighboring cells to regenerate by secreting SASP.

On the other side of the spectrum, senescent cells are known to accumulate in many tissues over time and to be more abundant in the elderly. Aged people are also more prone to develop inflammation, or rather the chronic inflammation which is typically found in aged individuals (*Lau et al., 2019*). Specific clearance of $p16^{Ink4a}$ -expressing cells has delayed the onset of age-related diseases in past work (*Baker et al., 2011*). Moreover, senescent pre-adipocytes treated with JAK inhibitors for the inhibition of SASP show significantly less inflammation in aged mice (*Biran et al., 2015*). In the context of hematopoiesis, and HSPCs transplant specifically, patients are usually treated with chemotherapy so that donor cells can engraft. In a transplant mouse model, the use of either irradiation or busulfan induced premature senescent in HSPCs in both cases (*Meng et al., 2003*), impairing their colony formation capacity and upregulating cell-cycle inhibitors, such as $p16^{Ink4a}$ and $p19^{ARF}$. Allogeneic HSPCs transplant patients also show accelerated T cell terminal differentiation and senescence and reduced peripheral T cell pool long-term. Given these results, the authors supported the hypothesis that long-term survivors of allogeneic HSPCs transplant are more susceptible to opportunistic infections due to senescence hampering a correct immune reconstitution (*Dougherty et al., 2017*).

Furthermore, there is the contradicting knowledge that many factors included in the SASP are also tumorigenic. The sustained secretion of ECM proteases, as well as growth factors,

induced the proliferation of malignant cells (*Ito et al., 2017; Lopes-Paciencia et al., 2019*). The cleavage of ECM proteins is also known to promote tumor migration and metastasis development (*Martínez-Zamudio et al., 2017*), as well as angiogenic factors often parts of the SASP (*Herranz and Gil, 2018*). In another study supporting these findings, senescent cell clearance in a pancreatic cancer mouse model reduced the neoplastic lesions (*Passos et al., 2010*). Nonetheless, in a mouse model of liver carcinoma, natural killer cells eliminated cancer cells thanks to the adjuvation of the SASP, a potential control mechanism against lesion development in the liver (*Zhuang et al., 2019*). This contradictory role of the SASP in tumor development could potentially be explained by the phenomenon of antagonistic pleiotropy (*Acosta et al., 2008*). Thus, senescence could have undergone positive selection in evolution because of the tumor-suppressive function it has in young cells and organisms. Instead, in processes such as aging, inflammatory diseases, or cancer, the harmful effects of SASP may outweigh its benefits.

1.3.3 The interaction between senescent cells and the immune system

The principal function of the release of SASP factors is to recruit immune cells so that they interact extensively with senescent cells (*Burton and Stolzing, 2018*). The clearance of senescent cells by the immune system was first observed in a hepatic tumor model (*Xue et al., 2007*). Interestingly, p53 activation, by inducing the secretion of chemokines such as MCP-1, or CCL2, can recall NK cells to eliminate senescent cancer cells (*Iannello et al., 2013*). SASP expression and immune cell recruitment are not merely dictated by transcriptional changes or alteration in the secretome but also by epigenetic regulation, since BRD4 can activate enhancers flanking SASP genes, resulting in enhanced immune clearance (*Tasdemir et al., 2016*). Immune cells that are recruited by SASP can be macrophages, dendritic cells, natural killer (NK) cells, neutrophils, and T cells.

Regarding macrophages, these innate immune cells are specialized in eliminating pathogens, such as bacteria, by recognizing pathogen-specific patterns, thus strongly involved during

infections (*Akira et al., 2006*). Macrophages can be divided into two different populations based on their phenotype: M1-like macrophages or M2-like macrophages. The M1 phenotype differentiates after specific stimuli, such as the secretion of IFNγ or lipopolysaccharide (LPS). M1-like macrophages, in turn, assist in eliminating pathogens with different mechanisms. These macrophages overexpress class II of major histocompatibility complex (*Boehm et al., 1997*) and produce nitric oxide (*MacMicking et al., 1997*). Furthermore, they secrete pro-inflammatory cytokines, such as IL-1β, IL-6, IL-8, TNFα, and other chemokines too (*Mills et al., 2017*). On the other hand, M2-like macrophages differentiate in response to IL-4 and IL-13 (*Hart et al., 1989*). These macrophages play a role in molding the microenvironment, by activating mechanisms of tissue repair and collagen production: they upregulate Arginase-1 to decrease nitric oxide production, as well as secreting IL-10, MMP12, CCL8, and CCL13 (*Hesse et al., 2001*). These changes could recruit basophils and eosinophils to ameliorate tissue damage after inflammation. The interplay between macrophages and senescent cells can be beneficial in some cases and deleterious in others. For example, after childbirth, senescent cells in the uterine stroma are efficiently cleared by macrophages (*Egashira et al., 2017*). Another work modeling chemical injury in the liver described the interaction between hepatic stellate cells and macrophages. During liver damage, hepatic stellate cells, through a p53-dependent senescent program, triggered the production of IL-6, ICAM, and IFNγ. The secretion of those cytokines promoted M1 polarization of macrophages, elimination of senescent cells, fibrosis reduction, and ultimately inhibited tumor development. The ablation of p53, on the other hand, prompted aberrant proliferation in hepatic stellate cells, the secretion of IL-3, IL-4, and IL-5, and overexpression of Mrc1 and Msr1, pointing towards M2-polarization and consequently favoring tumor development (*Lujambio et al., 2013*).

The interaction between senescent cells and macrophages is not entirely understood yet. It is widespread knowledge that macrophages also play a role in inflammation, accumulate in the elderly, and express some senescence-associated markers, such as SA-B-Gal, $p16^{Ink4a}$, and others (*Franceschi et al., 2003; Liu et al., 2019; Hall et al., 2016*). Additionally, clearance of senescent macrophages displaying M2-like polarization ameliorates inflammation (*Hall*

et al., 2017). Moreover, senescent cells can alter cell surface markers that might aid or prevent their clearance. One of these is CD47, a signal often defined as a "don't eat me" signal that macrophages recognize by the regulatory protein SIRPα. CD47 forms a clustered pattern in the lipid membrane of healthy cells, in order not to be a target of macrophage phagocytosis. In apoptotic cells or red blood cells, this specific pattern is disrupted, promoting phagocytosis of damaged cells (*Lv et al., 2015; Khandelwal et al., 2007*). Senescent cells show changes in the lipid rafts in the membrane, potentially altering the CD47 pattern on the surface (*Fulop et al., 2012*). In addition, it has been reported that senescent lung fibroblast overexpresses CD47, thus favoring immune evasion (*Hernández-Mercado et al., 2021*), in a similar way to what happens in cancer cells (*Takimoto et al., 2019*).

Dendritic cells also interact with senescent cells, with their antigen presenting role. In fact, dendritic cells can assemble antigens from pathogens and present them to B and T cells, in order to adjuvate immune response and clearance. With this function, they can enhance the elimination of senescent cells through the induction of NK and T cells (*Rahman and Aloman, 2013*). On the other hand, dendritic cells may also exacerbate chronic inflammation and immune suppression, favoring the resilience of senescent cells (*Bantsimba-Malanda et al., 2010*). Indeed, they play a role in the maturation of naïve CD4+ T cells into immunosuppressive regulatory T cells (*Kushwah and Hu, 2011*), as well as in the induction of T-cell senescence (*Ye et al., 2012*) similarly to what happens in the tumor microenvironment.

Natural killer (NK) cells are another significant immune cell type for immune clearance. NK cells respond to internal inflammation or external pathogens by interaction with toll-like receptors (TLRs) (*Sivori et al., 2014*), often overexpressed by senescent cells (*Shaw et al., 2013*). Studies on liver damage models have shown that senescent hepatic stellate cells can recall NK cells by secreting ECM proteins which activate NK receptors such as NKG2D and DNAM1 and limit fibrosis (*Krizhanovsky et al., 2008*). $CD8^+$ T cells also express the receptor NKG2D and are therefore able to similarly perform granular exocytosis (*Sagiv et al., 2013*). $CD4^+$ T cells, on the other hand, can be polarized with the same cytokine stimuli of macrophages, with the Th1-like profile producing pro-inflammatory cytokine, while the Th-

2-like profile secretes IL-4 and TGF-β, which are responsible for the downregulation of NKG2D in both NK and $CD8^+$ T cells. Thus, Th2 cells play an immunosuppressive role, while Th1 cells promote the immune response (*Kidd, 2003*). Interestingly, in a model of oncogene-induced tumors in the liver, hepatocytes first developed senescence, secreting SASP factors that attracted $CD4^+$ T cells and macrophages but not $CD8^+$ T cells and NK cells, suggesting that the former cell types play a larger role in the clearance of oncogene-induced senescent cells (*Kang et al., 2011*).

Overall, senescent cells interact intensely with immune cells to either endorse their elimination or, in some cases, promote immune evasion. In this regard, the nature of the SASP produced by senescent cells is pivotal to shaping both macrophages and CD4+ T cells toward an immune-promoting or immunosuppressive role.

1.4 BRAF V600E, oncogene-induced senescence and its enrichment in three rare hematological malignancies

Circa 8% of cancers display mutations in the BRAF gene, among which 60% of melanomas, 40% of thyroid cancers, 27% of ovarian cancers, 12% of colorectal cancers, and 3% of other cancer types (*Davies et al., 2002*). The BRAF gene is a proto-oncogene encoding for the serine/threonine-protein kinase B-Raf (*Sithanandam et al., 1990*). As previously mentioned, BRAF encodes for a signal transduction kinase, part of the RTK pathway, the MAPK/ERK pathway particularly, involved in cell division, growth, and survival (*McCain 2013*). The mechanism of action involves a growth factor binding an RTK, auto-phosphorylation of this receptor, and the triggering of RAS, RAF, MEK, and ERK phosphorylation cascade, in this order. Membrane-bound RAS-GTP recruits RAF and activates it (*Leevers et al., 1994*). RAF proteins are a family of kinases composed of ARAF, BRAF, and CRAF, and each of them has a similar structure, constituted by three conserved domains (CR) (**Figure 1.5**). CR1 is bound by active RAS (RAS-GTP) and a cysteine-rich domain, representing the regulatory domain of the protein, CR2 links CR1 with a serine-rich domain, while CR3 contains the P-loop, the catalytic portion of the kinase and the activation loop. The P-loop notably binds the activation loop, constituted of an ATP-binding domain, to stabilize the phosphate group of ATP so that the protein can form a fork-like structure (*Zaman et al. 2019*). Dimerization and phosphorylation of RAF family members are fundamental for their activation since BRAF and CRAF can both form homodimers and heterodimers (*Weber et al., 2001*). Mutations in BRAF usually cluster in the gene region coding for the P-loop and the catalytic portion between exon 11 and 15. The most frequent one (90%) is the V600E mutation, which substitutes glutamic acid for valine, disrupting the interaction between the P-loop and the activation domain, and thus constitutively activating the kinase domain of Braf (*Pratilas et al., 2012; Wan et al., 2004*).

In the context of the hematopoietic system, mutated BRAFV600E is found infrequently in liquid tumors, such as leukemia or lymphoma. However, it is enriched in three rare

hematological malignancies: Hairy Cell Leukemia, Langerhans Cell Histiocytosis, and Erdheim-Chester Disease (*Abdel-Wahab and Park, 2014*).

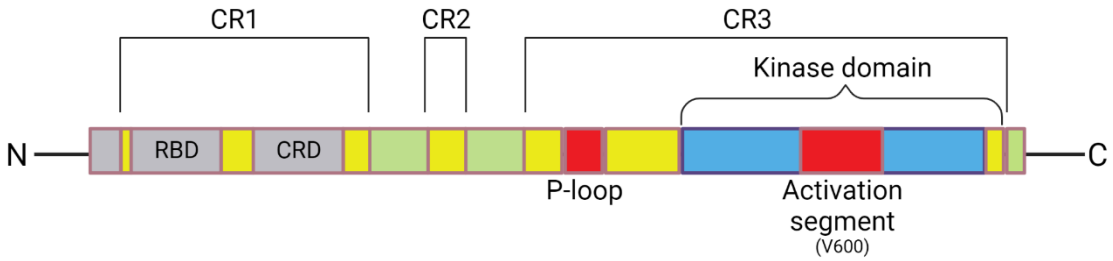

Figure 1.5 Representation of the conserved regions in the BRAF protein. *Red bars represent the two domains (Activation segment and P-loop) that interact with each other, which interaction is disrupted by the V600E mutation. Image generated with Biorender.*

1.4.1 Langerhans Cell Histiocytosis, Erdheim-Chester Disease, and Hairy Cell Leukemia: three rare BRAFV600E hematological malignancies

Hairy Cell Leukemia (HCL) is a rare B-cell leukemia, constituting 2% of all leukemias, with a chronic nature. Its frequency is in 1 every 100.000 individuals and targets males 4-5 times more frequently than females. Nearly 100% of HCL patients display the BRAFV600E mutation (*Tiacci et al., 2011*). The term "hairy" was given because of the morphological features that leukemic B-cells develop, which were later proven to be BRAF and MEK independent as their pharmacological inhibition reverted the HCL gene expression and morphological profile to normal (*Tiacci et al., 2015*). HCL leukemic cells show a mature B-cell phenotype, with the expression of CD19, and surface immunoglobulins, and can perform rearrangements of the heavy and light chain immunoglobulin genes (*Forconi et al., 2001; Maloum et al., 1998*). Nevertheless, HCL cells also show atypical markers, such as CD103, usually expressed in T cells (*Janik 2011*), and CD11c, a common marker of monocytes (*Juliusson et al., 1994*). HCL B-cells proliferate abnormally in the BM, preventing other hematopoietic cells from correctly differentiating and developing. As a result, HCL patients usually present low white blood cell count, making them more prone to infections, low platelet count, anemia, splenomegaly, and low lymph node involvement (*Polliack 2002*). A

seminal work in the field (*Chung et al., 2014*) investigated the cell of origin of HCL and discovered that HSCs of HCL patients displayed alteration in the generation of the progenitors, in particular skewing hematopoiesis towards abnormal B cell production. Moreover, variant allele frequency analysis in HSCs of HCL patients showed a 4.7% frequency of the BRAFV600E mutation. Expressing BrafV600E in mouse HSPCs resulted in mouse lethality, splenomegaly, and increased secretion of CD25, a common biomarker of HCL. Two considerations derive from this experiment: the first one is that the V600E mutation, for leukemia to develop, is required at a precursor stage, stem or progenitor, since BrafV600E expression restricted to only mature B cells did not produce a pathological phenotype. Secondly, only a small fraction of HSCs in HCL patients carries the V600E mutations, meaning that only a small portion of stem cells carrying the mutation is needed for leukemia development. Treatment of mice with Vemurafenib, a monoclonal antibody specific against BRAFV600E, resulted in amelioration of the phenotype, with erythroid and myeloid cells returning to normal counts and anemic symptoms emerging at later time points. This suggests that the elimination of mutated cells results in the reverse of the HCL phenotype. The gold standard for HCL is chemotherapy using purine analogs, which is successful in 95% of the patients. Five years after the therapy, however, half of the patients suffer from relapse, depending on their risk assessment. Splenomegaly, leukocytosis, hairy cells, and high levels of circulating beta-2 micro-globulin are associated with bad prognosis, as well as CD38 expression and mutations in the IGHV gene (*Maitre et al., 2019*). Interestingly, poor prognosis has been also correlated with telomere length in patients' cells (*Arons et al., 2011*). The second line of treatment involves either the second cycle of purine analogs or BRAF-specific inhibitors such as vemurafenib. Treatment with vemurafenib is successful with refractory patients non-responding to chemotherapy (*Tiacci et al., 2021*), although there are issues regarding the long-term adverse effect correlated to vemurafenib administration, such as skin integrity and the possibility of developing skin tumors (*Tham et al., 2022*).

Langerhans Cell Histiocytosis (LCH) and Erdheim-Chester Disease (ECD) are both hematological malignancies belonging to a broader family of rare disorders called

histiocytoses. Histiocytoses are all characterized by the abnormal infiltration of macrophages or dendritic cells in one or multiple organs or tissues (*Haroche et al., 2017*). LCH is distinguished between childhood and adult LCH while ECD occurs in adulthood. The incidence of childhood LCH amounts to 5-9 per million individuals (*Guyot-Goubin et al., 2008*), while adult LCH occurs in 0.07 per million individuals, although reports admit that this frequency is likely underestimated (*Goyal et al., 2018*). The frequency of ECD in the population is still unknown, with a prevalence of targeting patients with a median age of 55 years and males (73% of ECD cases) (*Cohen-Aubart et al., 2018*). Symptoms in LCH include bone fracture, lymphadenopathy, hepatosplenomegaly, diabetes insipidus, and others, depending on how many organs are affected by macrophage infiltration. ECD complications happen earlier and often involve the cardiac tissue and the central nervous system (CNS), while the involvement of the CNS is a late effect in LCH (*Emile et al., 2021*). This leads to ECD patients progressively developing neurodegeneration, with cognitive and behavioral impairment (*Haroche et al., 2017; Cohen-Aubart et al., 2014; Euskirchen et al., 2015*). After the emergence of symptoms, patients are diagnosed with either LCH or ECD firstly by assessing macrophage or dendritic cell infiltration in tissues, using the markers CD68 and CD163, and then the expression of the typical Langerhans Cell markers is assessed, using CD1a and CD207 (*Chu et al., 1987*). The driving causes of histiocytoses began to be unraveled when the first evidence of a BRAFV600E mutation in LCH patients was reported (*Badalian-Very et al., 2010*). Afterward, multiple studies confirmed the presence of BRAFV600E macrophages infiltrating the tissues of LCH patients (*Satoh et al., 2012; Haroche et al., 2012; Go et al., 2014*). In 90% of histiocytic patients, mutations involve at least one gene belonging to the MAPK pathway, with 60% of them carrying the BRAFV600E mutation (*Halbritter et al., 2019; Emile et al., 2014).* Other mutated genes are RAS genes or tyrosine kinase receptor genes (*Durham et al., 2019*). This, coupled with the previous notion that LCH showed clonality in patients (*Yu et al., 1994*), demonstrated that histiocytoses had neoplastic features. As with HCL, efforts have been made to understand the cell of origin of histiocytosis. Past studies have highlighted that BrafV600E expression in myeloid progenitor cells can induce a histiocytosis-like phenotype in mice (*Berres et al., 2014, Nelson et al., 2019).* One of these studies described BRAFV600E mutations in childhood LCH patients in

both monocytes and $CD34^+$ bone-marrow-derived cells, implying that histiocytosis may be a result of skewed hematopoiesis towards the myeloid lineage, resulting in exacerbated macrophage infiltration in tissues (*Berres et al., 2014*). Moreover, ECD patients are known to be more susceptible to myelodysplasia, myeloproliferative neoplasms, and leukemia development (*Papo et al., 2017; Ghobadi et al., 2019*).

Treatment of LCH usually involves chemotherapy as the first line of treatment (either vinblastine or cytarabine), while ECD patients are treated with IFN-alpha. As a second-line treatment, or for patients with risk organ involvement, vemurafenib or MEK inhibitors are currently employed (*Emile et al., 2021*). Vemurafenib was employed in the treatment of BRAFV600E hematopoietic malignancies after the successful results that were obtained in the treatment of BRAFV600E-specific melanomas, approved by the FDA in 2011 (*Chapman et al., 2011*). The V600E mutation is the most frequent BRAF variant, nevertheless, truncated forms of BRAF can also be found in different human cancers (i.e. thyroid carcinoma, melanoma, and prostate and gastric cancer), as a result of translocations or microdeletions (*Botton et al., 2019; Palanisamy et al., 2010*). Interestingly, melanoma cells in vitro have demonstrated resistance to vemurafenib through an aberrant splicing mechanism. This alteration generated a truncated form of BRAFV600E, lacking exons 4-8, the CR1 region bound by RAS for BRAF activation. The truncation of the protein enhances dimerization independently of RAS activation levels when compared to full-length BRAFV600E (*Poulikakos et al., 2011*). So far, this type of variant has not been characterized in ECD or LCH, although histiocytic and HCL patients are known to relapse multiple times since residual BRAFV600E cells have been reported to persist even after treatment with vemurafenib (*Tiacci et al., 2015; Donadieu et al., 2019*).

1.4.2 BRAFV600E and oncogene-induced senescence in HSPCs

As previously mentioned, OIS emerged as a protective cellular mechanism against the aberrant proliferation and tumor development (*Serrano et al., 1997*). Afterward, BRAFV600E-induced senescence has been described in human naevi, benign tumors which frequently carry the mutation and develop with an initial cell cycle progression and growth, followed by an arrest. The authors characterized naevi as senescent melanocytes carrying the V600E mutation, positive for SA-B-Gal staining and $p16^{Ink4a}$ expression (*Michaloglou et al., 2005*). BRAFV600E melanocytes did have an initial burst of proliferation, followed by cell cycle arrest, without telomere erosion, suggesting that senescence in naevi is strictly oncogene-dependent and not due to exhaustion in replication. A few years later, in experiments involving a mouse model lung tumor, authors highlighted BrafV600E-induced cell cycle arrest as protection against adenocarcinoma progression (*Dankort et al., 2007*). In the following years, ongoing studies concentrated on the role of BRAFV600E-induced senescence in solid tumors. In the context of hematopoiesis, the link between BRAFV600E and OIS started to be explored in 2014, when it was discovered that a small fraction of monocytes collected from ECD patients carried the BRAFV600E mutation, expressed activated MAPK/ERK proteins, and expressed the senescence marker $p16^{Ink4a}$ (*Cangi et al., 2015*). Moreover, it was already known that both ECD and LCH patients display elevated secretion of the following cytokines: IL-1, IL-6, IL8, CCL2, CCL5, and TNF-α (*Kannourakis and Abbas, 1994; Arnaud et al., 2011; Ferrero et al., 2014*). This abnormal cytokine production already resembled the context of senescence and the development of SASP. Furthermore, the involvement of the CNS in ECD and LCH resembles the induction of senescence occurring in neurodegenerative diseases (*Martinez-Cue and Rueda, 2020*).

In 2021, our group published results concerning a humanized mouse model, in which human HSPCs ($CD34^+$ cells) were transduced with a lentiviral vector for the expression of human BRAFV600E and were transplanted into immune-deficient NOD.Cg-$Prkdc^{scid}Il2rg^{tm1Wjl}$/SzJ (NSG) mice. All mice transplanted with BRAFV600E-expressing HSPCs succumbed due to BM failure. This hematopoietic phenotype showed impairment in total hematopoiesis (both mouse and human), impacting more aggressively on the lymphoid output, such as B cells,

thus generating an unbalance toward the myeloid compartment. The B cell impairment affected both oncogene-expressing and bystander cells, suggesting that paracrine senescence was occurring. Indeed, mice succumbed due to the onset of oncogene-induced-senescence, characterized by augmented levels of cell cycle inhibitors ($p16^{Ink4a}$; p21), DDR, and secretion of pro-inflammatory cytokines, among which TNFα, IL-1α, IL-1β, and MCP-1 were the most prominent and inversely correlated with mice survival. TNFα was specifically the key molecule inducing paracrine senescence and myeloid skewing, as its inhibition with a specific monoclonal antibody, i.e. infliximab, was able to partially reduce inflammation, prolong survival and partially restore the hematopoietic output. Gene expression analysis on sorted BRAFV600E-expressing and bystander myeloid ($CD33^{+}$) cells confirmed a shared transcriptional program between the two cell populations, and endorsed, at the same time, the pivotal role of TNFα signaling in the induction of inflammation. Histopathological evaluation of mice highlighted the presence of histiocytic lesions in multiple non-hematopoietic organs, especially the lungs, characterized by infiltration of inflammatory macrophages expressing BRAFV600E and $p16^{Ink4a}$. Altogether, this work was seminal in establishing the link between the induction of OIS in HSPCs and the onset of systemic inflammation characteristic of histiocytosis (*Biavasco, Lettera et al., 2021*).

In the same year, another collaborative work was published, showing how BRAFV600E expression in ECD activates trained immunity, leading to an alteration of several metabolic processes typically activated in response to pathogens. These changes include increased cytokine production and secretion, AKT signaling, glycolysis, glutaminolysis, and cholesterol synthesis. (*Molteni et al., 2021*). In the same year, Merad's group published another work, specifically linking BRAFV600E-induced senescence in human and mouse multipotent hematopoietic progenitor cells with Langerhans Cell Histiocytosis onset. The phenotype was characterized by growth arrest, resistance to apoptosis, and the SASP onset. Finally, specific senolysis of senescent cells ameliorated LCH symptoms in mice (*Bigenwald et al., 2021*). Regarding HCL, it is not known whether there is a possible link between BRAFV600E-induced senescence and its symptoms. Nevertheless, HCL cells can show anti-apoptotic behavior that can be reverted by BRAF inhibitors, since HCL cells treated with

vemurafenib become more susceptible to apoptosis (*Tiacci et al., 2017*). Nonetheless, the principal cell cycle inhibitor implicated in HCL, such as p27, is silenced in 100% of the patients, either by genetic disruption or reduction of gene expression (*Dietrich et al., 2015; Chilosi et al., 2000*). Moreover, KLF2, a gene carrying a loss of function mutations in circa 20% of HCL patients, encodes for a transcription factor regulating CDKN1a/p21, thus potentially inhibiting the expression of this cell cycle inhibitor (*Taniguchi et al., 2012; Wu et al., 2004*). KLF2, interestingly, has been reported to be a negative regulator of NFκB (*Das et al., 2006*), coherently with the fact that HCL patients show upregulation of NFκB signaling (*Nagel et al., 2015*), a key regulator of SASP, as previously mentioned. Altogether, these recent papers established OIS as a leading cause of the inflammation and complications present in LCH and ECD patients, opening the way for advanced treatments in the future.

2. Aim of the work

During this project, we were interested in studying the impact of the immunological condition of the host on the clearance or persistence of senescent cells. The previous humanized model has shown us that oncogene-expressing cells induce transcriptional reprogramming, which involves both hBRAFV600E cells and bystander cells. However, this reprogramming was specific to an immune-deficient humanized model. We hypothesize that, in an immune-competent context, gene expression could alter. Since the clearance of senescent cells greatly depends on the efficiency of the immunological system, we aimed to investigate the behavior and fate of oncogene-expressing senescent cells and their impact on hematopoiesis in the presence or absence of an active recipient immune system. The identification of transcriptional changes in persisting senescent cells in different genetic and immunological conditions could provide valuable molecular targets for their elimination. Thus, we expressed oncogene mBrafV600E or mBraf trunc in mouse hematopoietic stem and progenitor cells (HSPCs) transplanted into either immune-deficient or immune-competent recipients.

Although donor cells were collected from immune-competent donor mice, we hypothesized that the transplantation into immune-deficient mice would render them tolerant towards senescent cells, thus impairing their clearance. Thus, gene expression of the immune-deficient model would highlight the mechanisms of immune suppression toward the clearance of senescence. Additionally, by comparing the immune-deficient system with the humanized model, we could potentially identify differences and similarities between mouse and human senescence mechanisms.

On the other hand, an immune-competent recipient system represents a fundamental barrier against tumorigenesis. Therefore, we reasoned that an efficient immune system either would counteract senescent cells completely or that a small fraction of oncogene-expressing cells might persist over time. In that case, since the accumulation of senescent cells has been involved in an increased risk of cancer, our purpose would be to characterize the specific changes that occur in senescent cells resistant to immunological clearance.

3. Results

3.1 Experimental strategy

In practical terms, the focus of our work was to model OIS in immune-deficient or immune-competent mice. We reasoned that the use of these two models would highlight differences in multiple phenotypes: survival, hematopoietic output, cytokine secretion, and transcriptional alterations. To achieve this multi-faceted characterization, we transduced mouse HSPCs purified from the BM of donor C57BL/6 (C57) mice with a 3rd generation lentiviral vector expressing mBraf trunc, mBrafV600E, or only GFP (PGK.GFP) as a control. Transduced cells were transplanted into either lethally irradiated immune-competent C57 mice or sub-lethally irradiated immune-deficient NSG mice. One-month post-transplant we evaluated peripheral blood (PB) composition through Fluorescence Associated Cell Sorting (FACS) analysis, levels of the secreted factors in the plasma and we performed RNA-sequencing on sorted myeloid and B cells to assess gene expression perturbations. When the animals reached a severe disease-like state, we euthanized them and perform FACS analysis on the spleen and the bone marrow (BM).

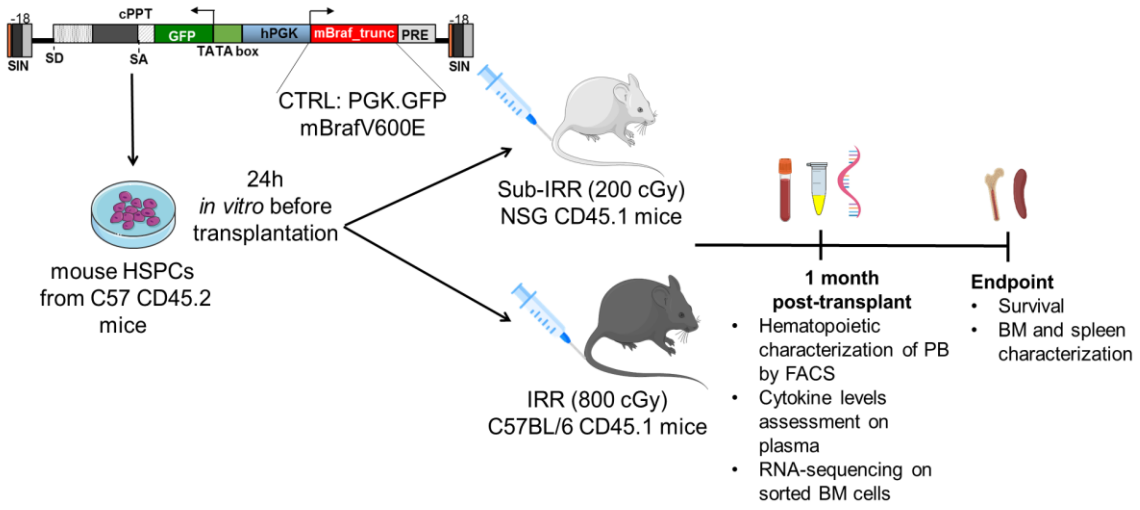

Figure 3.1. Experimental strategy for the project.

3.2 mBraf trunc expression in mouse HSPCs transplanted into NSG mice confers selective advantage to B cells.

For this project, we set out to perform our experiments in a complete murine system. Thus, we generated a bidirectional lentiviral vector (LV), expressing a constitutively active form of mouse Braf (lacking the regulatory N-terminal domain) and GFP (LV.mBraftrunc). This oncogenic truncated form was selected because it is involved in histiocytic sarcoma formation in *Cdkn2a*$^{-/-}$ mice as a result of LV or transposon-mediated insertional mutagenesis (*Cesana et al., 2014b; Collier et al., 2005; Keng et al., 2009; Montini et al., 2009; Ranzani et al., 2013*). Moreover, truncated forms of BRAF are found in a wide variety of human cancers, i.e. thyroid carcinoma, melanoma, and prostate and gastric cancer, as a result of translocations or microdeletions (*Botton et al., 2019; Palanisamy et al., 2010*). We transduced mouse HSPCs with LV.mBraf trunc or an LV expressing mBraf WT as control, at a specific MOI to reach transduction levels of 30%. Cells were transplanted into sub-lethally irradiated (*200 cGy*) NSG mice. Animals were monitored over time and Fluorescence Activated Cell Sorting (FACS) was performed on peripheral blood (PB) samples at 4, 8, and 24 weeks, following lineage composition markers: GFP for transduction, CD45.1 for engraftment, CD11b for myeloid cells, B220+ for B cells and CD3 for T cells. (**Figure 3.2a**). Firstly, we decided to observe the first phases of hematopoietic reconstitution by analyzing the major hematopoietic compartments at days 6, 9, 15, and 24 post-transplant. These time points were chosen to have a direct comparison with the time-course experiments performed in the previous humanized model (*Biavasco, Lettera et al. 2021*). We analyzed PB, BM, and spleen by FACS to determine engraftment, transduction levels, and lineage composition. Curiously, mice from the mBraf trunc group showed an expansion of vector-marked B cells in all of the major hematopoietic organs (**Figure 3.2b**). We also studied the long-term outcomes of mBraf trunc expression on hematopoiesis. Firstly, the selective advantage of mBraf trunc-B cells, when compared to mBraf WT expressing B cells, was also present in absolute counts 4 weeks post-transplant (**Figure 3.2c**). Moreover, percentages of engraftment in the mBraf trunc group lowered over time, until reaching a significant reduction at 22 weeks post-transplant (**Figure 3.2d**). Finally, the survival curve of mBraf trunc mice, compared to

their controls, slightly differs at the limits of significance (p=0.0532) (**Figure 3.2e**). These data suggest that mBraf trunc expression in mouse HSPCs results in the expansion of oncogene-expressing B cells, as opposed to the humanized model, in which lymphoid cells were strongly impaired in a matter of days post-transplant. However, the expression of this oncogene form in mouse HSPCs might not completely neutral, as it lowered the percentages of engraftment over time and slightly impacts the survival of recipient mice. Thus, mBraf trunc might negatively impact hematopoiesis more in the long term.

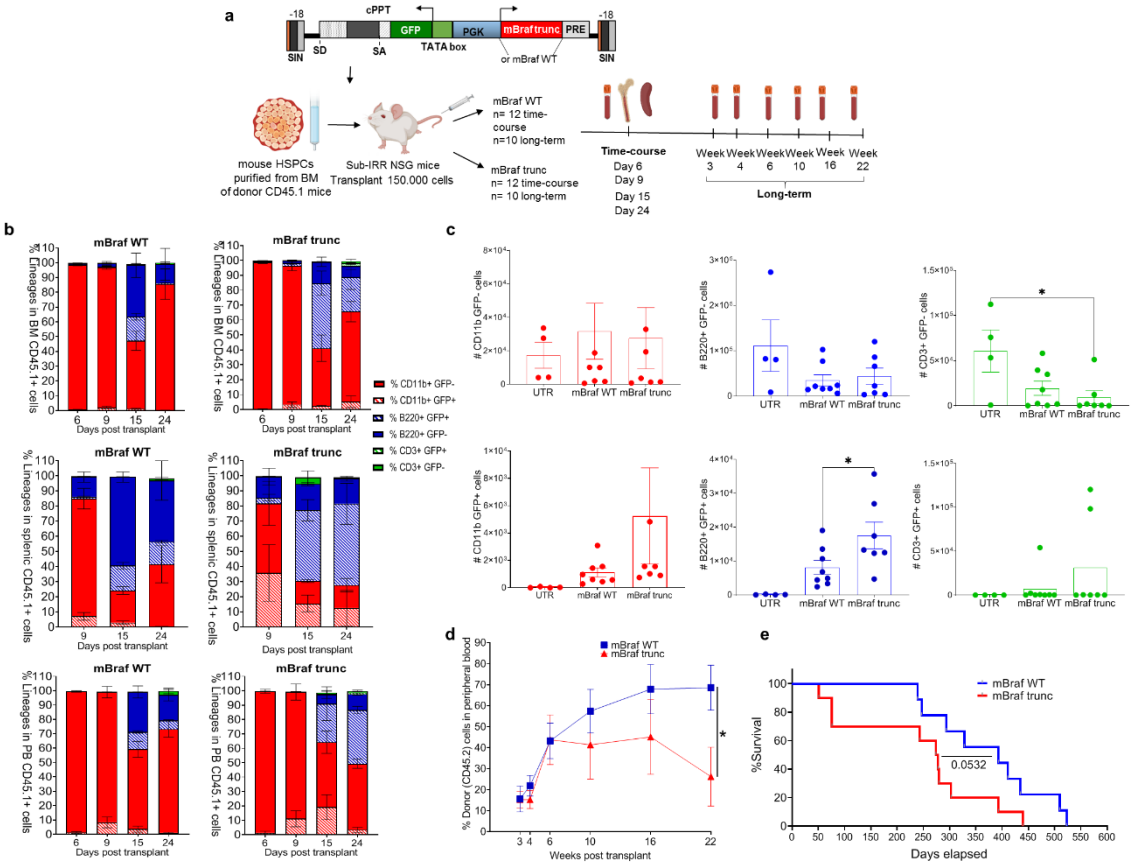

Figure 3.2. mBraf trunc expression in mouse HSPCs shows selective advantage of oncogene-expressing B cells. *(a) Experimental plan for the mBraf trunc experiments. (b) FACS analysis on BM, PB and spleen of NSG mice transplanted with HSPCs, transduced with a LV expressing mBraf WT or mBraf trunc. Mice were euthanized at 6, 9, 15 and 24 days post-transplant. BM, PB and spleen were collected and lineage composition was assessed. (c) Absolute counts on Myeloid, B and T cells (GFP+ and GFP-) of the mBraf trunc experiment. (d) Levels of engraftment of NSG mice of the mBraf trunc experiment over time (3, 4, 6, 10, 16, 22 weeks post-transplant). (e) Survival curve of mBraf trunc and mBraf WT mice. For statistical analysis, I performed One-way Anova through Prism. Asterisks represent significance in the p value: * < 0.05; ** < 0.01; *** < 0.001; **** < 0.0001.*

3.3 mBrafV600E expression in mouse HSPCs transplanted into NSG mice impairs cellularity and results in dose-dependent lethality

The unexpected selective advantage of oncogene-expressing B cells in mBraf trunc mice led us to hypothesize whether the contrasting results between our data and the previous humanized model were attributable to differences between mouse and human biology or due to differences between mutations. To answer this, we transplanted NSG mice with HSPCs transduced with LV expressing either GFP as control, mBraf trunc, or mBrafV600E (**Figure 3.3a**). FACS analysis on PB collected one month post-transplant showed comparable percentages of engraftment and transduction levels, with mBrafV600E mice to be potentially divided into two groups above or below 30% of transduction levels (**Figure 3.3b**). Absolute count analysis on PB revealed a decrease in total cellularity in mBrafV600E mice compared to PGK.GFP controls, which involved both donor and recipient cells. Of note, total cellularity was significantly reduced also in mBraf trunc mice, although less prominently than mBrafV600E mice, suggesting that mBraf trunc has a milder effect (**Figure 3.3c**). Additionally, we observed a lethal phenotype: indeed, 75% of mBrafV600E mice died within the first 40 days after transplant, while only two mBraf trunc mice died during this timeframe. Mice with a percentage of mBrafV600E-expressing cells in PB higher than (>) 30% died before 37 days post-transplant, while mBrafV600E mice with less than (<) 30% of transduced cells show a slower drop in the survival curve (median survival 33 days vs 44 days, p= 0.0307 *) suggesting that mBrafV600E expression results in dose-dependent lethality (**Figure 3.3d**). On the other hand, mBraf trunc mice also show a slight, but not significant, dose-dependent effect. The survival comparison between mBrafV600E > 30% mice with mBraf trunc > 30% mice shows a more rapid decline of the mBrafV600E group (median survival 33 days vs 136 days, p= 0.0364 *). A similar rapid decline is also observed in the mBrafV600E < 30% group when compared with the mBraf trunc < 30% group (median survival 44 days vs 176 days, p=0.0083 **). Although mBrafV600E expression resulted in strong and rapid lethality, its effect is slightly less pronounced compared to hBRAFV600E mice, which died even earlier (median 25.5 days, p<0.001 ***) despite the use of similar doses.

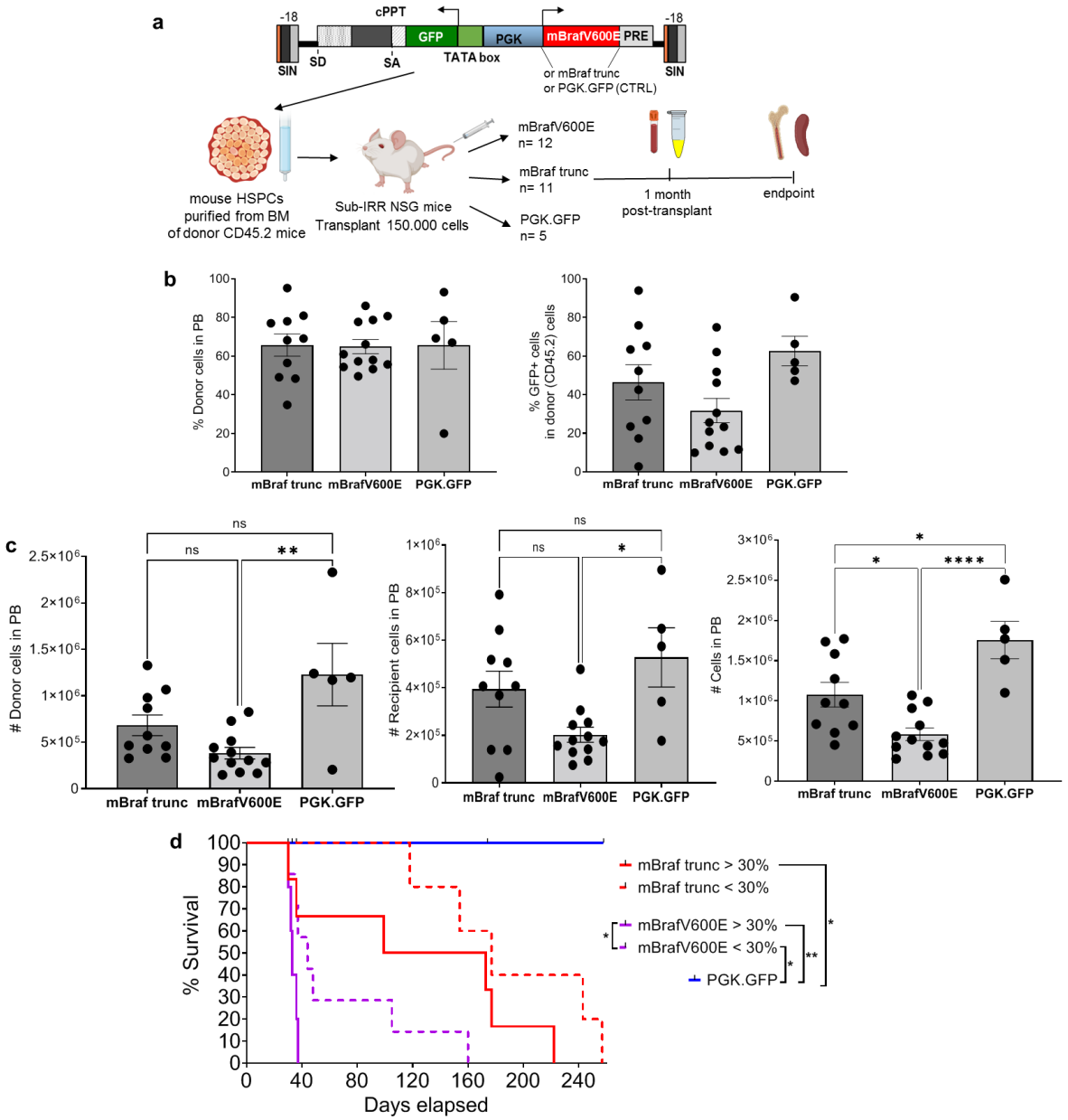

Figure 3.3 mBrafV600E expression in mouse HSPCs shows impairment in PB cellularity and dose-dependent lethality. *(a) Experimental plan for the mBrafV600E experiments. (b) Percentages of engraftment and transduction assessed through FACS analysis on mouse PB one-month post-transplant. (c) Absolute counts of donor (CD45.2), recipient (CD45.1) and total cells assessed through FACS analysis on mouse PB one-month post-transplant. (d) Survival curve of the mouse groups. Full lines of mBrafV600E and mBraf trunc mice represent groups with % of transduction higher than 30%, while dotted lines represent groups with % of transduction lower than 30%. Survival curve analysis was performed with GraphPad Prism, through the Log-rank (Mantel-Cox) test. For statistical analysis on cellularity, I performed One-way Anova through Prism. Asterisks represent significance in the p value: * < 0.05; ** < 0.01; *** < 0.001; **** < 0.0001.*

Hematopoietic characterization showed higher percentages of myeloid cells (36.93% vs 10.22%, p= 0.0265 *) and lower percentages of B cells in mBrafV600E mice compared to PGK.GFP controls (32.28% vs 60.18%, p=0.0149 *), thus displaying myeloid skewing (**Figure 3.4a**). Moreover, percentages of mBrafV600E cells directly correlated with percentages of myeloid cells and inversely correlated with levels of B cells in PB, suggesting that the higher the levels of oncogene expression, the higher the skewing toward the myeloid lineage (**Figure 3.4b**). This correlation was not observed in mBraf trunc mice, suggesting that this is a mBrafV600E-specific effect. Moreover, by distinguishing between oncogene-expressing (GFP+) and bystander (GFP-) cells, we observed a B and T cell impairment that is specific to only oncogene-expressing lymphoid cells, not bystander cells (**Figure 3.4c**). The impairment of only oncogene-expressing lymphoid cells differs from the one observed in the previously published humanized model, in which impairment affected both oncogene-expressing and bystander B cells. Myeloid cells in mBrafV600E mice, on the other hand, showed a tendency of higher levels of the un-transduced counterpart, while oncogene-expressing myeloid cells showed the same percentages as controls of mBraf trunc mice.

To further characterize the hematopoietic output, we performed an absolute count analysis, which slightly differs from the percentage analysis. The total number of myeloid cells in mBrafV600E mice does not differ from PGK.GFP controls ($1.09x10^5$ cells vs $1.16x10^5$, p=0.9593 ns), while we observe significant impairment in B cells ($6.90x10^4$ vs $8.02x10^5$, p=0.0094 **) and T cells numbers ($7.65x10^4$ vs $2.45x10^5$, p=0061 **) (**Figure 3.5a**). These results confirm that the observed myeloid skewing in the percentage analysis is not due to an expansion of myeloid cells but due to strong impairment of the lymphoid compartment. By distinguishing between oncogene-expressing (GFP+) and bystander (GFP-) cells, we also confirm that the impairment is specific to oncogene-expressing lymphoid cells, while untransduced B and T cells are not affected (**Figure 3.5b**). BM and spleen analysis of mBrafV600E mice confirmed impairment in total cellularity already observed in PB, again suggesting that mice succumbed to BM failure (**Figure 3.5c**). On the other hand, mBraf trunc mice showed a cellularity comparable to the controls. These results implying that the mild impairment of PB total cellularity, observed at one-month post-transplant, was rescued.

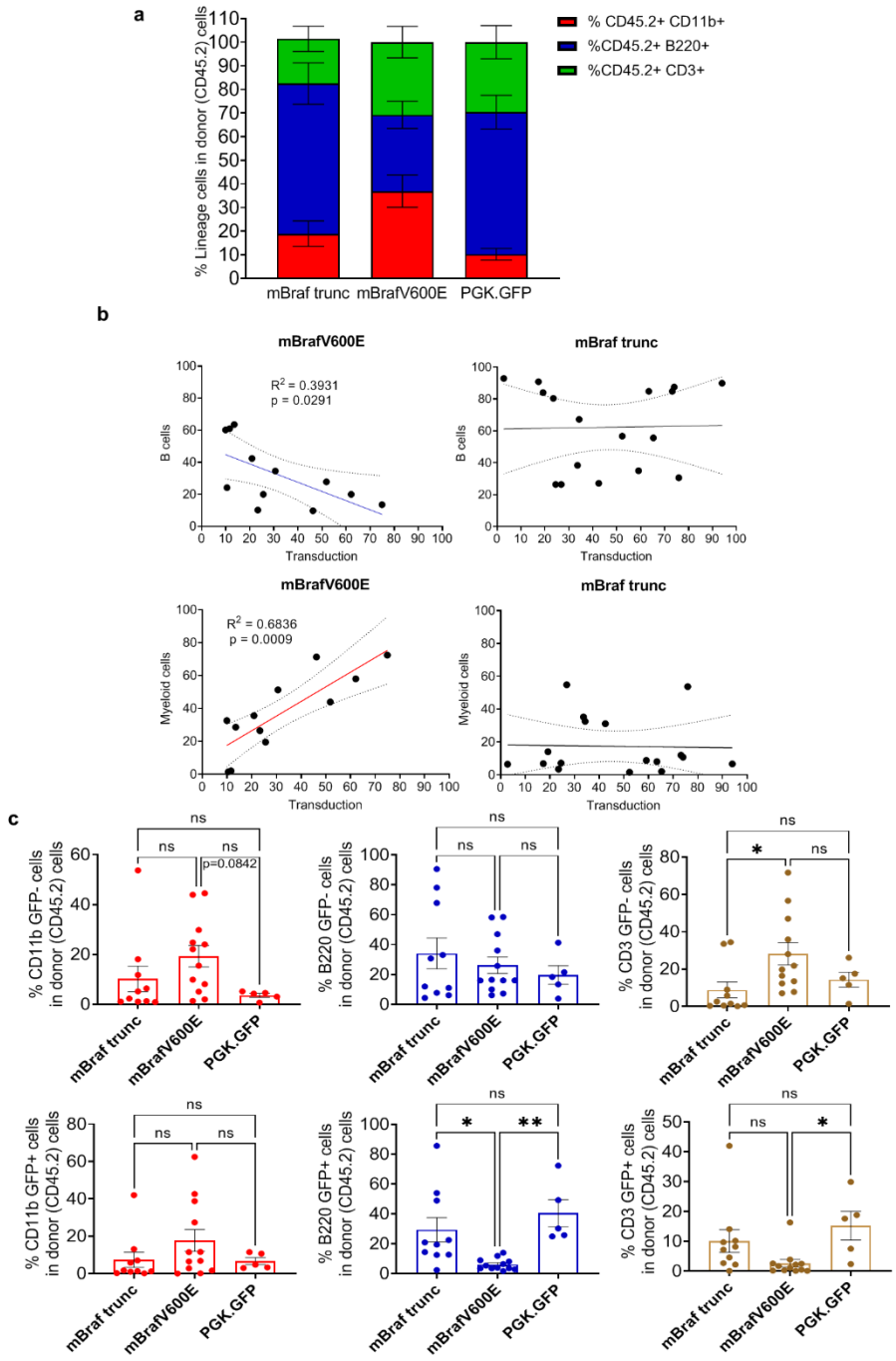

Figure 3.4. mBrafV600E expression results in myeloid skewing and lymphoid impairment. *(a) Hematopoietic composition (% Myeloid, B, and T cells) of donor cells was assessed by FACS analysis of PB collected one-month post-transplant. For statistical analysis, Mann-Whitney test was performed through GraphPad Prism. (b) Correlation graphs of percentages of B cells (top) and percentages of myeloid cells (bottom) with transduction levels, corresponding with the levels of oncogene expression, in mBrafV600E (left) and mBraf trunc (right) groups. Linear regression analysis was performed through GraphPad Prism. (c) Percentages of myeloid (left), B cells (center),*

*and T cells (right) separated by fraction of bystander cells (GFP-, top) and oncogene-expressing cells (GFP+, bottom). For statistical analysis, One-way Anova was performed through GraphPad Prism. Asterisks represent significance in the p value: * < 0.05; ** < 0.01; *** < 0.001; **** < 0.0001.*

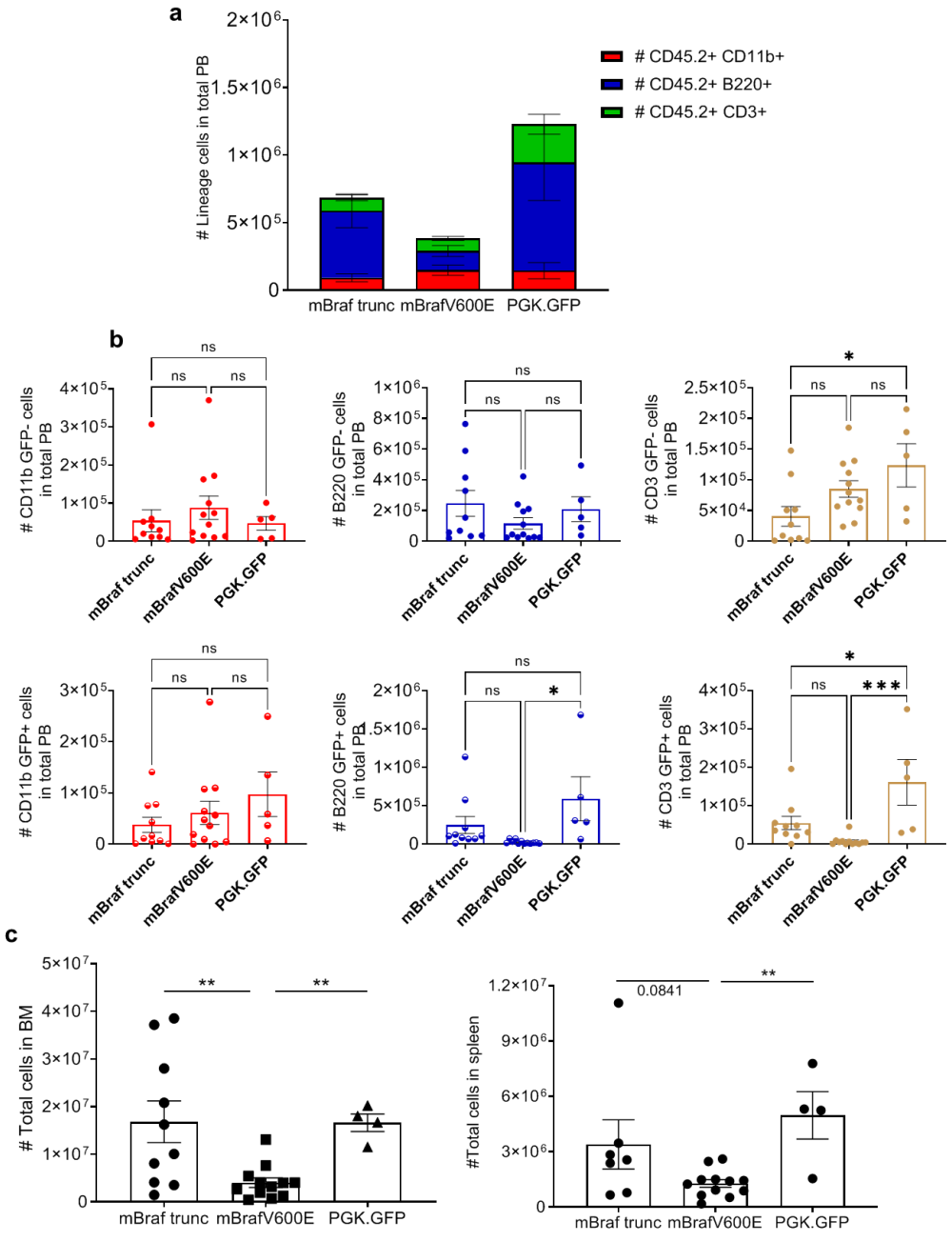

Figure 3.5. Absolute count analysis confirms specific impairment of oncogene-expressing B and T cells. *(a) Hematopoietic composition in absolute counts (# Myeloid, B, and T cells) of donor cells was assessed by FACS analysis of PB collected one-month post-transplant. For statistical analysis, Mann-Whitney test was performed through GraphPad Prism. (b) Absolute counts of myeloid (left), B*

*cells (center), and T cells (right) separated by fraction of bystander cells (GFP-, top) and oncogene-expressing cells (GFP+, bottom). (c) Cellularity observed in total BM and spleen at the endpoint of the animals. For statistical analysis, One-way Anova was performed through GraphPad Prism. Asterisks represent significance in the p value: * < 0.05; ** < 0.01; *** < 0.001; **** < 0.0001.*

3.4 mBrafV600E expression causes alteration in the secretion of pro-inflammatory molecules in NSG mice

Since we observed similarities with the humanized mouse models, such as impairment in cellularity specific to B cells, but also differences, such as the impairment of only oncogene-expressing lymphoid cells and not bystander cells, we hypothesized that the secretory phenotype of our murine model also presented differences compared to the humanized. To verify this hypothesis, we performed a multiplex assay on pro-inflammatory cytokines in the plasma of peripheral blood collected one-month post-transplant. Interestingly, we found an increased secretion of cytokines IL-2, IL-6, and IL-12, chemokines CCL2, CCL3, CCL4, and CCL5, a tendency of higher levels of IFNγ and higher levels of G-CSF in the plasma of mBrafV600E mice (**Figure 3.6a**). In the plasma of mBraf trunc mice, we only observed a tendency of higher levels of CCL2 and IL-2, again confirming a milder effect on the oncogene in inflammation compared to mBrafV600E expression, which is still not completely neutral. The cytokine secretion profile of mBrafV600E is strongly related to myeloid cells, especially macrophages, as the observed chemokines are associated with their inflammatory activity. Interestingly, we also observe an alteration of G-CSF, a factor that is responsible for the mobilization of cells from the BM to the peripheral blood. G-CSF also inversely correlated with the survival of mice and with the overall BM cellularity (**Figure 3.6b**). CCL2, already characterized in the humanized model, inversely correlates with survival and BM cellularity as well. Overall, this cytokine profile showed similarities and differences from the humanized mouse model, in which we observed similar overproduction of IL-6, CCL2 and CCL4 but also IL-1α and IL-1β, cytokines that were not altered in our immune-deficient mouse model (**Figure 3.6a**).

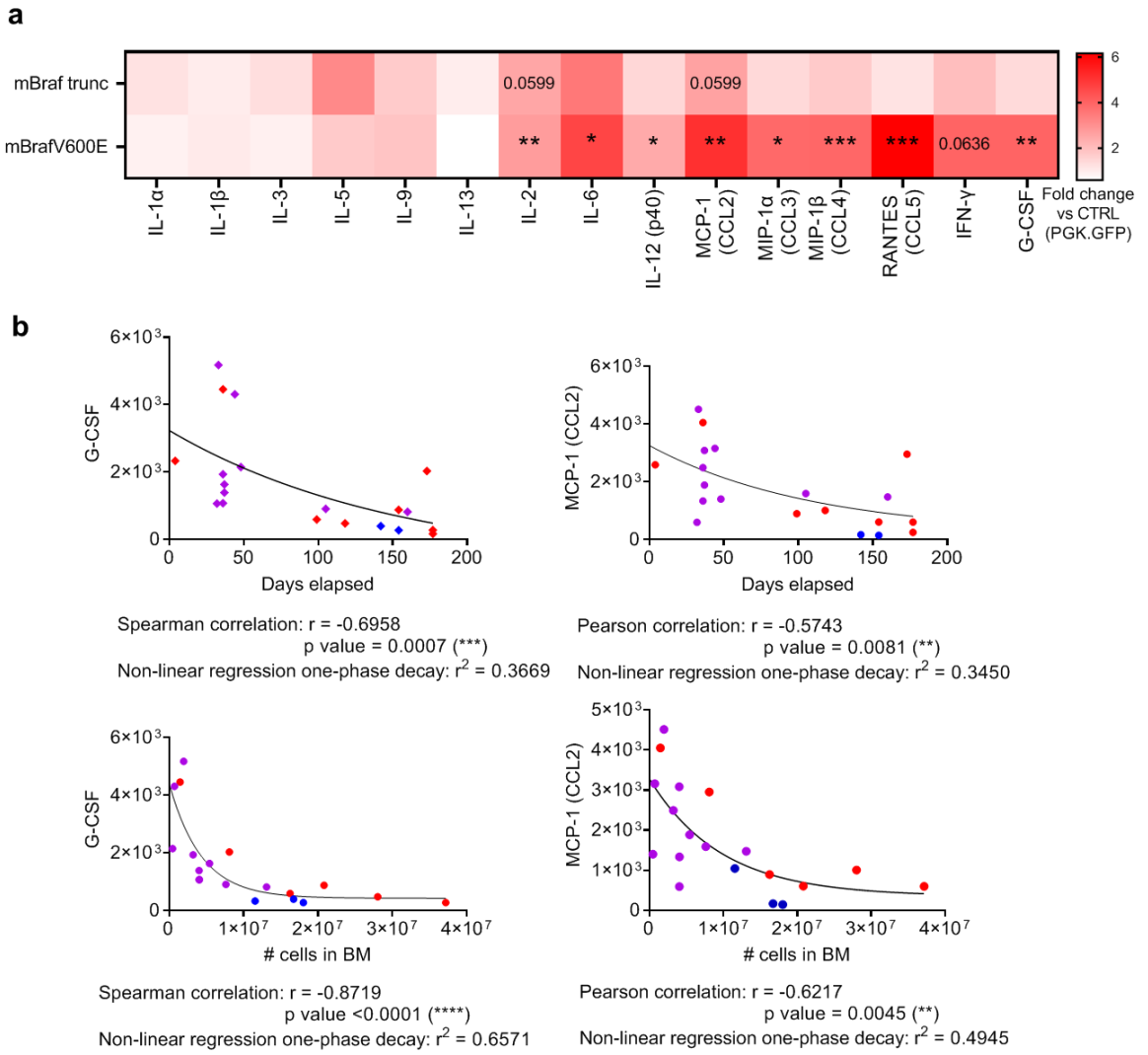

Figure 3.6. mBrafV600E expression alters the secretion of pro-inflammatory molecules. *(a) Quantifications of pro-inflammatory molecules in mouse plasma collected one-month post-transplant. (b) Correlation graphs of levels of G-CSF and MCP-1 with survival (top) and absolute counts of cells in the BM (bottom). Linear regression analysis was performed with GraphPad Prism. Red dots, violet and blue dots represents plasma levels in mBraf trunc, mBrafV600E, and PGK.GFP mice respectively.*

3.5 Characterization of oncogene-expressing cells transplanted into immune-competent mice

Given this aggressive phenotype in NSG mice after mBrafV600E expression in HSPCs, characterized by dose-dependent lethality, lymphoid impairment and enhanced secretion of inflammatory cytokines, we sought to understand whether the presence of an efficient immune system of the host would dampen inflammation and prolong the survival of transplanted mice. To do so, we performed transplantation of mouse HSPCs transduced with LV.mBrafV600E, LV.mBraftrunc, or LV.PGK.GFP in recipient C57 mice. First of all, peripheral blood analysis 4 weeks post-transplant showed a reduction of total cellularity in mBrafV600E mice compared to mBraf trunc and PGK.GFP. This result resembled the one in NSG mice, however, to a lesser degree, since reduction compared to controls is 2.2 fold, compared to the 3.6 fold observed before in immune-deficient mice (**Figure 3.7a**). Moreover, hematopoietic characterization of donor cells showed impairment of the B cell compartment (**Figure 3.7b**), in particular of oncogene-expressing B cells (**Figure 3.7c**). Again, the B cell impairment in immune-competent mice is less aggravating, 1.45 fold compared to the 11.4 fold observed in the immune-deficient model. We also turned our attention to recipient cells, which were impaired both in the B and in the T compartment (**Figure 3.7d**), suggesting that senescent cells in the mBrafV600E group could impair adaptive immune cells, in order to prevent their clearance. Luminex assay on cytokine levels in the plasma of mice showed elevated levels of only chemokines CCL3, CCL4 and CCL5, but not of interleukins like in the immune-deficient model, suggesting that the conserved upregulated chemokines are independent of potential immunological clearance (**Figure 3.7e**). Survival analysis on these mice showed an initial wave of lethality in mBrafV600E mice, which only affected 60% of them, while a portion of the mice survived (**Figure 3.7f**). We performed peripheral blood analysis also 12 weeks post-transplant to assess again the hematopoietic phenotype and found that the levels of oncogene-expressing cells in surviving mBrafV600E mice dropped to zero, suggesting that clearance of senescent cells occurred in these mice (**Figure 3.7g**). Moreover, their peripheral blood composition 12 weeks post-transplant was restored to similar levels compared to control mice, while at 4 weeks they showed myeloid skewing (**Figure 3.7h**).

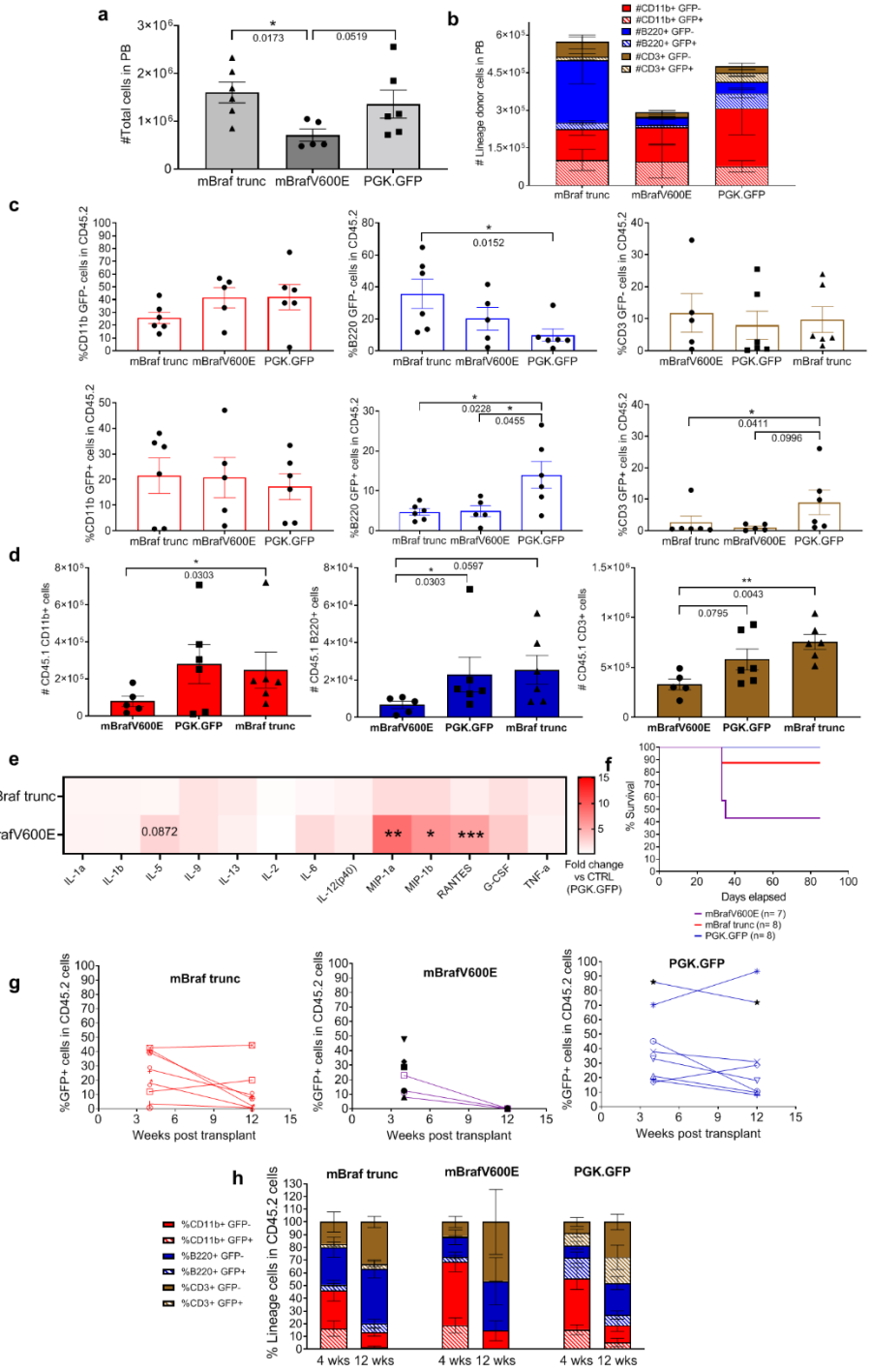

Figure 3.7. Oncogene expression in mouse HSPCs transplanted in immune-competent recipients. *(a) Total cellularity in mouse peripheral blood sampled 4 weeks post-transplant. (b) Overview of hematopoietic cell composition of the peripheral blood sampled 4 weeks post-transplant. (c) Absolute counts of donor myeloid (left), B (center) and T cells (right), separated in bystander (top graphs) or oncogene-expressing (bottom graphs). (d) Absolute counts of recipient cells in mouse peripheral blood 4 weeks post-transplant. (e) Levels of inflammatory proteins in the plasma of mice 4 weeks post-transplant, represented as fold levels compared to their controls (PGK.GFP mice). (f) Survival*

*curve of immune-competent mice. (g) Percentage of GFP+ cells in donor cells in the peripheral blood at 4 and 12 weeks post-transplant. (h) Hematopoietic characterization of mice at 4 and 12 weeks post-transplant in percentages. For statistical analysis, I performed One-way Anova on GraphPad Prism. Asterisks represent significance in the FDR of the DEGs: * < 0.05; ** < 0.01; *** < 0.001; **** < 0.0001.*

3.6 mBrafV600E expression in mouse HSPCs activates transcription of senescence, inflammatory and immune genes

We decided to further characterize at a transcriptional level the alterations driven by mBrafV600E, the intriguing differences between mouse and human senescence, and the differences in immunological clearance in the two recipient systems. Thus, we performed RNA-sequencing on sorted BM-derived myeloid and B cells from the mBrafV600E, the mBraf trunc, and the control (PGK.GFP) group (**Figure 8a and b**). We sorted cells one-month post-transplant, to understand the transcriptional signatures at a biologically relevant time point since mBrafV600E started showing a lethal phenotype at that time point. Firstly, principal component analysis on the top 5000 genes showed a distinct transcriptional signature of mBrafV600E samples. In NSG mice, both B and myeloid cells of the mBrafV600E group separated between the different populations and separately from the other groups. In C57 mice, only B cells of the mBrafV600E group clustered separately from the other populations, while myeloid cells were positioned at the same levels as control and mBraf trunc samples. On the other hand, mBraf trunc samples clustered similarly with the control samples in both systems (**Figure 3.8c**). Data were filtered to identify differentially expressed genes (DEGs), by filtering for a logFC higher than +1 or lower than -1 and with an FDR lower than 0.05 for significance. In NSG mice, the 4 mBrafV600E populations showed more DEGs compared to the truncated ones, except for mBraf trunc-expressing myeloid cells, which had the most deregulated genes of all samples (1772 DEGs in total) (**Figure 3.9a and b**). Curiously, in the mBrafV600E group, bystander myeloid and B cells showed more DEGs compared to their oncogene-expressing counterpart (1399 vs 945 for myeloid cells, 590 vs 199 DEGs for B cells) (**Figure 3.9a**).

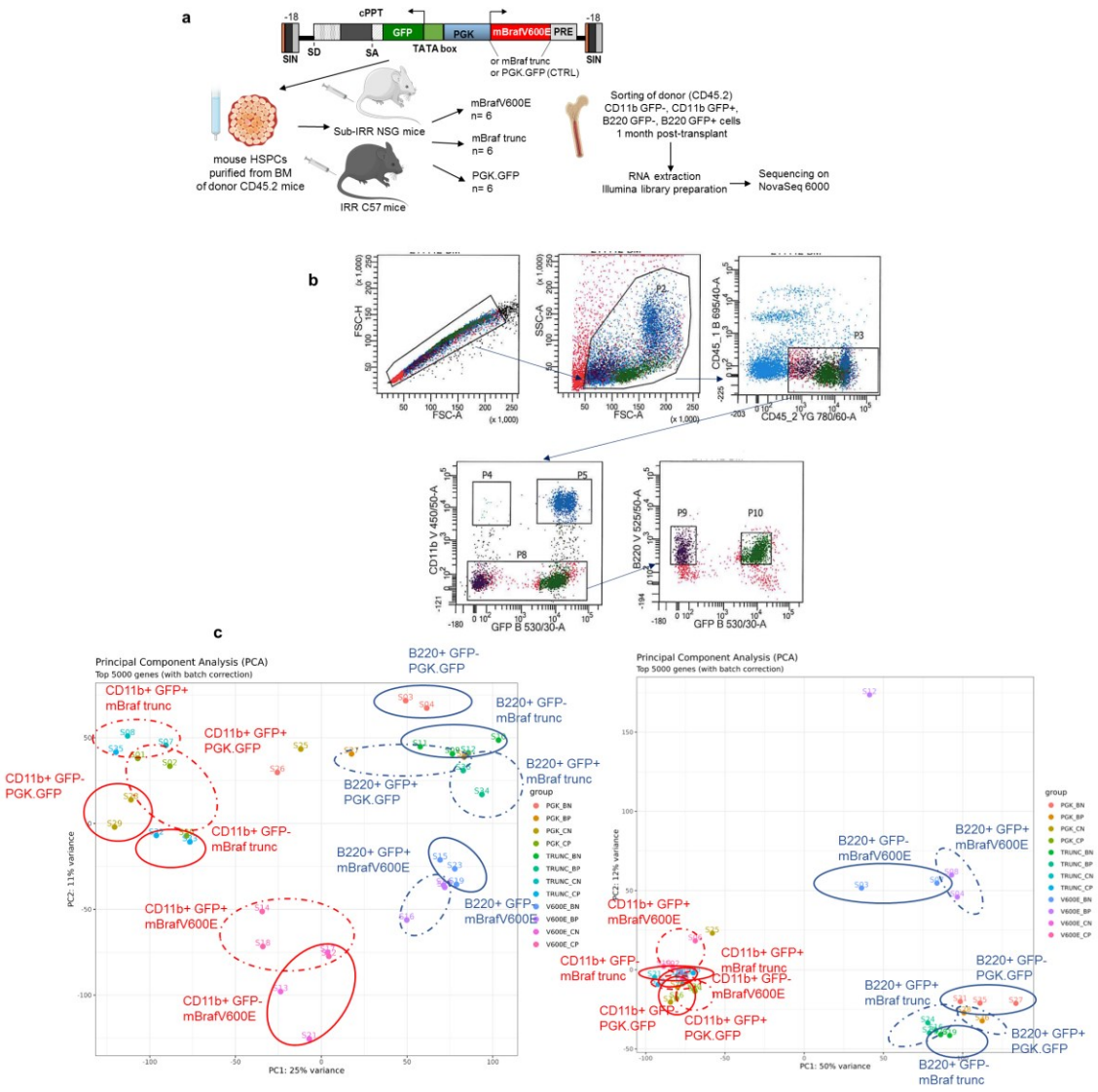

Figure 3.8. ***Gene expression experiment set up.*** *(a) Experimental plan of the cell sorting experiment. Four populations were sorted: oncogene-expressing (mBrafV600E or mBraf trunc) myeloid cells (CD11b+ GFP+), bystander myeloid cells (CD11b+ GFP-), oncogene-expressing B cells (B220+ GFP+), and bystander B cells (B220+ GFP-). (b) Gating strategy for FACS sorting. (c) Principal component analysis of the RNA-sequencing of NSG recipients (left) and C57 recipients (right) using the top 5000 deregulated genes of the sequenced cDNA samples.*

B cells expressing mBrafV600E showed the least number of DEGs, a peculiar observation, considering that this population was the most impaired in vivo (**Figure 3.4c and 3.5b**). It is worth noticing that some of the DEGs with the lowest p-value in myeloid cells of both oncogene groups are unusual for myeloid cells since they are related to the production of the

heavy and light immunoglobulin chains, IgH and IgK genes, respectively (**Figure 3.9a and 3.9b**). In C57 mice, we surprisingly observed that the populations with the highest DEGs are oncogene-expressing and bystander B cells of the mBrafV600E group (3017 and 2096 DEGs, respectively) while myeloid cells and all 4 populations of the mBraf trunc groups show little to no deregulation (**Figure 3.10a and 3.10b**).

To better dissect the deregulated pathways in our population, an enrichment analysis of the data was performed. Upregulated and downregulated hallmarks of each population, using the MSigDB mouse hallmarks as a reference, are represented in **Figure 3.11**. In NSG mice, upregulated pathways in the mBrafV600E-expressing CD11b population included: TNFα signaling via NFκB, reactive oxygen species (ROS) pathway, hypoxia, coagulation, apoptosis, allograft rejection, and MTORC1 signaling. Bystander myeloid cells of the same group showed upregulated TNFα signaling and coagulation, while bystander B cells other than coagulation, curiously displayed upregulated epithelial-mesenchymal transition genes, other than angiogenesis and myogenesis pathways. B cells expressing mBrafV600E did not show any upregulated pathways (**Figure 3.11a**). Downregulated hallmarks in mBrafV600E-expressing CD11b cells included: mostly IFN type I and II responses, and allograft rejection. Bystander myeloid showed downregulated allograft rejection, IL2-STAT5 signaling, inflammatory response, as well as estrogen response late pathway. Bystander B cells, other than the pathways already mentioned, also downregulated IL6 signaling. B cells expressing mBrafV600E only showed downregulated hallmarks, such as IFN-gamma, allograft rejection, and IL2-STAT5 signaling (**Figure 3.11b**). Regarding mBraf trunc samples, only the B220+ GFP+ population showed deregulated pathways, such as upregulated TNFα signaling, inflammatory response, complement, and coagulation, and downregulated epithelial-mesenchymal transition and coagulation pathways, suggesting again a not entirely neutral role of the mBraf trunc mutation in B cells.

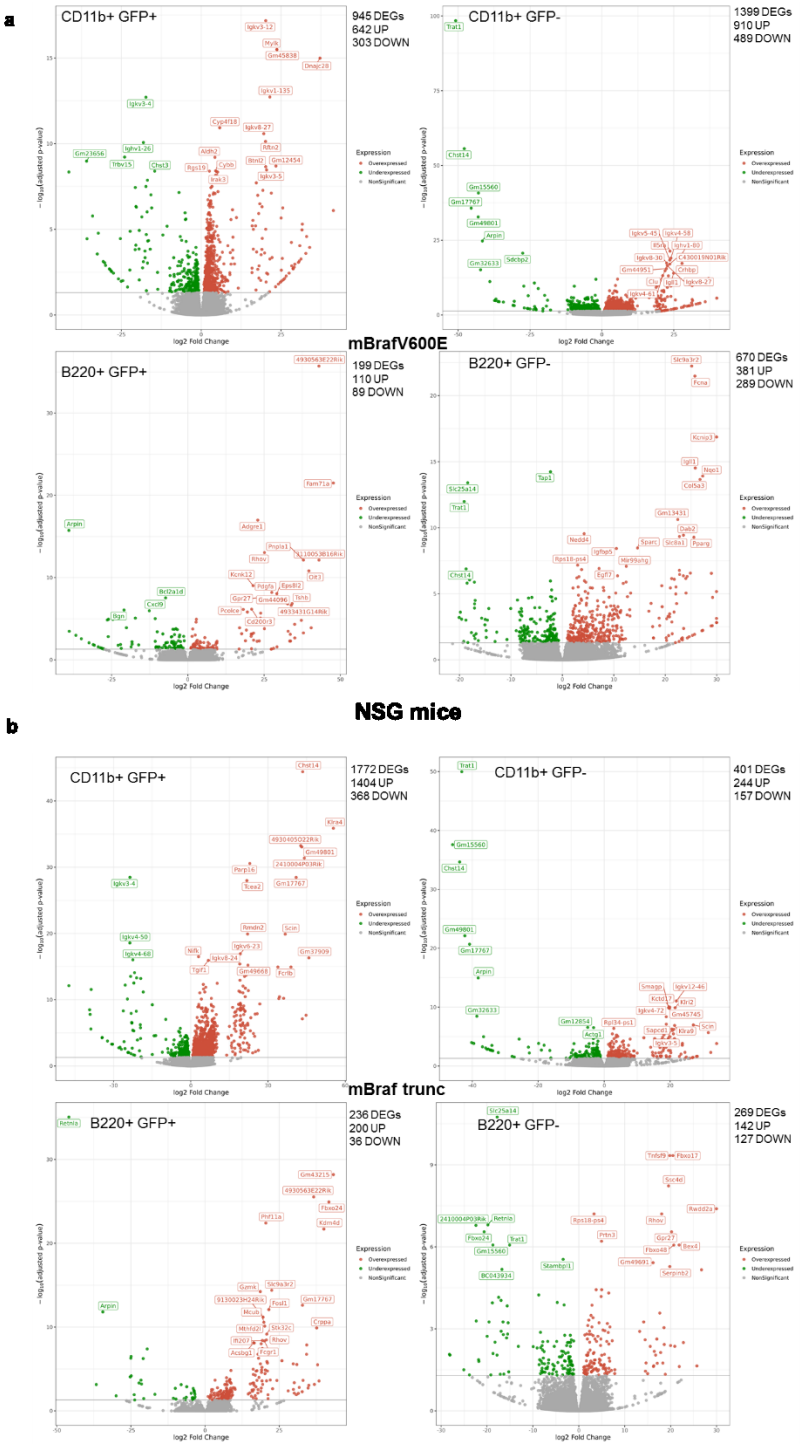

Figure 3.9. Differentially expressed genes (DEGs) in NSG recipients. *(a) Volcano plots representing upregulated (red) or downregulated (green) genes in NSG recipients transplanted with mBrafV600E-expressing HSPCs. (b) Volcano plots representing upregulated (red) or downregulated (green) genes in NSG recipients transplanted with mBraf trunc-expressing HSPCs.*

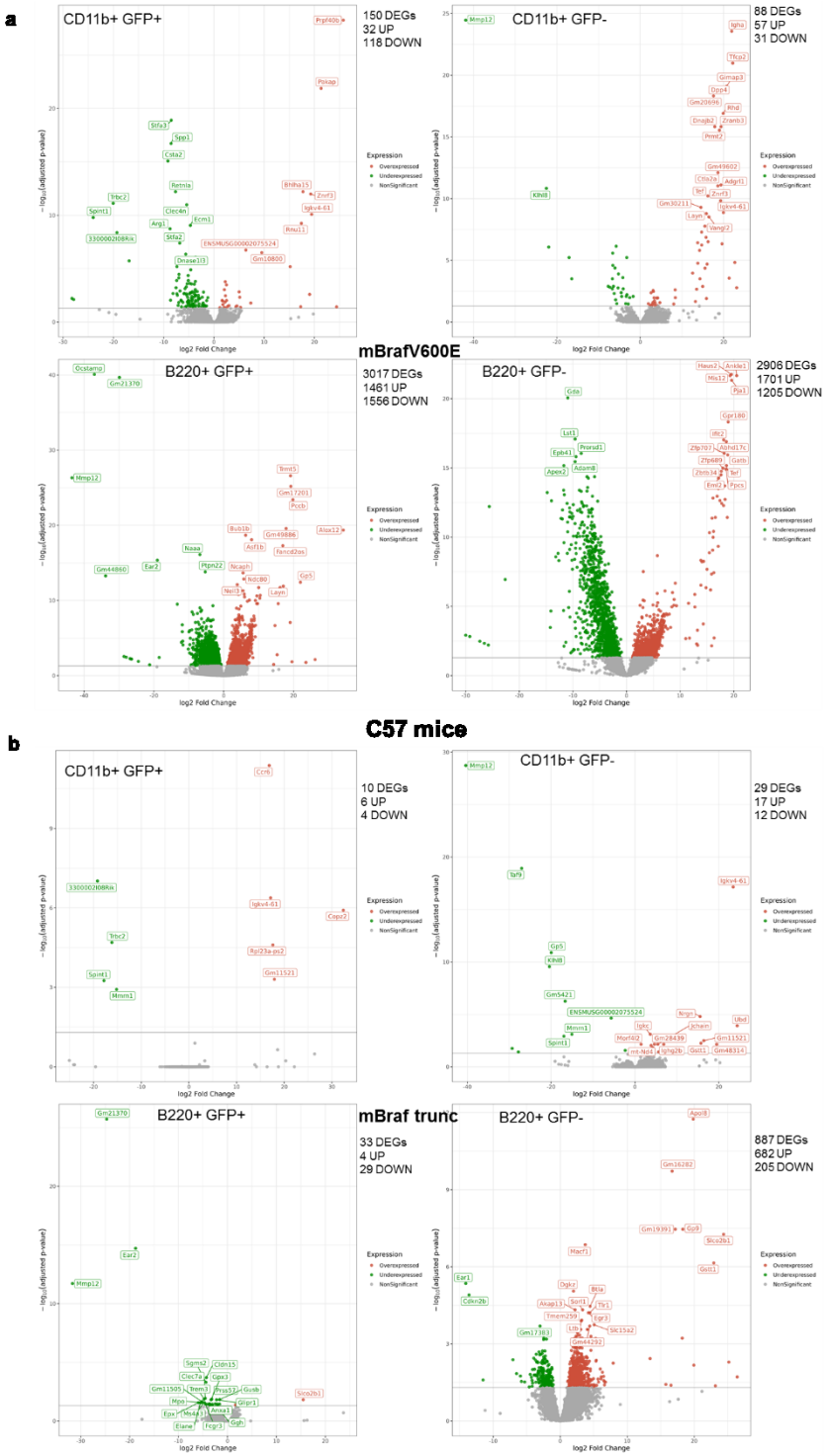

Figure 3.10. Differentially expressed genes (DEGs) in C57 recipients. *(a) Volcano plots representing upregulated (red) or downregulated (green) genes in C57 recipients transplanted with mBrafV600E-expressing HSPCs. (b) Volcano plots representing upregulated (red) or downregulated (green) genes in C57 recipients transplanted with mBraf trunc-expressing HSPCs.*

In C57 recipients, we observed different hallmarks: firstly there was a clear upregulation of G2/M checkpoint and E2F target hallmarks in both oncogene-expressing and bystander B cells, and upregulation of mitotic spindle hallmark in bystander B cells. Moreover, oncogene-expressing and bystander B cells show downregulation of IFN-γ response signaling, and heme metabolism. Oncogene-expressing myeloid and B cells share downregulation of TNFα signaling, IL6 JAK-STAT3 signaling, inflammatory response, complement, and apoptosis. The mBraf trunc group of C57 mice, on the other hand, showed downregulation of metabolism-related hallmarks in bystander B cells, such as glycolysis, oxidative phosphorylation, and fatty acid metabolism, as well as downregulation of E2F targets (**Figure 3.11a and b**).

Given that mBrafV600E cell populations showed an inflammatory phenotype in their hallmarks, also characterized by oxidation hallmarks, we performed deeper characterization. Firstly, we checked the levels of expression of cell cycle inhibitors. Interestingly, in NSG mice, Cdkn2d was the most upregulated in mBrafV600E and bystander myeloid cells, suggesting that $p19^{Ink4d}$ is the main player in cell cycle blockade of mBrafV600E and bystander cells, by blocking Cdk4/Cdk6 activation. Another upregulated gene in these two populations was Cdk2ap2, also known as p14, which inhibits Cdk2 activation. Surprisingly, Cdkn1a, encoding for p21, is only overexpressed in bystander B cells, while we observe downregulation of Cdkn2a, encoding for $p16^{Ink4a}$, in bystander myeloid and B cells and no change in expression in oncogene-expressing myeloid and B cells. The commonality in upregulation of $p19^{Ink4d}$ and p14 in both oncogene-expressing and bystander myeloid cells, along with the common upregulation of TNFα signaling in both populations, supports the hypothesis that a phenomenon of paracrine senescence is occurring. In mBraf trunc-expressing myeloid cells, we observed overexpression of Cdk2ap2, while in bystander myeloid cells Cdkn2a is downregulated, similarly to what happened in the same population of the mBrafV600E group (**Figure 3.11c**). In C57 recipients, mBrafV600E- expressing B cells show upregulation of Cdkn2d, as well as Cdkn3, known as CIP2, an

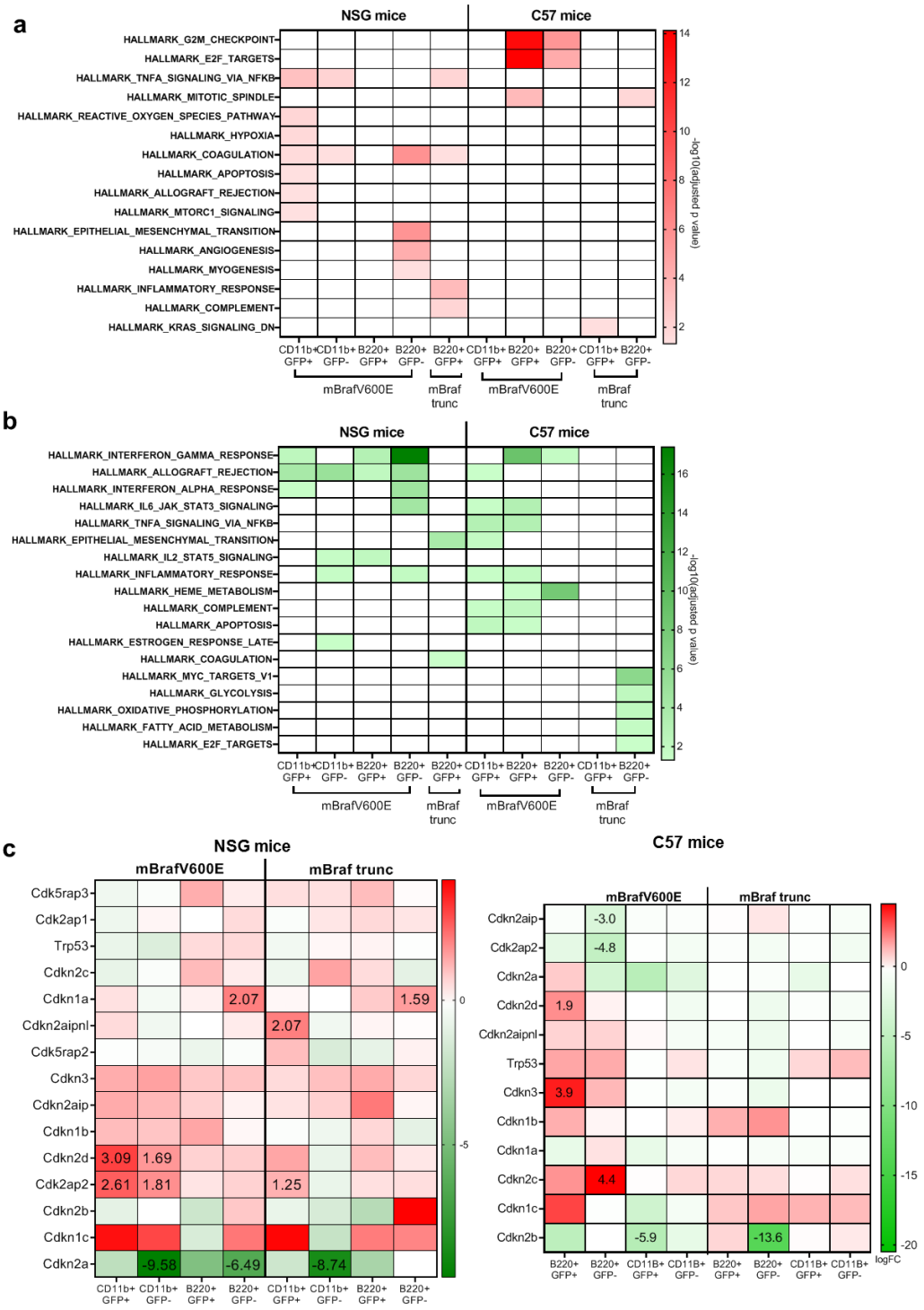

Figure 3.11. Hallmarks of inflammation and senescence in mBrafV600E and mBraf trunc samples. *(a) Upregulated MsgDB Hallmarks in the different populations. (b) Downregulated hallmarks in the different populations. Adjusted p value is represented in –log10 measurement, and*

colored cells indicate statistical significance. (c) Expression levels of genes encoding for cell cycle inhibitors in the different populations. Cells that show the logFC number represent the significant genes (FDR <0.05, logFC > 1) in our dataset.

inhibitor of Cdk2 kinase. Bystander B cells of the mBrafV600E group, on the other hand, show upregulation of Cdkn2c, such as $p18^{Ink4c}$, inhibitor of Cdk4/6 kinase, and downregulated levels of Cdk2ap2 and Cdkn2aip. Other populations, as well as all the mBraf trunc populations, did not show upregulated levels of cell cycle inhibitors gene expression (**Figure 3.11c**).

Afterward, to understand differences in the response upon oncogene activation depending on the immune system, we analyzed gene ontology (GO) results, focusing on the biological processes (BP) negatively or positively regulated in each population. Regarding mBrafV600E-expressing myeloid cells, we observed similar BP deregulation in NSG and C57 mice (**Figure 3.12a and c**). In particular, different processes regulating adaptive immune response, such as T cell proliferation, activation, differentiation, and T cell type I immune response were downregulated, as well as antigen presentation, such as MHC class II molecules, and response to IFN stimulus in both NSG and C57 mBrafV600E-expressing myeloid cells. Of note, we observed downregulation of ribosome biogenesis and ribosomal RNA processing, upregulation of processes involved in cell motility, lamellipodia, cytoskeleton, cell adhesion, and metabolic processes, such as NADP metabolism, glycolysis, metal ion transport, and lipids only in NSG mice (**Figure 3.12a**). Regarding bystander myeloid cells of the mBrafV600E group, adaptive immune response, antigen presentation, and IFN signaling were similarly downregulated in both NSG and C57 mice (**Figure 3.12b and d**). Again, we observed the upregulation of processes that are specific to bystander myeloid cells in NSG mice, such as phagocytosis, defense response, coagulation, MAPK activity, and different metabolic processes (**Figure 3.12b**). The comparison of NSG mice to C57 mice highlighted similarities and differences in the BP of B cells from the mBrafV600E groups. On one hand, both recipients showed negative deregulation of adaptive immune response and T cell signaling in both mBrafV600E-expressing and bystander B cells (**Figure 3.12e, f, g, h**).

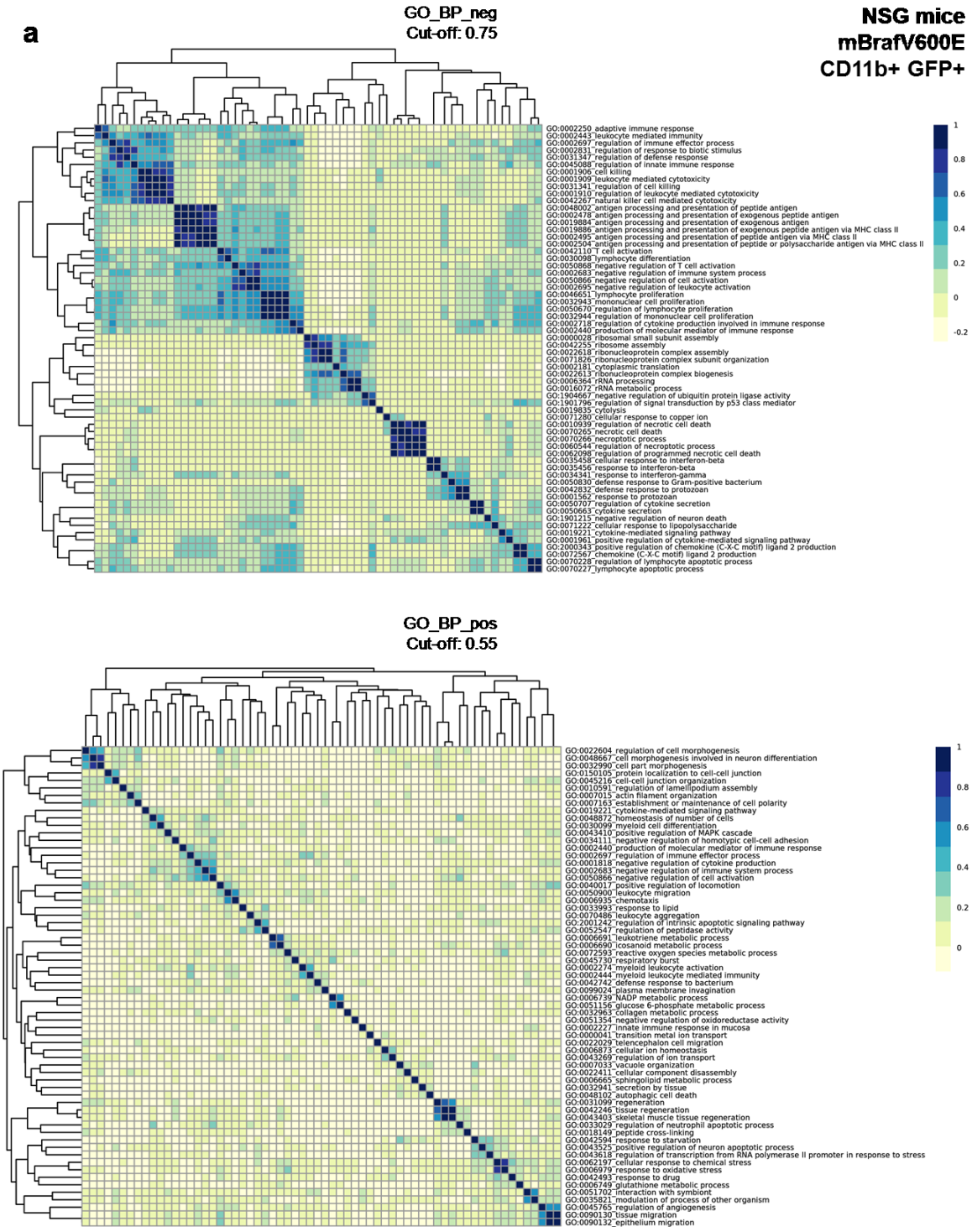
a
GO_BP_neg
Cut-off: 0.75
NSG mice
mBrafV600E
CD11b+ GFP+
GO:0002250_adaptive immune response
GO:0002443_leukocyte mediated immunity
GO:0002697_regulation of immune effector process
GO:0002831_regulation of response to biotic stimulus
GO:0031347_regulation of defense response
GO:0045088_regulation of innate immune response
GO:0001906_cell killing
GO:0001909_leukocyte mediated cytotoxicity
GO:0031341_regulation of cell killing
GO:0001910_regulation of leukocyte mediated cytotoxicity
GO:0042267_natural killer cell mediated cytotoxicity
GO:0048002_antigen processing and presentation of peptide antigen
GO:0002478_antigen processing and presentation of exogenous peptide antigen
GO:0019884_antigen processing and presentation of exogenous antigen
GO:0019886_antigen processing and presentation of exogenous peptide antigen via MHC class II
GO:0002495_antigen processing and presentation of peptide antigen via MHC class II
GO:0002504_antigen processing and presentation of peptide or polysaccharide antigen via MHC class II
GO:0042110_T cell activation
GO:0030098_lymphocyte differentiation
GO:0050868_negative regulation of T cell activation
GO:0002683_negative regulation of immune system process
GO:0050866_negative regulation of cell activation
GO:0002695_negative regulation of leukocyte activation
GO:0046651_lymphocyte proliferation
GO:0032943_mononuclear cell proliferation
GO:0050670_regulation of lymphocyte proliferation
GO:0032944_regulation of mononuclear cell proliferation
GO:0002718_regulation of cytokine production involved in immune response
GO:0002440_production of molecular mediator of immune response
GO:0000028_ribosomal small subunit assembly
GO:0042255_ribosome assembly
GO:0022618_ribonucleoprotein complex assembly
GO:0071826_ribonucleoprotein complex subunit organization
GO:0002181_cytoplasmic translation
GO:0022613_ribonucleoprotein complex biogenesis
GO:0006364_rRNA processing
GO:0016072_rRNA metabolic process
GO:1904667_negative regulation of ubiquitin protein ligase activity
GO:1901796_regulation of signal transduction by p53 class mediator
GO:0019835_cytolysis
GO:0071280_cellular response to copper ion
GO:0010939_regulation of necrotic cell death
GO:0070265_necrotic cell death
GO:0070266_necroptotic process
GO:0060544_regulation of necroptotic process
GO:0062098_regulation of programmed necrotic cell death
GO:0035458_cellular response to interferon-beta
GO:0035456_response to interferon-beta
GO:0034341_response to interferon-gamma
GO:0050830_defense response to Gram-positive bacterium
GO:0042832_defense response to protozoan
GO:0001562_response to protozoan
GO:0050707_regulation of cytokine secretion
GO:0050663_cytokine secretion
GO:1901215_negative regulation of neuron death
GO:0071222_cellular response to lipopolysaccharide
GO:0019221_cytokine-mediated signaling pathway
GO:0001961_positive regulation of cytokine-mediated signaling pathway
GO:2000343_positive regulation of chemokine (C-X-C motif) ligand 2 production
GO:0072567_chemokine (C-X-C motif) ligand 2 production
GO:0070228_regulation of lymphocyte apoptotic process
GO:0070227_lymphocyte apoptotic process
1
0.8
0.6
0.4
0.2
0
-0.2
GO_BP_pos
Cut-off: 0.55
GO:0022604_regulation of cell morphogenesis
GO:0048667_cell morphogenesis involved in neuron differentiation
GO:0032990_cell part morphogenesis
GO:0150105_protein localization to cell-cell junction
GO:0045216_cell-cell junction organization
GO:0010591_regulation of lamellipodium assembly
GO:0007015_actin filament organization
GO:0007163_establishment or maintenance of cell polarity
GO:0019221_cytokine-mediated signaling pathway
GO:0048872_homeostasis of number of cells
GO:0030099_myeloid cell differentiation
GO:0043410_positive regulation of MAPK cascade
GO:0034111_negative regulation of homotypic cell-cell adhesion
GO:0002440_production of molecular mediator of immune response
GO:0002697_regulation of immune effector process
GO:0001818_negative regulation of cytokine production
GO:0002683_negative regulation of immune system process
GO:0050866_negative regulation of cell activation
GO:0040017_positive regulation of locomotion
GO:0050900_leukocyte migration
GO:0006935_chemotaxis
GO:0033993_response to lipid
GO:0070486_leukocyte aggregation
GO:2001242_regulation of intrinsic apoptotic signaling pathway
GO:0052547_regulation of peptidase activity
GO:0006691_leukotriene metabolic process
GO:0006690_icosanoid metabolic process
GO:0072593_reactive oxygen species metabolic process
GO:0045730_respiratory burst
GO:0002274_myeloid leukocyte activation
GO:0002444_myeloid leukocyte mediated immunity
GO:0042742_defense response to bacterium
GO:0099024_plasma membrane invagination
GO:0006739_NADP metabolic process
GO:0051156_glucose 6-phosphate metabolic process
GO:0032963_collagen metabolic process
GO:0051354_negative regulation of oxidoreductase activity
GO:0002227_innate immune response in mucosa
GO:0000041_transition metal ion transport
GO:0022029_telencephalon cell migration
GO:0006873_cellular ion homeostasis
GO:0043269_regulation of ion transport
GO:0007033_vacuole organization
GO:0022411_cellular component disassembly
GO:0006665_sphingolipid metabolic process
GO:0032941_secretion by tissue
GO:0048102_autophagic cell death
GO:0031099_regeneration
GO:0042246_tissue regeneration
GO:0043403_skeletal muscle tissue regeneration
GO:0033029_regulation of neutrophil apoptotic process
GO:0018149_peptide cross-linking
GO:0042594_response to starvation
GO:0043525_positive regulation of neuron apoptotic process
GO:0043618_regulation of transcription from RNA polymerase II promoter in response to stress
GO:0062197_cellular response to chemical stress
GO:0006979_response to oxidative stress
GO:0042493_response to drug
GO:0006749_glutathione metabolic process
GO:0051702_interaction with symbiont
GO:0035821_modulation of process of other organism
GO:0045765_regulation of angiogenesis
GO:0090130_tissue migration
GO:0090132_epithelium migration
1
0.8
0.6
0.4
0.2
0

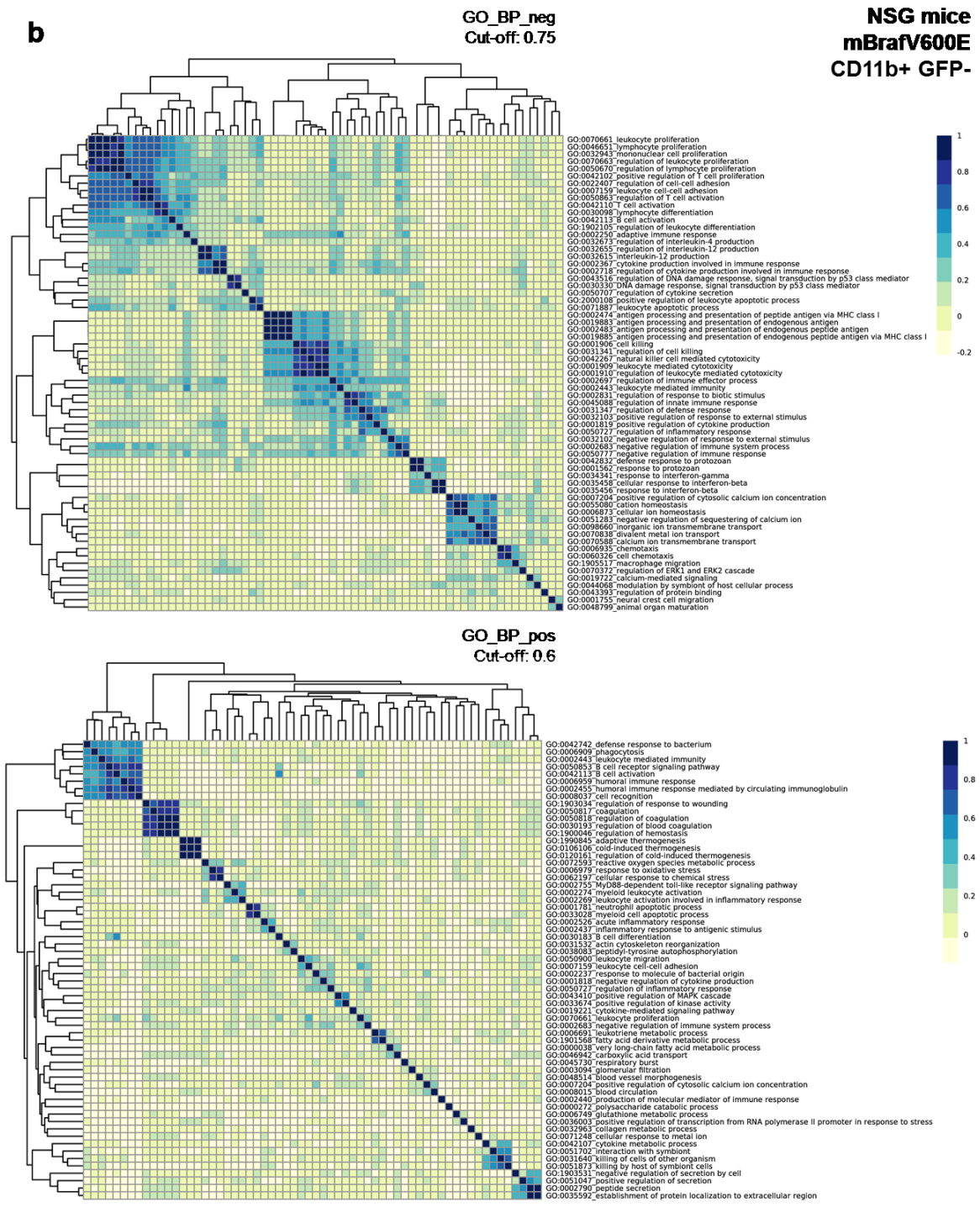
b
GO_BP_neg
Cut-off: 0.75
NSG mice
mBrafV600E
CD11b+ GFP-
GO:0070661_leukocyte proliferation
GO:0046651_lymphocyte proliferation
GO:0032943_mononuclear cell proliferation
GO:0070663_regulation of leukocyte proliferation
GO:0050670_regulation of lymphocyte proliferation
GO:0042102_positive regulation of T cell proliferation
GO:0022407_regulation of cell-cell adhesion
GO:0007159_leukocyte cell-cell adhesion
GO:0050863_regulation of T cell activation
GO:0042110_T cell activation
GO:0030098_lymphocyte differentiation
GO:0042113_B cell activation
GO:1902105_regulation of leukocyte differentiation
GO:0002250_adaptive immune response
GO:0032673_regulation of interleukin-4 production
GO:0032655_regulation of interleukin-12 production
GO:0032615_interleukin-12 production
GO:0002367_cytokine production involved in immune response
GO:0002718_regulation of cytokine production involved in immune response
GO:0043516_regulation of DNA damage response, signal transduction by p53 class mediator
GO:0030330_DNA damage response, signal transduction by p53 class mediator
GO:0050707_regulation of cytokine secretion
GO:2000108_positive regulation of leukocyte apoptotic process
GO:0071887_leukocyte apoptotic process
GO:0002474_antigen processing and presentation of peptide antigen via MHC class I
GO:0019883_antigen processing and presentation of endogenous antigen
GO:0002483_antigen processing and presentation of endogenous peptide antigen
GO:0019885_antigen processing and presentation of endogenous peptide antigen via MHC class I
GO:0001906_cell killing
GO:0031341_regulation of cell killing
GO:0042267_natural killer cell mediated cytotoxicity
GO:0001909_leukocyte mediated cytotoxicity
GO:0001910_regulation of leukocyte mediated cytotoxicity
GO:0002697_regulation of immune effector process
GO:0002443_leukocyte mediated immunity
GO:0002831_regulation of response to biotic stimulus
GO:0045088_regulation of innate immune response
GO:0031347_regulation of defense response
GO:0032103_positive regulation of response to external stimulus
GO:0001819_positive regulation of cytokine production
GO:0050727_regulation of inflammatory response
GO:0032102_negative regulation of response to external stimulus
GO:0002683_negative regulation of immune system process
GO:0050777_negative regulation of immune response
GO:0042832_defense response to protozoan
GO:0001562_response to protozoan
GO:0034341_response to interferon-gamma
GO:0035458_cellular response to interferon-beta
GO:0035456_response to interferon-beta
GO:0007204_positive regulation of cytosolic calcium ion concentration
GO:0055080_cation homeostasis
GO:0006873_cellular ion homeostasis
GO:0051283_negative regulation of sequestering of calcium ion
GO:0098660_inorganic ion transmembrane transport
GO:0070838_divalent metal ion transport
GO:0070588_calcium ion transmembrane transport
GO:0006935_chemotaxis
GO:0060326_cell chemotaxis
GO:1905517_macrophage migration
GO:0070372_regulation of ERK1 and ERK2 cascade
GO:0019722_calcium-mediated signaling
GO:0044068_modulation by symbiont of host cellular process
GO:0043393_regulation of protein binding
GO:0001755_neural crest cell migration
GO:0048799_animal organ maturation
1
0.8
0.6
0.4
0.2
0
-0.2
GO_BP_pos
Cut-off: 0.6
GO:0042742_defense response to bacterium
GO:0006909_phagocytosis
GO:0002443_leukocyte mediated immunity
GO:0050853_B cell receptor signaling pathway
GO:0042113_B cell activation
GO:0006959_humoral immune response
GO:0002455_humoral immune response mediated by circulating immunoglobulin
GO:0008037_cell recognition
GO:1903034_regulation of response to wounding
GO:0050817_coagulation
GO:0050818_regulation of coagulation
GO:0030193_regulation of blood coagulation
GO:1900046_regulation of hemostasis
GO:1990845_adaptive thermogenesis
GO:0106106_cold-induced thermogenesis
GO:0120161_regulation of cold-induced thermogenesis
GO:0072593_reactive oxygen species metabolic process
GO:0006979_response to oxidative stress
GO:0062197_cellular response to chemical stress
GO:0002755_MyD88-dependent toll-like receptor signaling pathway
GO:0002274_myeloid leukocyte activation
GO:0002269_leukocyte activation involved in inflammatory response
GO:0001781_neutrophil apoptotic process
GO:0033028_myeloid cell apoptotic process
GO:0002526_acute inflammatory response
GO:0002437_inflammatory response to antigenic stimulus
GO:0030183_B cell differentiation
GO:0031532_actin cytoskeleton reorganization
GO:0038083_peptidyl-tyrosine autophosphorylation
GO:0050900_leukocyte migration
GO:0007159_leukocyte cell-cell adhesion
GO:0002237_response to molecule of bacterial origin
GO:0001818_negative regulation of cytokine production
GO:0050727_regulation of inflammatory response
GO:0043410_positive regulation of MAPK cascade
GO:0033674_positive regulation of kinase activity
GO:0019221_cytokine-mediated signaling pathway
GO:0070661_leukocyte proliferation
GO:0002683_negative regulation of immune system process
GO:0006691_leukotriene metabolic process
GO:1901568_fatty acid derivative metabolic process
GO:0000038_very long-chain fatty acid metabolic process
GO:0046942_carboxylic acid transport
GO:0045730_respiratory burst
GO:0003094_glomerular filtration
GO:0048514_blood vessel morphogenesis
GO:0007204_positive regulation of cytosolic calcium ion concentration
GO:0008015_blood circulation
GO:0002440_production of molecular mediator of immune response
GO:0000272_polysaccharide catabolic process
GO:0006749_glutathione metabolic process
GO:0036003_positive regulation of transcription from RNA polymerase II promoter in response to stress
GO:0032963_collagen metabolic process
GO:0071248_cellular response to metal ion
GO:0042107_cytokine metabolic process
GO:0051702_interaction with symbiont
GO:0031640_killing of cells of other organism
GO:0051873_killing by host of symbiont cells
GO:1903531_negative regulation of secretion by cell
GO:0051047_positive regulation of secretion
GO:0002790_peptide secretion
GO:0035592_establishment of protein localization to extracellular region
1
0.8
0.6
0.4
0.2
0

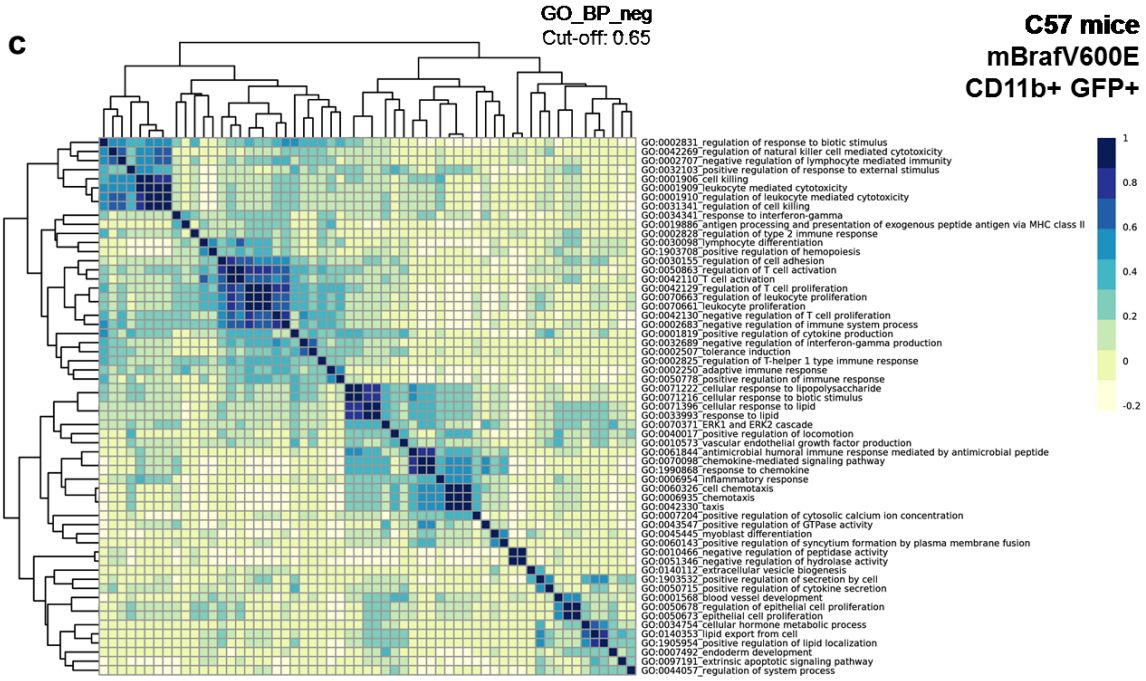
c
GO_BP_neg
Cut-off: 0.65
C57 mice
mBrafV600E
CD11b+ GFP+
GO:0002831_regulation of response to biotic stimulus
GO:0042269_regulation of natural killer cell mediated cytotoxicity
GO:0002707_negative regulation of lymphocyte mediated immunity
GO:0032103_positive regulation of response to external stimulus
GO:0001906_cell killing
GO:0001909_leukocyte mediated cytotoxicity
GO:0001910_regulation of leukocyte mediated cytotoxicity
GO:0031341_regulation of cell killing
GO:0034341_response to interferon-gamma
GO:0019886_antigen processing and presentation of exogenous peptide antigen via MHC class II
GO:0002828_regulation of type 2 immune response
GO:0030098_lymphocyte differentiation
GO:1903708_positive regulation of hemopoiesis
GO:0030155_regulation of cell adhesion
GO:0050863_regulation of T cell activation
GO:0042110_T cell activation
GO:0042129_regulation of T cell proliferation
GO:0070663_regulation of leukocyte proliferation
GO:0070661_leukocyte proliferation
GO:0042130_negative regulation of T cell proliferation
GO:0002683_negative regulation of immune system process
GO:0001819_positive regulation of cytokine production
GO:0032689_negative regulation of interferon-gamma production
GO:0002507_tolerance induction
GO:0002825_regulation of T-helper 1 type immune response
GO:0002250_adaptive immune response
GO:0050778_positive regulation of immune response
GO:0071222_cellular response to lipopolysaccharide
GO:0071216_cellular response to biotic stimulus
GO:0071396_cellular response to lipid
GO:0033993_response to lipid
GO:0070371_ERK1 and ERK2 cascade
GO:0040017_positive regulation of locomotion
GO:0010573_vascular endothelial growth factor production
GO:0061844_antimicrobial humoral immune response mediated by antimicrobial peptide
GO:0070098_chemokine-mediated signaling pathway
GO:1990868_response to chemokine
GO:0006954_inflammatory response
GO:0060326_cell chemotaxis
GO:0006935_chemotaxis
GO:0042330_taxis
GO:0007204_positive regulation of cytosolic calcium ion concentration
GO:0043547_positive regulation of GTPase activity
GO:0045445_myoblast differentiation
GO:0060143_positive regulation of syncytium formation by plasma membrane fusion
GO:0010466_negative regulation of peptidase activity
GO:0051346_negative regulation of hydrolase activity
GO:0140112_extracellular vesicle biogenesis
GO:1903532_positive regulation of secretion by cell
GO:0050715_positive regulation of cytokine secretion
GO:0001568_blood vessel development
GO:0050678_regulation of epithelial cell proliferation
GO:0050673_epithelial cell proliferation
GO:0034754_cellular hormone metabolic process
GO:0140353_lipid export from cell
GO:1905954_positive regulation of lipid localization
GO:0007492_endoderm development
GO:0097191_extrinsic apoptotic signaling pathway
GO:0044057_regulation of system process
1
0.8
0.6
0.4
0.2
0
-0.2

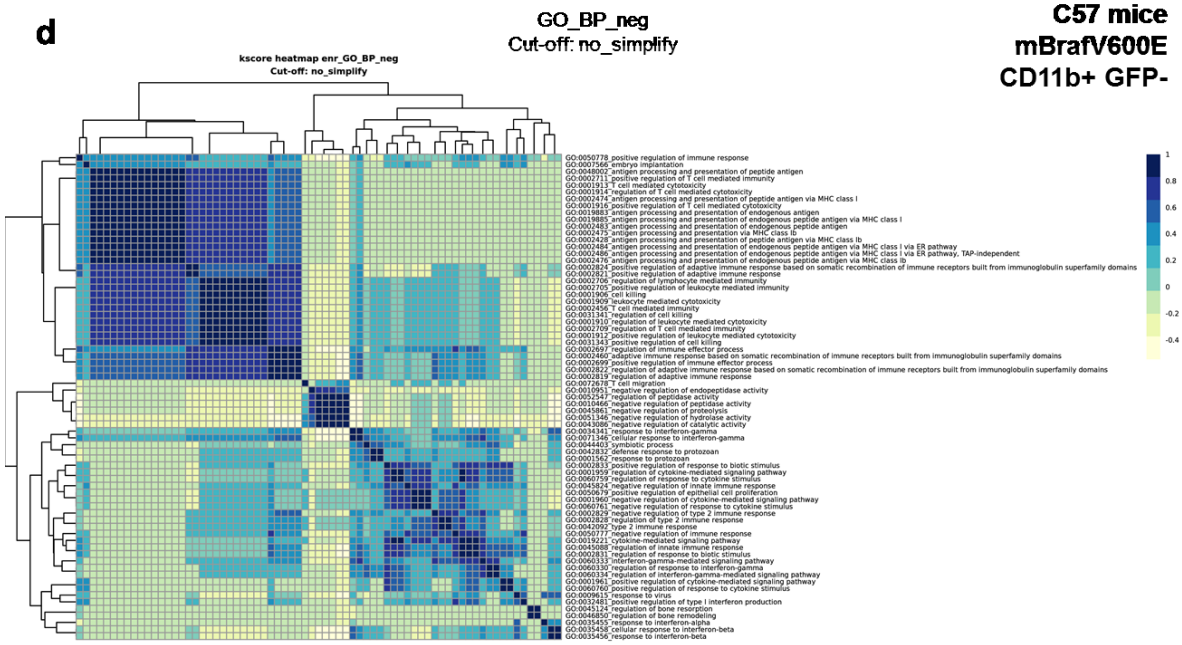
d
GO_BP_neg
Cut-off: no_simplify
C57 mice
mBrafV600E
CD11b+ GFP-
kscore heatmap enr_GO_BP_neg
Cut-off: no_simplify
GO:0050778_positive regulation of immune response
GO:0007566_embryo implantation
GO:0048002_antigen processing and presentation of peptide antigen
GO:0002711_positive regulation of T cell mediated immunity
GO:0001913_T cell mediated cytotoxicity
GO:0001914_regulation of T cell mediated cytotoxicity
GO:0002474_antigen processing and presentation of peptide antigen via MHC class I
GO:0001916_positive regulation of T cell mediated cytotoxicity
GO:0019883_antigen processing and presentation of endogenous antigen
GO:0019885_antigen processing and presentation of endogenous peptide antigen via MHC class I
GO:0002483_antigen processing and presentation of endogenous peptide antigen
GO:0002478_antigen processing and presentation of exogenous antigen via MHC class Ib
GO:0002484_antigen processing and presentation of endogenous peptide antigen via MHC class I via ER pathway
GO:0002486_antigen processing and presentation of endogenous peptide antigen via MHC class I via ER pathway, TAP-independent
GO:0002476_antigen processing and presentation of endogenous peptide antigen via MHC class Ib
GO:0002824_positive regulation of adaptive immune response based on somatic recombination of immune receptors built from immunoglobulin superfamily domains
GO:0002821_positive regulation of adaptive immune response
GO:0002708_regulation of lymphocyte mediated immunity
GO:0002705_positive regulation of leukocyte mediated immunity
GO:0001906_cell killing
GO:0001909_leukocyte mediated cytotoxicity
GO:0002456_T cell mediated immunity
GO:0031341_regulation of cell killing
GO:0001910_regulation of leukocyte mediated cytotoxicity
GO:0002709_regulation of T cell mediated immunity
GO:0001912_positive regulation of leukocyte mediated cytotoxicity
GO:0031343_positive regulation of cell killing
GO:0002697_regulation of immune effector process
GO:0002460_adaptive immune response based on somatic recombination of immune receptors built from immunoglobulin superfamily domains
GO:0002699_positive regulation of immune effector process
GO:0002822_regulation of adaptive immune response based on somatic recombination of immune receptors built from immunoglobulin superfamily domains
GO:0002819_regulation of adaptive immune response
GO:0072678_T cell migration
GO:0010951_negative regulation of endopeptidase activity
GO:0052547_regulation of peptidase activity
GO:0010466_negative regulation of peptidase activity
GO:0045861_negative regulation of proteolysis
GO:0051346_negative regulation of hydrolase activity
GO:0043086_negative regulation of catalytic activity
GO:0034341_response to interferon-gamma
GO:0071346_cellular response to interferon-gamma
GO:0044403_symbiotic process
GO:0042832_defense response to protozoan
GO:0001562_response to protozoan
GO:0002833_positive regulation of response to biotic stimulus
GO:0001959_regulation of cytokine-mediated signaling pathway
GO:0060759_regulation of response to cytokine stimulus
GO:0045824_negative regulation of innate immune response
GO:0050679_positive regulation of epithelial cell proliferation
GO:0001960_negative regulation of cytokine-mediated signaling pathway
GO:0060761_negative regulation of response to cytokine stimulus
GO:0002829_negative regulation of type 2 immune response
GO:0002828_regulation of type 2 immune response
GO:0042092_type 2 immune response
GO:0050777_negative regulation of immune response
GO:0019221_cytokine-mediated signaling pathway
GO:0045088_regulation of innate immune response
GO:0002831_regulation of response to biotic stimulus
GO:0060333_interferon-gamma-mediated signaling pathway
GO:0060330_regulation of response to interferon-gamma
GO:0060334_regulation of interferon-gamma-mediated signaling pathway
GO:0001961_positive regulation of cytokine-mediated signaling pathway
GO:0060760_positive regulation of response to cytokine stimulus
GO:0009615_response to virus
GO:0032481_positive regulation of type I interferon production
GO:0045124_regulation of bone resorption
GO:0046850_regulation of bone remodeling
GO:0035455_response to interferon-alpha
GO:0035458_cellular response to interferon-beta
GO:0035456_response to interferon-beta
1
0.8
0.6
0.4
0.2
0
-0.2
-0.4

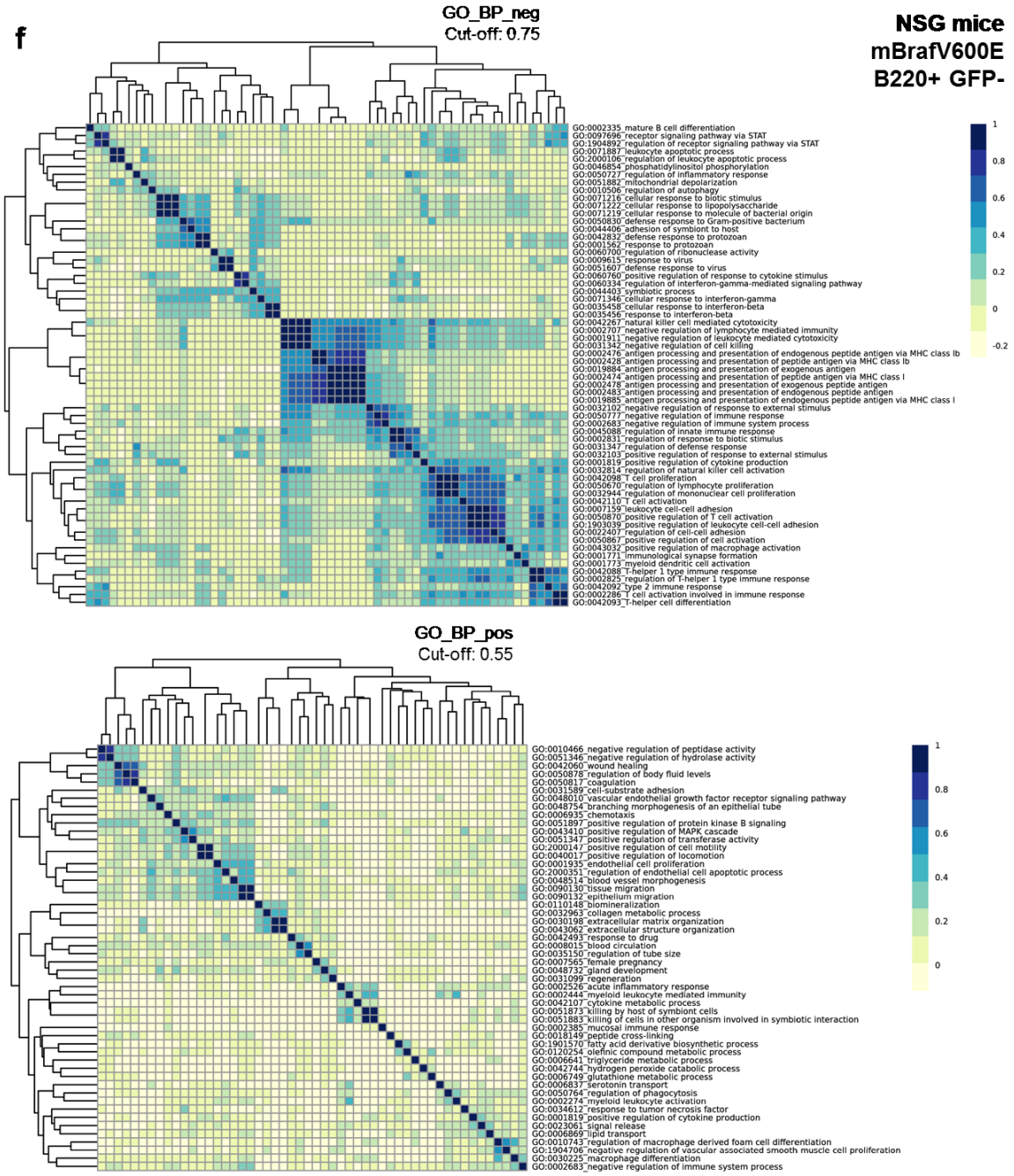
f
GO_BP_neg
Cut-off: 0.75
NSG mice
mBrafV600E
B220+ GFP-
GO:0002335 mature B cell differentiation
GO:0097696 receptor signaling pathway via STAT
GO:1904892 regulation of receptor signaling pathway via STAT
GO:0071887 leukocyte apoptotic process
GO:2000106 regulation of leukocyte apoptotic process
GO:0046854 phosphatidylinositol phosphorylation
GO:0050727 regulation of inflammatory response
GO:0051882 mitochondrial depolarization
GO:0010506 regulation of autophagy
GO:0071216 cellular response to biotic stimulus
GO:0071222 cellular response to lipopolysaccharide
GO:0071219 cellular response to molecule of bacterial origin
GO:0050830 defense response to Gram-positive bacterium
GO:0044406 adhesion of symbiont to host
GO:0042832 defense response to protozoan
GO:0001562 response to protozoan
GO:0060700 regulation of ribonuclease activity
GO:0009615 response to virus
GO:0051607 defense response to virus
GO:0060760 positive regulation of response to cytokine stimulus
GO:0060334 regulation of interferon-gamma-mediated signaling pathway
GO:0044403 symbiotic process
GO:0071346 cellular response to interferon-gamma
GO:0035458 cellular response to interferon-beta
GO:0035456 response to interferon-beta
GO:0042267 natural killer cell mediated cytotoxicity
GO:0002707 negative regulation of lymphocyte mediated immunity
GO:0001911 negative regulation of leukocyte mediated cytotoxicity
GO:0031342 negative regulation of cell killing
GO:0002476 antigen processing and presentation of endogenous peptide antigen via MHC class Ib
GO:0002428 antigen processing and presentation of peptide antigen via MHC class Ib
GO:0019884 antigen processing and presentation of exogenous antigen
GO:0002474 antigen processing and presentation of peptide antigen via MHC class I
GO:0002478 antigen processing and presentation of exogenous peptide antigen
GO:0002483 antigen processing and presentation of endogenous peptide antigen
GO:0019885 antigen processing and presentation of endogenous peptide antigen via MHC class I
GO:0032102 negative regulation of response to external stimulus
GO:0050777 negative regulation of immune response
GO:0002683 negative regulation of immune system process
GO:0045088 regulation of innate immune response
GO:0002831 regulation of response to biotic stimulus
GO:0031347 regulation of defense response
GO:0032103 positive regulation of response to external stimulus
GO:0001819 positive regulation of cytokine production
GO:0032814 regulation of natural killer cell activation
GO:0042098 T cell proliferation
GO:0050670 regulation of lymphocyte proliferation
GO:0032944 regulation of mononuclear cell proliferation
GO:0042110 T cell activation
GO:0007159 leukocyte cell-cell adhesion
GO:0050870 positive regulation of T cell activation
GO:1903039 positive regulation of leukocyte cell-cell adhesion
GO:0022407 regulation of cell-cell adhesion
GO:0050867 positive regulation of cell activation
GO:0043032 positive regulation of macrophage activation
GO:0001771 immunological synapse formation
GO:0001773 myeloid dendritic cell activation
GO:0042088 T-helper 1 type immune response
GO:0002825 regulation of T-helper 1 type immune response
GO:0042092 type 2 immune response
GO:0002286 T cell activation involved in immune response
GO:0042093 T-helper cell differentiation
1
0.8
0.6
0.4
0.2
0
-0.2
GO_BP_pos
Cut-off: 0.55
GO:0010466 negative regulation of peptidase activity
GO:0051346 negative regulation of hydrolase activity
GO:0042060 wound healing
GO:0050878 regulation of body fluid levels
GO:0050817 coagulation
GO:0031589 cell-substrate adhesion
GO:0048010 vascular endothelial growth factor receptor signaling pathway
GO:0048754 branching morphogenesis of an epithelial tube
GO:0006935 chemotaxis
GO:0051897 positive regulation of protein kinase B signaling
GO:0043410 positive regulation of MAPK cascade
GO:0051347 positive regulation of transferase activity
GO:2000147 positive regulation of cell motility
GO:0040017 positive regulation of locomotion
GO:0001935 endothelial cell proliferation
GO:2000351 regulation of endothelial cell apoptotic process
GO:0048514 blood vessel morphogenesis
GO:0090130 tissue migration
GO:0090132 epithelium migration
GO:0110148 biomineralization
GO:0032963 collagen metabolic process
GO:0030198 extracellular matrix organization
GO:0043062 extracellular structure organization
GO:0042493 response to drug
GO:0008015 blood circulation
GO:0035150 regulation of tube size
GO:0007565 female pregnancy
GO:0048732 gland development
GO:0031099 regeneration
GO:0002526 acute inflammatory response
GO:0002444 myeloid leukocyte mediated immunity
GO:0042107 cytokine metabolic process
GO:0051873 killing by host of symbiont cells
GO:0051883 killing of cells in other organism involved in symbiotic interaction
GO:0002385 mucosal immune response
GO:0018149 peptide cross-linking
GO:1901570 fatty acid derivative biosynthetic process
GO:0120254 olefinic compound metabolic process
GO:0006641 triglyceride metabolic process
GO:0042744 hydrogen peroxide catabolic process
GO:0006749 glutathione metabolic process
GO:0006837 serotonin transport
GO:0050764 regulation of phagocytosis
GO:0002274 myeloid leukocyte activation
GO:0034612 response to tumor necrosis factor
GO:0001819 positive regulation of cytokine production
GO:0023061 signal release
GO:0006869 lipid transport
GO:0010743 regulation of macrophage derived foam cell differentiation
GO:1904706 negative regulation of vascular associated smooth muscle cell proliferation
GO:0030225 macrophage differentiation
GO:0002683 negative regulation of immune system process
1
0.8
0.6
0.4
0.2
0

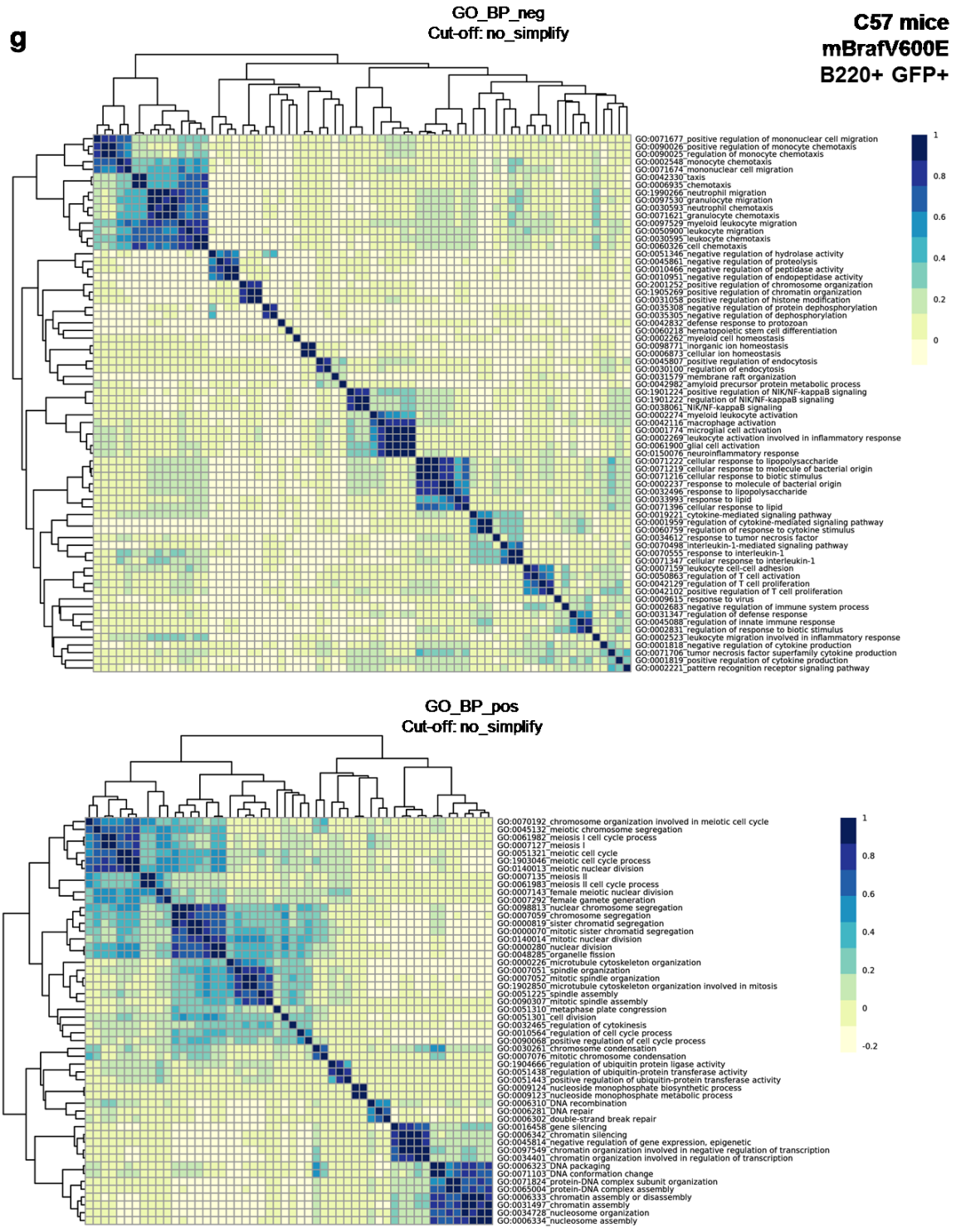
g
GO_BP_neg
Cut-off: no_simplify
C57 mice
mBrafV600E
B220+ GFP+
GO:0071677_positive regulation of mononuclear cell migration
GO:0090026_positive regulation of monocyte chemotaxis
GO:0090025_regulation of monocyte chemotaxis
GO:0002548_monocyte chemotaxis
GO:0071674_mononuclear cell migration
GO:0042330_taxis
GO:0006935_chemotaxis
GO:1990266_neutrophil migration
GO:0097530_granulocyte migration
GO:0030593_neutrophil chemotaxis
GO:0071621_granulocyte chemotaxis
GO:0097529_myeloid leukocyte migration
GO:0050900_leukocyte migration
GO:0030595_leukocyte chemotaxis
GO:0060326_cell chemotaxis
GO:0051346_negative regulation of hydrolase activity
GO:0045861_negative regulation of proteolysis
GO:0010466_negative regulation of peptidase activity
GO:0010951_negative regulation of endopeptidase activity
GO:2001252_positive regulation of chromosome organization
GO:1905269_positive regulation of chromatin organization
GO:0031058_positive regulation of histone modification
GO:0035308_negative regulation of protein dephosphorylation
GO:0035305_negative regulation of dephosphorylation
GO:0042832_defense response to protozoan
GO:0060218_hematopoietic stem cell differentiation
GO:0002262_myeloid cell homeostasis
GO:0098771_inorganic ion homeostasis
GO:0006873_cellular ion homeostasis
GO:0045807_positive regulation of endocytosis
GO:0030100_regulation of endocytosis
GO:0031579_membrane raft organization
GO:0042982_amyloid precursor protein metabolic process
GO:1901224_positive regulation of NIK/NF-kappaB signaling
GO:1901222_regulation of NIK/NF-kappaB signaling
GO:0038061_NIK/NF-kappaB signaling
GO:0002274_myeloid leukocyte activation
GO:0042116_macrophage activation
GO:0001774_microglial cell activation
GO:0002269_leukocyte activation involved in inflammatory response
GO:0061900_glial cell activation
GO:0150076_neuroinflammatory response
GO:0071222_cellular response to lipopolysaccharide
GO:0071219_cellular response to molecule of bacterial origin
GO:0071216_cellular response to biotic stimulus
GO:0002237_response to molecule of bacterial origin
GO:0032496_response to lipopolysaccharide
GO:0033993_response to lipid
GO:0071396_cellular response to lipid
GO:0019221_cytokine-mediated signaling pathway
GO:0001959_regulation of cytokine-mediated signaling pathway
GO:0060759_regulation of response to cytokine stimulus
GO:0034612_response to tumor necrosis factor
GO:0070498_interleukin-1-mediated signaling pathway
GO:0070555_response to interleukin-1
GO:0071347_cellular response to interleukin-1
GO:0007159_leukocyte cell-cell adhesion
GO:0050863_regulation of T cell activation
GO:0042129_regulation of T cell proliferation
GO:0042102_positive regulation of T cell proliferation
GO:0009615_response to virus
GO:0002683_negative regulation of immune system process
GO:0031347_regulation of defense response
GO:0045088_regulation of innate immune response
GO:0002831_regulation of response to biotic stimulus
GO:0002523_leukocyte migration involved in inflammatory response
GO:0001818_negative regulation of cytokine production
GO:0071706_tumor necrosis factor superfamily cytokine production
GO:0001819_positive regulation of cytokine production
GO:0002221_pattern recognition receptor signaling pathway
1
0.8
0.6
0.4
0.2
0
GO_BP_pos
Cut-off: no_simplify
GO:0070192_chromosome organization involved in meiotic cell cycle
GO:0045132_meiotic chromosome segregation
GO:0061982_meiosis I cell cycle process
GO:0007127_meiosis I
GO:0051321_meiotic cell cycle
GO:1903046_meiotic cell cycle process
GO:0140013_meiotic nuclear division
GO:0007135_meiosis II
GO:0061983_meiosis II cell cycle process
GO:0007143_female meiotic nuclear division
GO:0007292_female gamete generation
GO:0098813_nuclear chromosome segregation
GO:0007059_chromosome segregation
GO:0000819_sister chromatid segregation
GO:0000070_mitotic sister chromatid segregation
GO:0140014_mitotic nuclear division
GO:0000280_nuclear division
GO:0048285_organelle fission
GO:0000226_microtubule cytoskeleton organization
GO:0007051_spindle organization
GO:0007052_mitotic spindle organization
GO:1902850_microtubule cytoskeleton organization involved in mitosis
GO:0051225_spindle assembly
GO:0090307_mitotic spindle assembly
GO:0051310_metaphase plate congression
GO:0051301_cell division
GO:0032465_regulation of cytokinesis
GO:0010564_regulation of cell cycle process
GO:0090068_positive regulation of cell cycle process
GO:0030261_chromosome condensation
GO:0007076_mitotic chromosome condensation
GO:1904666_regulation of ubiquitin protein ligase activity
GO:0051438_regulation of ubiquitin-protein transferase activity
GO:0051443_positive regulation of ubiquitin-protein transferase activity
GO:0009124_nucleoside monophosphate biosynthetic process
GO:0009123_nucleoside monophosphate metabolic process
GO:0006310_DNA recombination
GO:0006281_DNA repair
GO:0006302_double-strand break repair
GO:0016458_gene silencing
GO:0006342_chromatin silencing
GO:0045814_negative regulation of gene expression, epigenetic
GO:0097549_chromatin organization involved in negative regulation of transcription
GO:0034401_chromatin organization involved in regulation of transcription
GO:0006323_DNA packaging
GO:0071103_DNA conformation change
GO:0071824_protein-DNA complex subunit organization
GO:0065004_protein-DNA complex assembly
GO:0006333_chromatin assembly or disassembly
GO:0031497_chromatin assembly
GO:0034728_nucleosome organization
GO:0006334_nucleosome assembly
1
0.8
0.6
0.4
0.2
0
-0.2

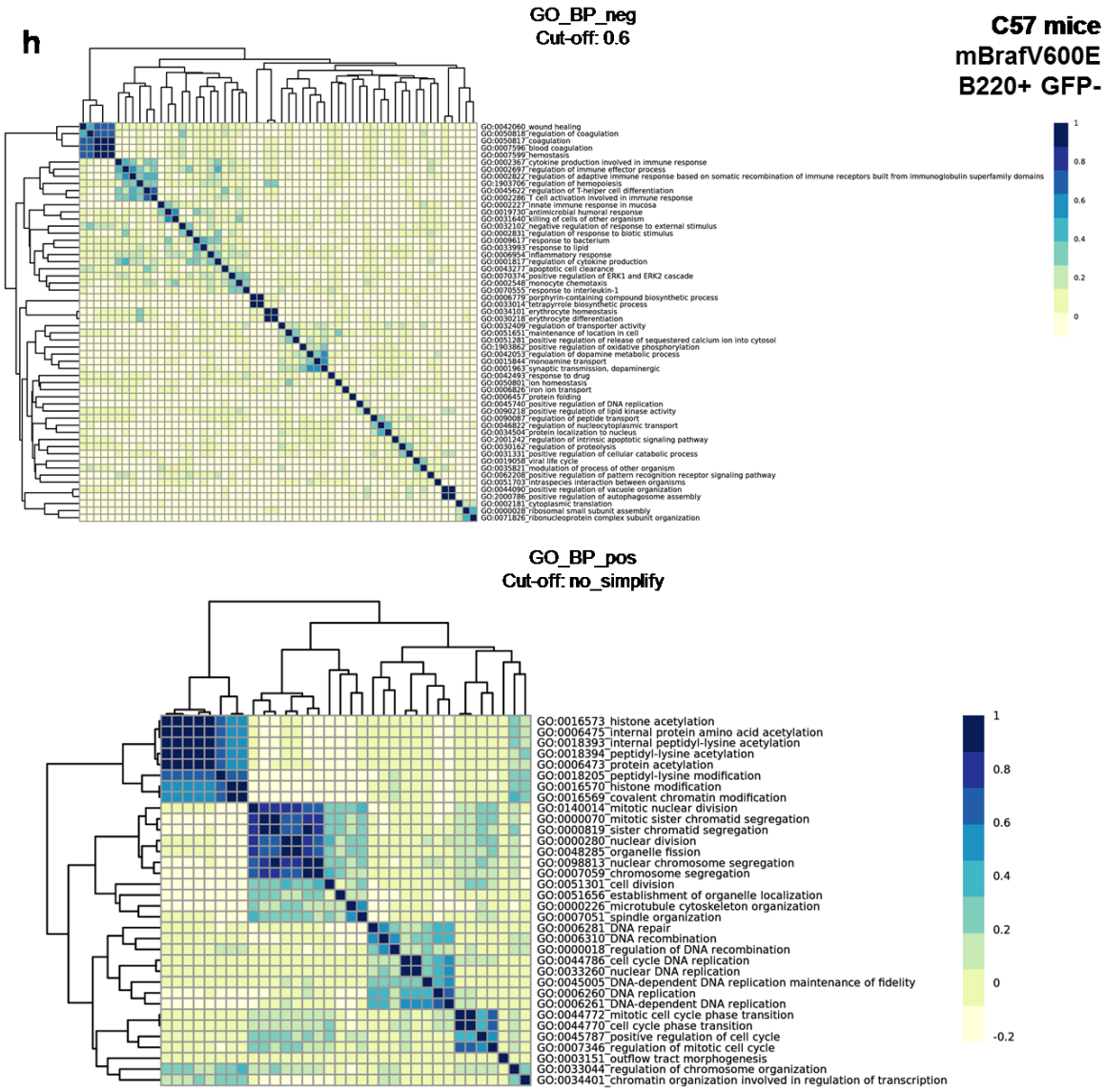
h
GO_BP_neg
Cut-off: 0.6
C57 mice
mBrafV600E
B220+ GFP-
GO:0042060 wound healing
GO:0050818 regulation of coagulation
GO:0050817 coagulation
GO:0007596 blood coagulation
GO:0007599 hemostasis
GO:0002367 cytokine production involved in immune response
GO:0002697 regulation of immune effector process
GO:0002822 regulation of adaptive immune response based on somatic recombination of immune receptors built from immunoglobulin superfamily domains
GO:1903706 regulation of hemopoiesis
GO:0045622 regulation of T-helper cell differentiation
GO:0002286 T cell activation involved in immune response
GO:0002227 innate immune response in mucosa
GO:0019730 antimicrobial humoral response
GO:0031640 killing of cells of other organism
GO:0032102 negative regulation of response to external stimulus
GO:0002831 regulation of response to biotic stimulus
GO:0009617 response to bacterium
GO:0033993 response to lipid
GO:0006954 inflammatory response
GO:0001817 regulation of cytokine production
GO:0043277 apoptotic cell clearance
GO:0070374 positive regulation of ERK1 and ERK2 cascade
GO:0002548 monocyte chemotaxis
GO:0070555 response to interleukin-1
GO:0006779 porphyrin-containing compound biosynthetic process
GO:0033014 tetrapyrrole biosynthetic process
GO:0034101 erythrocyte homeostasis
GO:0030218 erythrocyte differentiation
GO:0032409 regulation of transporter activity
GO:0051651 maintenance of location in cell
GO:0051281 positive regulation of release of sequestered calcium ion into cytosol
GO:1903862 positive regulation of oxidative phosphorylation
GO:0042053 regulation of dopamine metabolic process
GO:0015844 monoamine transport
GO:0001963 synaptic transmission, dopaminergic
GO:0042493 response to drug
GO:0050801 ion homeostasis
GO:0006826 iron ion transport
GO:0006457 protein folding
GO:0045740 positive regulation of DNA replication
GO:0090218 positive regulation of lipid kinase activity
GO:0090087 regulation of peptide transport
GO:0046822 regulation of nucleocytoplasmic transport
GO:0034504 protein localization to nucleus
GO:2001242 regulation of intrinsic apoptotic signaling pathway
GO:0030162 regulation of proteolysis
GO:0031331 positive regulation of cellular catabolic process
GO:0019058 viral life cycle
GO:0035821 modulation of process of other organism
GO:0062208 positive regulation of pattern recognition receptor signaling pathway
GO:0051703 intraspecies interaction between organisms
GO:0044090 positive regulation of vacuole organization
GO:2000786 positive regulation of autophagosome assembly
GO:0002181 cytoplasmic translation
GO:0000028 ribosomal small subunit assembly
GO:0071826 ribonucleoprotein complex subunit organization
1
0.8
0.6
0.4
0.2
0
GO_BP_pos
Cut-off: no_simplify
GO:0016573 histone acetylation
GO:0006475 internal protein amino acid acetylation
GO:0018393 internal peptidyl-lysine acetylation
GO:0018394 peptidyl-lysine acetylation
GO:0006473 protein acetylation
GO:0018205 peptidyl-lysine modification
GO:0016570 histone modification
GO:0016569 covalent chromatin modification
GO:1140014 mitotic nuclear division
GO:0000070 mitotic sister chromatid segregation
GO:0000819 sister chromatid segregation
GO:0000280 nuclear division
GO:0048285 organelle fission
GO:0098813 nuclear chromosome segregation
GO:0007059 chromosome segregation
GO:0051301 cell division
GO:0051656 establishment of organelle localization
GO:0000226 microtubule cytoskeleton organization
GO:0007051 spindle organization
GO:0006281 DNA repair
GO:0006310 DNA recombination
GO:0000018 regulation of DNA recombination
GO:0044786 cell cycle DNA replication
GO:0033260 nuclear DNA replication
GO:0045005 DNA-dependent DNA replication maintenance of fidelity
GO:0062260 DNA replication
GO:0006261 DNA-dependent DNA replication
GO:0044772 mitotic cell cycle phase transition
GO:0044770 cell cycle phase transition
GO:0045787 positive regulation of cell cycle
GO:0007346 regulation of mitotic cell cycle
GO:0003151 outflow tract morphogenesis
GO:0033044 regulation of chromosome organization
GO:0034401 chromatin organization involved in regulation of transcription
1
0.8
0.6
0.4
0.2
0
-0.2

i

NSG mice
mBraf trunc
CD11b+ GFP+

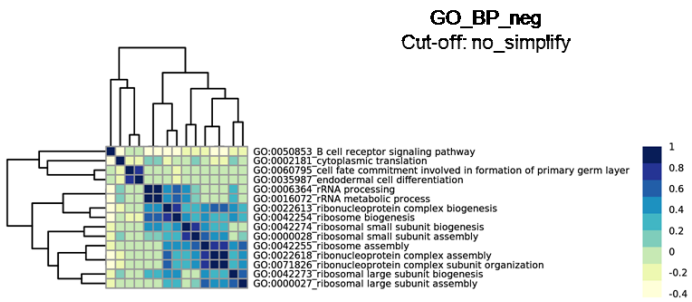

j

NSG mice
mBraf trunc
CD11b+ GFP-

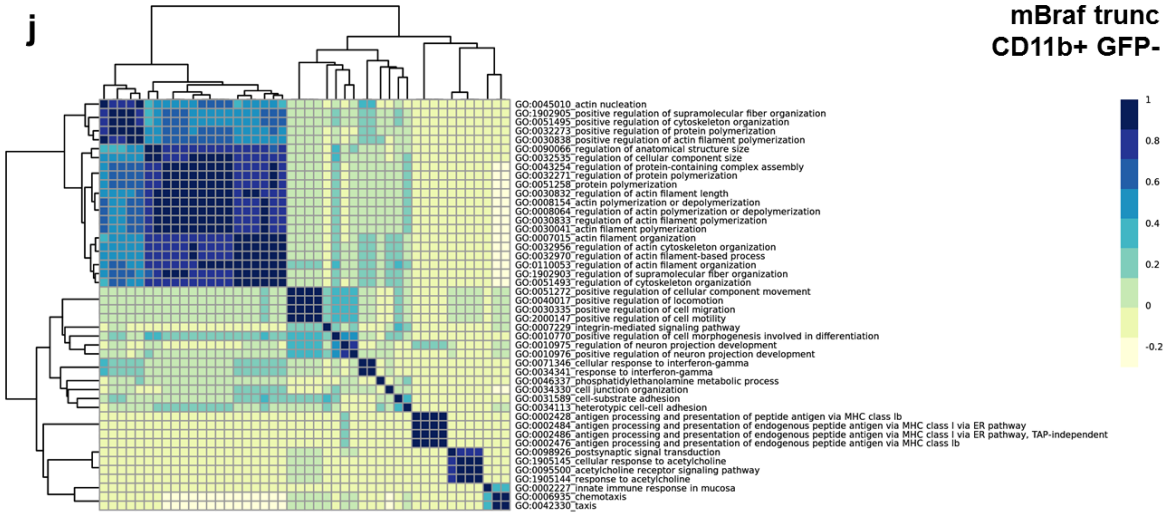

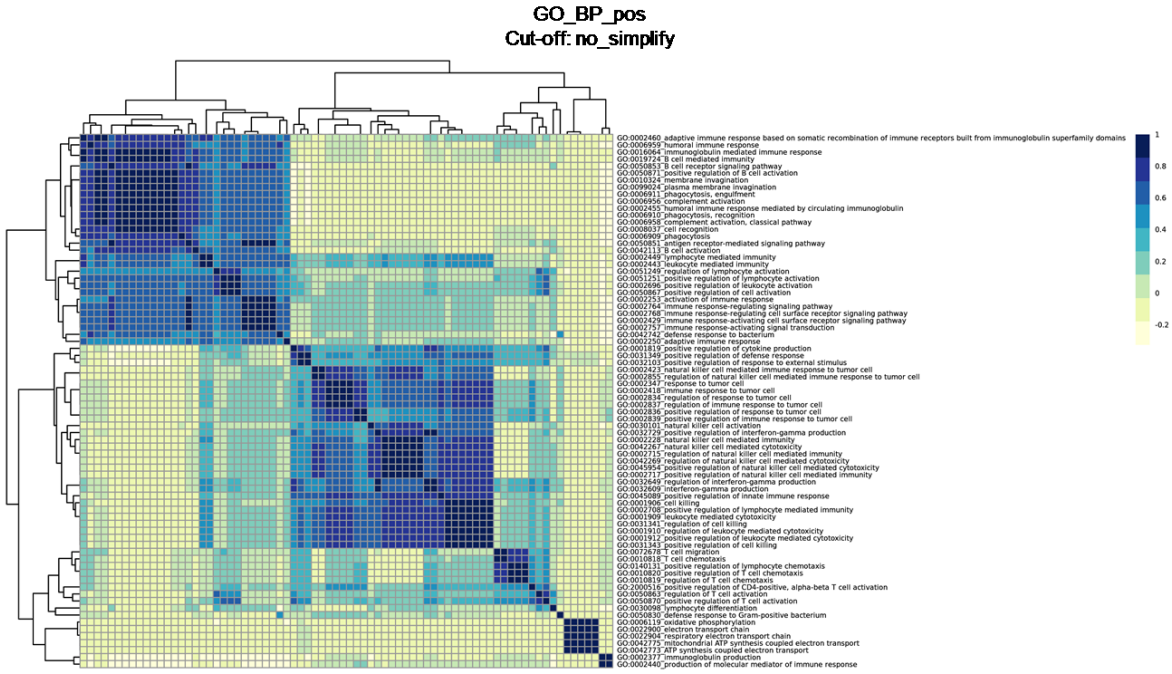

k

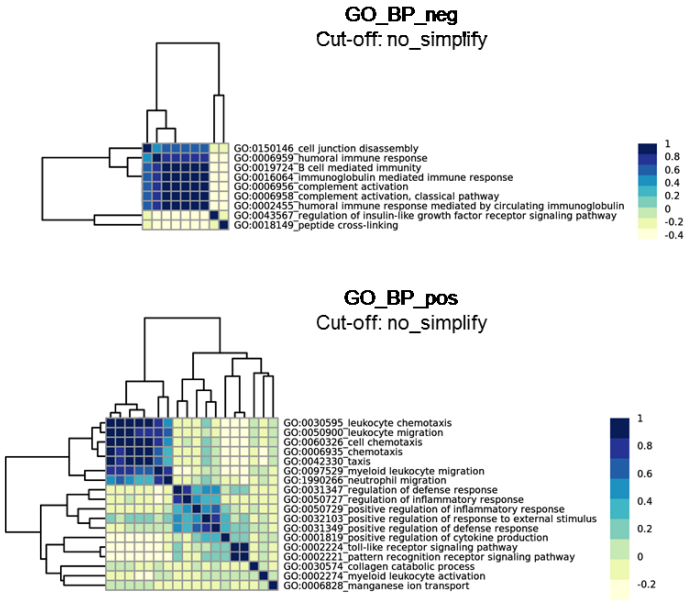

NSG mice
mBraf trunc
B220+ GFP+

l

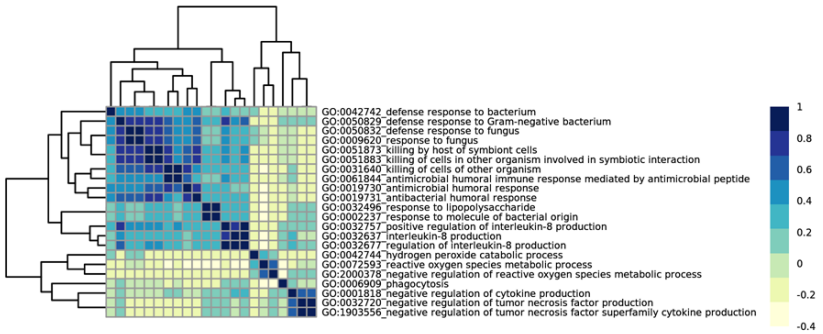

NSG mice
mBraf trunc
B220+ GFP-


m
GO_BP
Cut-off: no_simplify
C57 mice
mBraf trunc
CD11b+ GFP-
GO:0009451 RNA modification
GO:0006399 tRNA metabolic process
GO:0008033 tRNA processing
GO:0034660 ncRNA metabolic process
GO:0034470 ncRNA processing
GO:0016072 rRNA metabolic process
GO:0006364 rRNA processing
GO:0022613 ribonucleoprotein complex biogenesis
GO:0042254 ribosome biogenesis
GO:0030099 myeloid cell differentiation
GO:0002573 myeloid leukocyte differentiation
GO:0048872 homeostasis of number of cells
GO:0002262 myeloid cell homeostasis
GO:0034101 erythrocyte homeostasis
GO:0030218 erythrocyte differentiation
GO:0051052 regulation of DNA metabolic process
GO:0060249 anatomical structure homeostasis
GO:0000723 telomere maintenance
GO:0032200 telomere organization
GO:0008015 blood circulation
GO:0003013 circulatory system process
GO:0030198 extracellular matrix organization
GO:0043062 extracellular structure organization
GO:0140053 mitochondrial gene expression
GO:0006790 sulfur compound metabolic process
GO:0060759 regulation of response to cytokine stimulus
GO:0042060 wound healing
GO:0045861 negative regulation of proteolysis
GO:0042113 B cell activation
GO:0050864 regulation of B cell activation
GO:0050871 positive regulation of B cell activation
GO:0019724 B cell mediated immunity
GO:0016064 immunoglobulin mediated immune response
GO:0002250 adaptive immune response
GO:0002443 leukocyte mediated immunity
GO:0002449 lymphocyte mediated immunity
GO:0002460 adaptive immune response based on somatic recombination of immune receptors built from immunoglobulin superfamily domains
GO:0002253 activation of immune response
GO:0050851 antigen receptor-mediated signaling pathway
GO:0002764 immune response-regulating signaling pathway
GO:0002768 immune response-regulating cell surface receptor signaling pathway
GO:0002757 immune response-activating signal transduction
GO:0002429 immune response-activating cell surface receptor signaling pathway
GO:0006956 complement activation
GO:0002455 humoral immune response mediated by circulating immunoglobulin
GO:0006958 complement activation, classical pathway
GO:0050853 B cell receptor signaling pathway
GO:0006910 phagocytosis, recognition
GO:0006911 phagocytosis, engulfment
GO:0006959 humoral immune response
GO:0008037 cell recognition
GO:0002706 regulation of lymphocyte mediated immunity
GO:0002708 positive regulation of lymphocyte mediated immunity
GO:0002700 regulation of production of molecular mediator of immune response
GO:0002440 production of molecular mediator of immune response
GO:0002377 immunoglobulin production
GO:0050867 positive regulation of cell activation
GO:0002696 positive regulation of leukocyte activation
GO:0051251 positive regulation of lymphocyte activation
GO:0022409 positive regulation of cell-cell adhesion
GO:1903039 positive regulation of leukocyte cell-cell adhesion
GO:0050870 positive regulation of T cell activation
GO:0042110 T cell activation
GO:0022407 regulation of cell-cell adhesion
GO:0050863 regulation of T cell activation
GO:0007159 leukocyte cell-cell adhesion
GO:1903037 regulation of leukocyte cell-cell adhesion
1
0.8
0.6
0.4
0.2
0

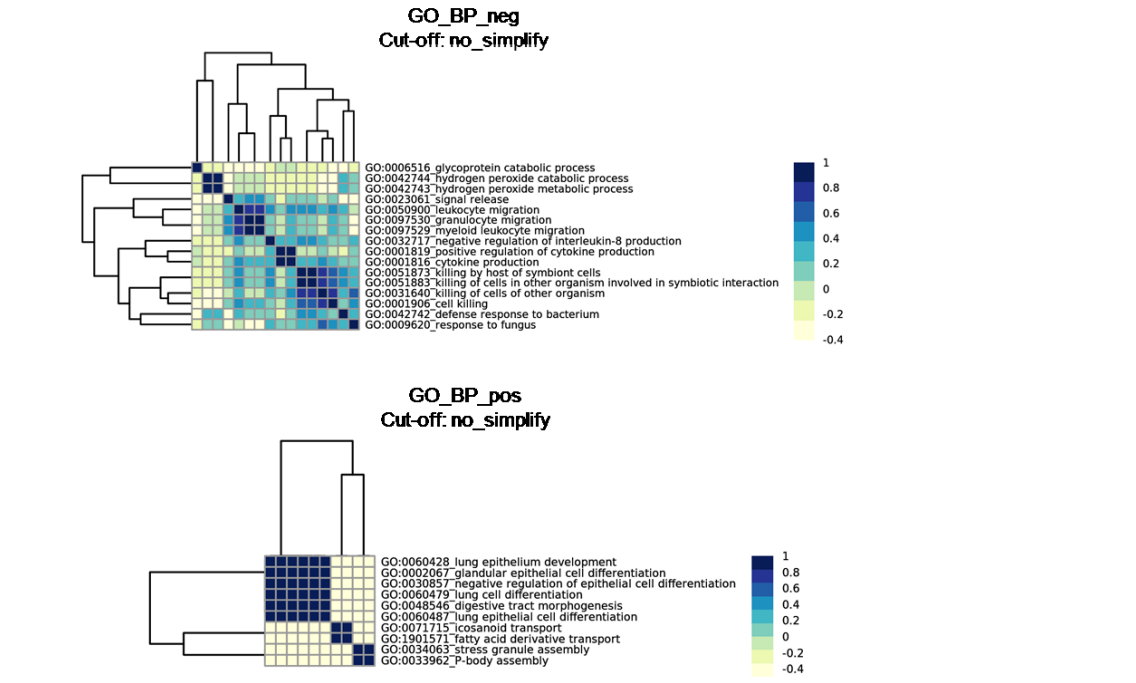
n
C57 mice
mBraf trunc
B220+ GFP+
GO_BP_neg
Cut-off: no_simplify
GO:0006516 glycoprotein catabolic process
GO:0042744 hydrogen peroxide catabolic process
GO:0042743 hydrogen peroxide metabolic process
GO:0023061 signal release
GO:0050900 leukocyte migration
GO:0097530 granulocyte migration
GO:0097529 myeloid leukocyte migration
GO:0032717 negative regulation of interleukin-8 production
GO:0001819 positive regulation of cytokine production
GO:0001816 cytokine production
GO:0051873 killing by host of symbiont cells
GO:0051883 killing of cells in other organism involved in symbiotic interaction
GO:0031640 killing of cells of other organism
GO:0001906 cell killing
GO:0042742 defense response to bacterium
GO:0009620 response to fungus
1
0.8
0.6
0.4
0.2
0
-0.2
-0.4
GO_BP_pos
Cut-off: no_simplify
GO:0060428 lung epithelium development
GO:0002067 glandular epithelial cell differentiation
GO:0030857 negative regulation of epithelial cell differentiation
GO:0060479 lung cell differentiation
GO:0048546 digestive tract morphogenesis
GO:0060487 lung epithelial cell differentiation
GO:0071715 icosanoid transport
GO:1901571 fatty acid derivative transport
GO:0034063 stress granule assembly
GO:0033962 P-body assembly
1
0.8
0.6
0.4
0.2
0
-0.2
-0.4

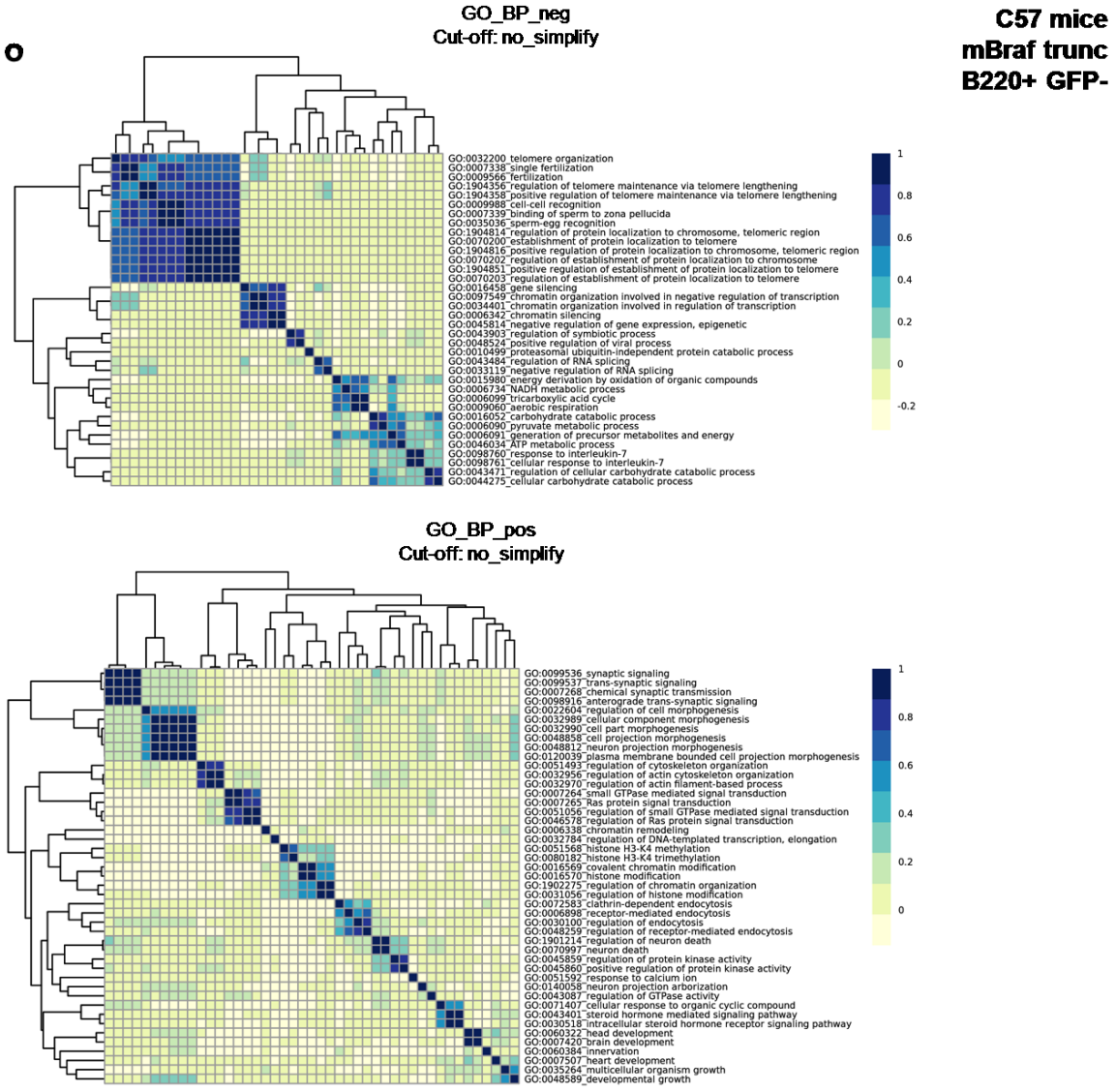

Figure 3.12. Kscore heatmaps of the enrichment analysis on gene ontology biological processes for each population.

Moreover, bystander B cells in NSG mice showed upregulation of BP involved in the ECM composition, regulation of peptidase and hydrolase, MAPK cascade, as well as upregulation of glutathione and hydrogen peroxide metabolism (**Figure 3.12f**). On the other hand, both mBrafV600E-expressing B cells and bystander B cells in C57 mice showed positive regulation of meiosis (surprisingly), mitosis, cell division, chromatin and chromosome organization, as well as DNA repair and DNA replication maintenance of fidelity (**Figure**

3.12g and h). Bystander B cells in C57 mice also negatively regulate ribosome biogenesis (**Figure 3.12h**).

In mBraf trunc mice, BP deregulation involved downregulation of ribosome biogenesis in oncogene-expressing myeloid cells in NSG mice (**Figure 3.12i**). Bystander myeloid cells in NSG mice, on the other hand, showed downregulation of antigen processing, similarly to their mBrafV600E counterpart, IFN signaling, reduction in cell motility, cytoskeleton regulation, and upregulation of lymphocyte activation, B-cell, T-cell, and natural killer cell mediated immunity (**Figure 3.12j**). Bystander myeloid cells in C57 mice similarly regulated cell motility and the immune response (**Figure 3.12m**). In mBraf trunc-expressing B cells we observed activation of the immune process, leukocyte migration, and reactive oxygen species metabolism in both NSG and C57 mice (**Figure 3.12k and 3.12n**). Interestingly, in bystander B cells in C57 telomere function, chromatin organization, splicing, and remodeling in transcriptional sites stood out (**Figure 3.12o**).

Intrigued by these findings, mostly correlating with the immune response, we decided to perform further analysis. Firstly, we checked for the expression of the genes encoding for ribosomal proteins in each population. As anticipated by the previous GO results, mBrafV600E-expressing myeloid cells and mBraf trunc-expressing myeloid cells in NSG mice, as well as bystander B cells of the mBrafV600E group in C57 mice, showed substantial downregulation of ribosomal proteins. Bystander B cells of the mBraf trunc group in C57 mice, as well, showed a tendency of downregulation of the ribosomal subunits (**Figure 3.13a**). Moreover, we detected deregulation in HLA molecules expression. Of note, mBrafV600E-expressing myeloid cells in NSG mice displayed upregulation of the orthologous MHC class I molecules (MHC-A,-B,-C,-E,-F,-G), such as H2-D1 and H2-Q1. On the other hand, MHC class II molecules, encoded by mouse genes H2-Ab1, H2-Aa, and H2-Eb1, are downregulated. Also, mBrafV600E-expressing myeloid cells in C57 mice and mBraf trunc-expressing myeloid cells in NSG mice displayed downregulation of genes encoding for MHC class II molecules (**Figure 3.13b**).

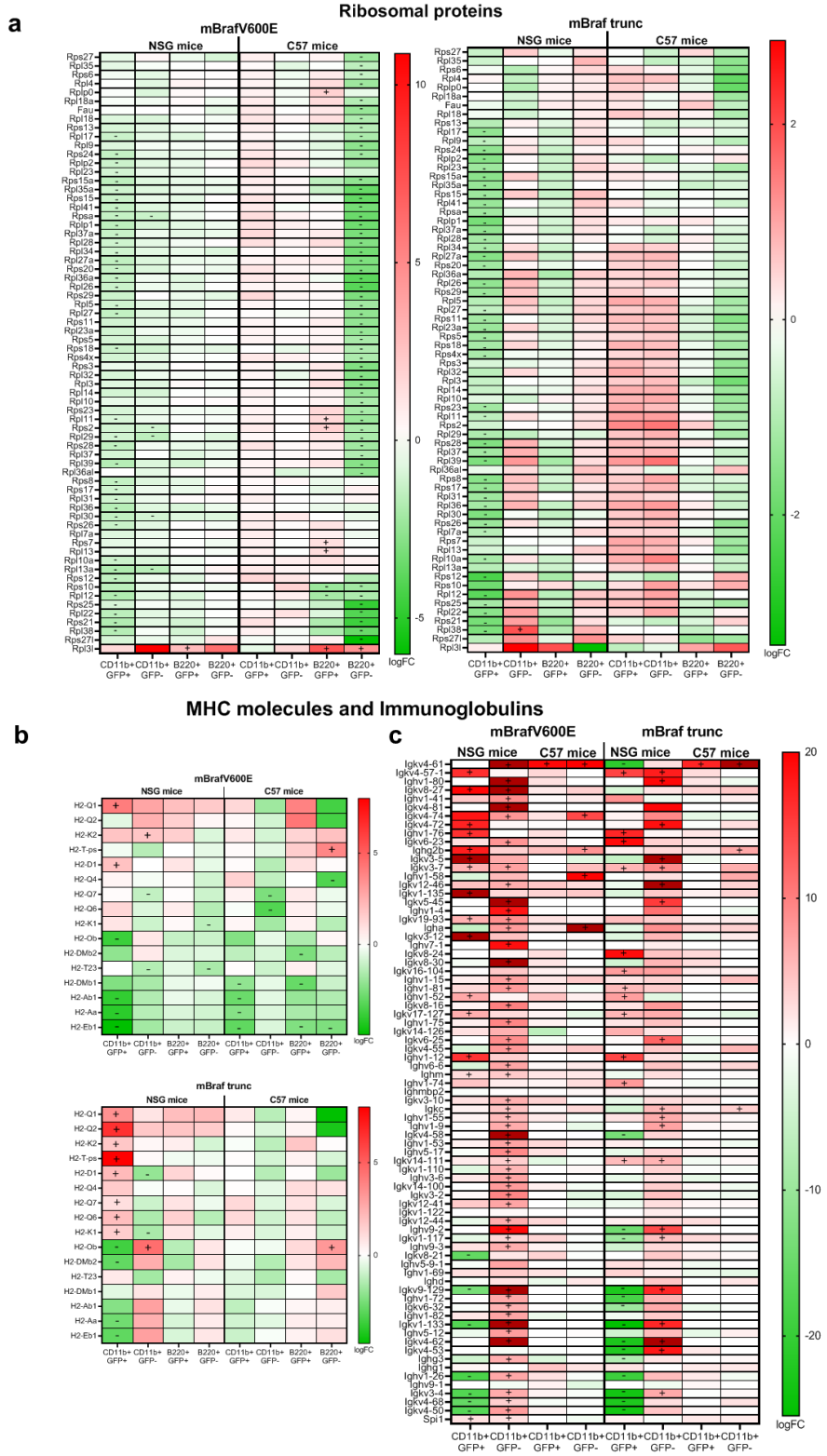

Figure 3.13. Deregulation of ribosome biogenesis, HLA molecules, and immunoglobulins. *(a) logFC of genes encoding for ribosomal proteins in each population of mBrafV600E (left) and mBraf*

trunc mice (right). Symbols – and + indicate significantly (FDR <0.05, logFC >1 downregulated or upregulated genes). The list of ribosomal proteins is the one indicated by the KEGG_RIBOSOME dataset. (b) logFC of HLA genes in each population of mBrafV600E (top) or mBraf trunc (bottom) mice. (c) logFC of heavy chain (Igh genes) and light chain (Igk genes) immunoglobulin subunits.

Finally, mBrafV600E myeloid cells in NSG mice, along with bystander myeloid cells, peculiarly deregulated (mostly through upregulation) the expression of genes encoding for the heavy chain (IgH genes) and the light chain (IgK genes) of immunoglobulins (**Figure 3.13c**). The expression of mBraf trunc also deregulated part of these genes, but to a lesser extent, suggesting a common deregulated pathway in the two oncogenic forms. These type of genes were the most significant and noticeable ones in our datasets, based on logFC and on adjusted p value (**Figure 3.9a and b**). Of note, Spi1, a transcription factor which regulates immunoglobulin production and rearrangement, was significantly upregulated in both oncogene-expressing and bystander myeloid cells in mBrafV600E NSG mice. In C57 mice we observed deregulation of only a few of the IgH and IgK genes.

In summary, gene expression analysis in NSG and C57 mice subjected to transplantation with mBraV600E-expressing HSPCs strongly downregulated pathways related to innate and adaptive immunity in both systems, with C57 mice showing positive regulation of DNA replication and chromosome organization, as well as DNA repair mechanisms.

4. Discussion

Through this PhD project, we evaluated the outcomes of the forced expression of two oncogenic mutated forms of murine Braf (mBraf trunc and mBrafV600E) in HSPCs transplanted into an immune-deficient and an immune-competent recipient. The main objectives were: (i) understanding the effects of the two Braf mutations on hematopoietic reconstitution, (ii) dissecting the similarities and differences in OIS between mouse and human cells, (iii) investigating the role of the recipient's immune system in the clearance of oncogene-expressing cells.

As for the first aim, both oncogene forms caused dose-dependent lethality in NSG mice. However, the mBraf trunc form clearly showed a delayed effect on survival compared to mBrafV600E. Moreover, we observed impairment in peripheral blood cellularity in both mBraf groups one-month post-transplant, but NSG mBraf trunc mice did not show impairment in BM or spleen cellularity like NSG mice of the mBrafV600E group. Expression of mBrafV600E resulted in impairment of B and T cells, while mBraf trunc-expressing B cells showed a selective advantage, especially in the first days of hematopoietic reconstitution. The basis of these differences in survival and hematopoiesis were possibly due to the variances in cytokine secretion between the two mBraf groups. Cytokine secretion in NSG mBrafV600E mice was exacerbated, with IL-2, IL-6, IL-12, CCL-2, CCL-3, CCL-4, CCL-5, G-CSF, while NSG mBraf trunc mice only showed a tendency of higher CCL-2 and IL-2. Thus, we show that the different mutations in Braf results in a different inflammatory response and lethality.

Moreover, these differences were further exacerbated when, instead of transplanting NSG mice, we transplanted immune-competent C57 mice. Indeed, only 60% of mBrafV600E mice died, while only 10% of mBraf trunc mice died. Furthermore, C57 mBraf trunc mice did not show any differences in hematopoietic reconstitution compared to controls, while C57 mBrafV600E mice still showed impaired hematopoiesis, with decreased PB and BM cellularity. C57 mBrafV600E mice showed higher chemokines levels (CCL-3,-4,-5), while C57 mBraf trunc mice did not show any alteration in the secretion of inflammatory cytokines.

Indeed, these differences in the impact of mBrafV600E or mBraf trunc mice on survival and hematopoiesis are also reflected in gene expression analysis on myeloid and B cells collected from NSG and C57 mice. Indeed, all cell types of the mBrafV600E groups showed upregulation in inflammatory hallmarks, while mBraf trunc mice only showed deregulation in oncogene-expressing B cells in NSG mice, oncogene-expressing myeloid cells and bystander B cells in C57 mice. However, we observed also similarities in mBrafV600E and mBraf trunc myeloid cells in NSG mice, as both groups showed downregulation of MHC class II molecules, ribosome biogenesis, and upregulation of immunoglobulin genes.

In order to explain why the mBrafV600E form is more detrimental in hematopoiesis compared to the mBraf trunc form, we should consider their frequency in human tumors. The V600E mutation, in fact, is the most frequent Braf mutation in tumors. Braf mutations in melanoma are in 75% of cases V600E mutations, while the rest are non-V600E. Even considering non-V600E mutations, the most frequent ones still have the same phenotypic effect as the V600E, which is the disruption of the interaction between the P-loop and the activation domain. This results in constitutive activation of the Braf kinase (*Greaves et al., 2013*). Truncated forms of BRAF, on the other hand, lose the N-terminal portion, regulated by RAS phosphorylation, and can be found in thyroid carcinoma, melanoma, and prostate and gastric cancer, as a result of translocations or microdeletions (*Botton et al., 2019; Palanisamy et al., 2010*). Still, the truncated form only contains the catalytic portion of the Braf kinase. Previous literature reports that the catalytic domain of Braf alone mostly functions as a monomer (*Lavoie et al., 2013*). Most studies on the kynetics of Braf activity, as well as the development of drugs against this kinase, one of them being vemurafenib, have been performed on truncated Braf, however full length Braf, compared to truncated Braf, showed strong differences in kinetics and interactions with other proteins. Indeed, full-length Braf formed homodimers instead of monomers, and was 20-fold more active than the truncated counterpart. Thus, the dimerization of Braf per se rendered the protein in a more active state that only the catalytic domain. Moreover, the interaction of MEK1 with full length Braf promoted auto-phosphorylation of the activation loop. Finally, full length Braf, in contrast with truncated Braf, is able to form heterodimers with CRAF, which is more

catalytically active than Braf homodimers (*Cope et al., 2018*). Thus, the lack of the N-terminal region in mBraf trunc may limit both the catalytic potential and the interaction with other proteins for downstream signaling.

In summary, we have shown that both types of mBraf mutation, as well as the immunological status of the recipient mice, has a profound impact on mouse survival. The dissimilar outcomes in the two mBraf groups are a result of a different cytokine secretion profile triggered by the different mutations, as well as the interaction of the transplanted cells with the surrounding microenvironment. Moreover, we also observed drastic differences from the previous humanized model (*Biavasco, Lettera, et al., 2021*), which showed a SASP characterized by IL1α, IL1β, TNFα, IL8, IL6, CCL-2, and CCL4, while in our case we showed delayed mortality and secretion of other cytokines and chemokines. In particular, in our NSG mBrafV600E mouse group, IL1α, IL1β, and TNFα are not altered, while only IL-6, CCL-2, and CCL-4 overlapped with the cytokine profile from humanized mice, on top of higher levels of IL-2, IL-12, G-CSF, CCL-3, and CCL-5. The C57 mBrafV600E mice group shared only CCL-4 with the human cytokine profile. Therefore, this data suggests that differences in secretory profiles between the humanized models and the murine models might explain the differences in survival and paracrine effect on bystander cells. In the humanized model, higher levels of IL1α, IL1β, and TNFα inversely correlated with the survival of treated mice, and inhibition of TNFα by infliximab treatment abrogated paracrine senescence in vivo (*Biavasco, Lettera et al., 2021*). This suggests that the lack of secretion of TNFα signature might explain the lack of paracrine senescence on bystander B cells and the delay on mortality.

Regarding other senescence markers, gene expression analysis revealed overexpression of cell cycle inhibitors such as Cdkn2d, encoding for $p19^{Ink4d}$, and Cdk2ap2, encoding for p14, in oncogene-expressing mouse cells. On the other hand, genes of common senescence markers such as Cdkn2a, encoding for $p16^{Ink4a}$ and $p19^{Arf}$, and Cdkn1a, encoding for $p21^{Cip}$, overexpressed in the humanized model, were not present or even downregulated in both NSG or C57 mice transplanted with mBrafV600E or mBraf trunc HSPCs.

Concerning the inconsistencies between mouse and human senescence, literature reports that replicative senescence of mouse cells does not resemble human cells. Human fibroblasts undergo proliferation only to a certain extent until the extensive shortening of telomeres blocks the cell cycle and induces senescence. Furthermore, human fibroblasts in culture do not immortalize spontaneously, since it would require the inactivation of both p53 and $p16^{Ink4a}$, other than the telomere shortening (*Wright and Shay, 2000*). Mouse cells, on the other hand, can undergo senescence, but in a telomere-independent fashion, suggesting that the trigger of senescence has a different nature in mice (*Prowse and Greider 1995*). Moreover, mouse fibroblasts cultured under physiological oxygen conditions (3%) do not undergo replicative senescence, while under atmospheric oxygen conditions (20%) they do, but again with a mechanism of accumulation of DNA damage that is telomere-independent. The same study also showed that mouse cells are more sensitive to oxidative stress compared to human cells (*Parrinello et al., 2003*). This can be explained by the higher expression levels of the DNA repair genes in human cells compared to mouse cells (*MacRae et al., 2015*). Interestingly, the ROS signaling pathway and hypoxia are two of the most significant hallmarks in oncogene-expressing myeloid cells, which is the population driving inflammation in our model, based on our gene expression data. Thus, it is plausible that the observed senescent phenotype in our murine system might not be related to telomere shortening, but to the accumulation of DNA damage that is telomere-independent. To confirm this hypothesis, further experiments will be performed in the future.

Oxygen levels are also known to influence the production of SASP in mouse cells, as physiological levels confer mouse senescent cells a human-like SASP (*Coppé et al., 2010*). In our in vivo model, however, thus in physiological oxygen levels, we show NFκB activation, as well as a mouse SASP, but with exclusion of IL-1 production. This shows that mouse SASP, in the context of oncogene-induced-senescence, did not induce IL-1 production. Inhibition of NFκB signaling in senescent cells decreases the levels of all SASP factors except IL-1, meaning that the production and the secretion of that particular cytokine are both independent and upstream of NFκB signaling (*Kang et al., 2015*). Lau and David (*Lau and David, 2019*) suggested that chromatin fragments, after the onset of senescence,

activated the cGAS-STING pathway, thus triggering different downstream signaling, one of them being the inflammasome and IL-1 production. Thus, there could be differences between mouse and human cells in the activation of IL-1-specific SASP that are still currently indefinite in the field. It could be possible that, in our mouse model of OIS, we only upregulated NFκB signaling without triggering IL-1-specific signaling. To test this hypothesis, in vitro experiments regarding the activation of the inflammasome in mouse HSPCs after expression of mBrafV600E or mBraf trunc will be performed.

Regarding other differences between human and mouse senescence, we observed upregulation of cell cycle inhibitors such as Cdkn2d ($p19^{Ink4d}$) and Cdk2ap2 (p14), inhibiting Cdk4/6 and Cdk2 respectively. "Traditional" cell cycle inhibitors such as Cdkn1a ($p21^{Cip}$) or Cdkn2a ($p16^{Ink4a}$), were either upregulated only in bystander B cells of the NSG mBrafV600E and mBraf trunc groups, or downregulated, respectively. The absence of $p16^{Ink4a}$ upregulation in mouse senescent cells is not uncommon, since its activity is more human-specific (*Buj et al., 2021*). In our case, however, $p19^{Ink4d}$ plays a greater role in cell cycle inhibition. Literature reports that $p19^{INK4D}$ in human has a role in cell cycle regulation in HSCs, terminally differentiated erythrocytes, and AML cells, but not in healthy myeloid or lymphoid cells (*Tschan et al., 1999*). In mice, $p19^{Ink4d}$ is described to inhibit the entrance of HSCs into the cell cycle, by halting them in the G_0 phase (*Hilpert et al., 2014*). Furthermore, pharmacological stress induction in $Cdkn2d^{-/-}$ cells increases cell mortality and apoptosis, suggesting a protective and anti-apoptotic role in hematopoietic stem cells. Of note, the same paper shows higher total cellularity in the BM of 8-week-old $Cdkn2d^{-/-}$ mice than controls, as well as a skewing toward the lymphoid population. This result is peculiar, considering that our donor and recipient experimental mice are of the same age. In our model, in which $p19^{Ink4d}$ is upregulated in myeloid cells of mBrafV600E NSG and oncogene-expressing B cells in C57 mice, we observe: impairment of oncogene-expressing lymphoid cells, as well as impairment in total BM cellularity. Future experiments performing quantitative PCR on in vitro samples will validate RNA-sequencing data for specific genes of interest, especially the variation of expression of these cell cycle inhibitor genes (for examples, Cdkn2a). To our knowledge, our work highlights for the first time the specific role of $p19^{Ink4d}$ in OIS in mouse

HSPCs. Also given the distinct role that $p19^{Ink4d}$ has in hematopoiesis, our results could suggest that the activation of specific cell cycle inhibitors could be dictated by the cell type, species, and the immunological background of the microenvironment in which senescence is occurring.

Regarding the similarities and differences between an immune-deficient and an immune-competent host, in both C57 and NSG mice biological processes involving innate and adaptive immune response were negatively regulated, with impairment of T and B cells proliferation, activation, and downregulation of MHC Class II molecules. In contrast, we observe that, in an immune-competent host, oncogene-expressing cells can be eliminated in 40% of the mice, ameliorating their phenotype and their survival. Moreover, we observe the upregulation of hallmarks and biological processes related to G2/M checkpoint, E2F targets, mitosis, and DNA repair in both mBrafV600E-expressing and bystander B cells of C57 mice.

In particular, negative regulation of T cell toxicity and T-helper 1 type immune response was observed in NSG mice, processes that are correlated with immune escape by tumor cells (*Raskov et al., 2021; Basu et al., 2021*). Moverover, the downregulation of MHC class II molecules is one of the distinctive markers of tumor-associated macrophages (TAMs), commonly known as immune-suppressive macrophages in the tumor microenvironment (*Wang et al., 2011)*. Moreover, Tap1, a fundamental gene for antigen presentation through MHC class I molecules, is significantly downregulated in all populations of NSG mBrafV600E mice, as well as B cells in C57 mBrafV600E mice (Shown in **Appendix**). Myeloid cells in C57 mBrafV600E mice, however, do not downregulate Tap1, suggesting that antigen presentation processing of MHC Class I molecules in the myeloid cells of C57 mice is preserved. MHC class I molecules presentation is fundamental for the differentiation of type 1 T helper cells, known for their anti-tumoral pro-inflammatory role (*Kidd,* 2003).

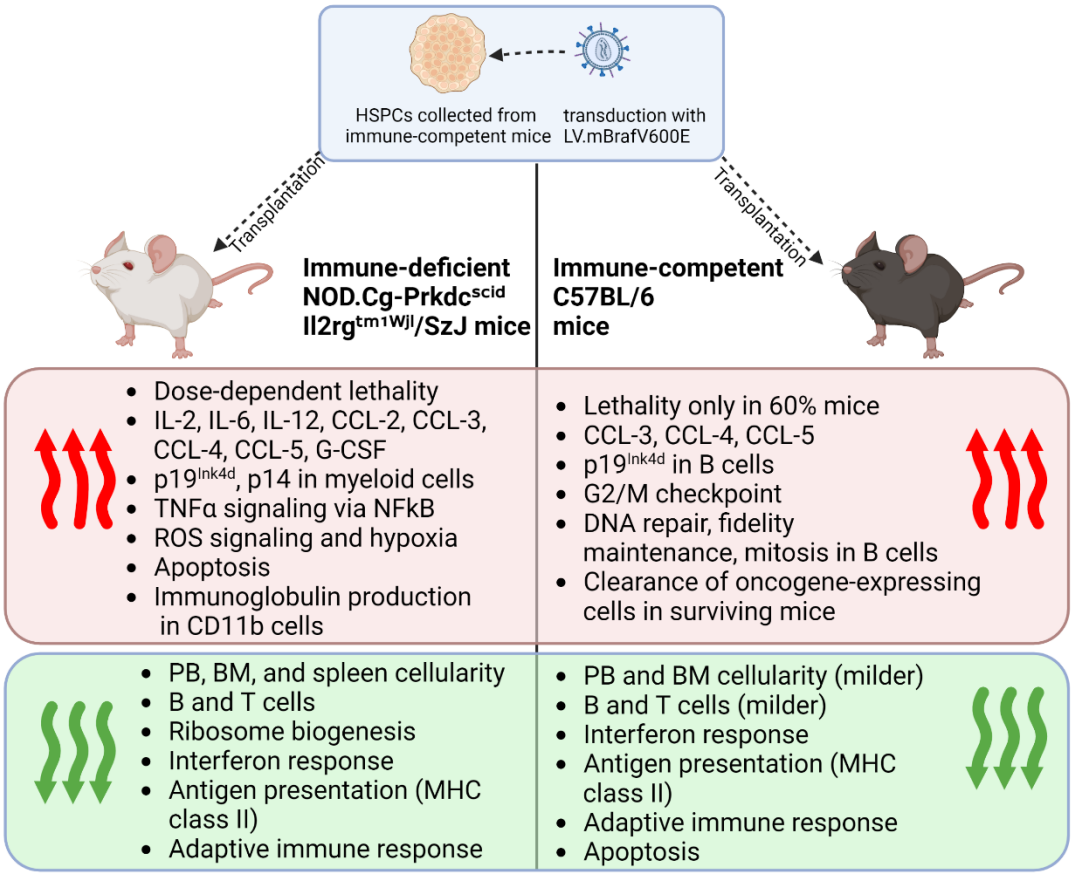

Figure 4.1 Summary of the results obtained in this project. *Red arrows represent positive regulation/upregulation, green arrows represent negative regulation/downregulation/impairment. Figure generated with BioRender.*

The downregulation of antigen presentation is in part discordant with previous literature, in which the acquisition of mutations like BRAFV600E caused OIS and led to upregulation of MHC Class II molecules and secretion of IL1β, favoring melanoma suppression and clearance by the immune system (*van Tuyn et al., 2017*). In our case, we observe the opposite effect, with absence of secretion of IL1β and downregulation of MHC Class II molecules, together with other signs of tumor suppression. This constransting result may be explained by the different type of senescent stimuli that we observe. Indeed, in the case of the work by van Tuyn et al, OIS was the result of the activation of a protective mechanism against melanoma progression, favoring a more "acute" response that may favor the clearance of senescent cells. In our case, on the other hand, the integration of a LV expressing constitutively active Braf constantly clearly generates a chronic an immunesuppressive

microenvironment, similarly to what happens in tumors (*Wang et al., 2011*). Moreover, we observe upregulation of genes such as H2-Q1 and H2-D1 in NSG mice of the mBrafV600E and mBraf trunc group. These genes are the orthologs of the human HLA-E gene, which encodes for non-canonical MHC class molecules. A study on the interaction between senescent cells and the immune system showed that senescent cells can upregulated HLA-E molecules in order to escape clearance by NK cells and T CD8+ cells (*Pereira et al., 2019)*. Interestingly, H2-Q1 and H2-D1 in immune-competent recipients are not upregulated, further confirming that the immunological competence of recipient mice is less immunosuppressive.

Another interesting observation is that both oncogene-expressing and bystander myeloid cells of the NSG mBrafV600E group, but not C57 mice, overexpress CD47, commonly known as a "do not eat me" molecule (Showed in **Appendix**). CD47 is often overexpressed at the surface of tumor cells and exploited as a means of immune escape (*Takimoto et al., 2019*). Moreover, a previous study observed that senescent lung fibroblasts overexpress CD47 and favor immune evasion (*Hernández-Mercado et al., 2021*). Between the downregulated hallmarks and the negatively regulated processes, we observe impairment in IFNα or IFNγ responses in mBrafV600E mice, in both immune-deficient and immune-competent mice. Indeed, induction of type I IFN response is a novel anti-tumoral therapeutic approach (*Cao et al., 2021*). Type II IFN response, on the other hand, and its role in tumors is a debated subject. IFNγ is a cytokine with both pro-tumoral and anti-tumoral roles (*Gocher et al., 2022*). Mostly produced by T cells, it can also be secreted by a subset of B cells (CD11ahiCD16/CD32hi) against bacterial infection (*Ballesteros-Tato et al., 2014*), however, the role of this specific subset in the tumor microenvironment is not known. Both myeloid and B cells show downregulation of IFN signaling, meaning that deficiency in these pathways has a detrimental effect on the whole system. This data shows combined negative regulation of type I and type II IFN responses, impaired adaptive immune system, and impaired antigen presentation process. These findings might suggest that mBrafV600E-expressing HSPCs have generated an immune-suppressive microenvironment that impedes the elimination of senescent cells by the immune system, leading to the progression of the disease.

Despite immune suppression, a percentage of immune-competent recipients could eliminate oncogene-expressing cells and survive, also reconstituting correct hematopoiesis. Furthermore, the impairment in cellularity after oncogene expression, specifically of B cells, is milder in C57 recipients compared to NSG mice. B cells are the lymphocyte subset most sensitive to DNA damage (*Felgentreff et al., 2021*) however, the differences in severity of the impairment depending on the recipient strain are fascinating. Both recipients were transplanted with HSPCs collected from donor immune-competent (C57 CD45.2) mice. Thus, the only biological differences between the two experimental conditions are the residual recipient HSPCs and stromal cells, constituting the recipient's microenvironment in which donor cells engrafted. The microenvironment around immune cells is known to support their survival and function. For example, in the context of DNA damage and telomere erosion, a recent study showed that antigen-presenting cells exchange vesicles containing telomere portions and the recombination factor Rad51 with T cells, to preserve them from replication exhaustion (*Lanna et al., 2022*). Recipient cells in NSG mice, however, have mutations in genes that are fundamental for the correct function of immune cells (*Shultz et al., 2007*), in particular macrophage phagocytosis, antigen presentation and vesicle formation. Thus, we hypothesize that antigen-presenting recipient cells in NSG mice, impaired in their immune function, were unable to aid donor immune cells to avoid exhaustion. This resulted in the inability to eliminate oncogene-expressing cells when mBrafV600E expression generated an inflammatory and immune-suppressive microenvironment.

Other differences between NSG and C57 mBrafV600E mice concern the apoptotic process. Indeed, mBrafV600E-expressing myeloid cells in NSG upregulated pro-apoptotic genes. In C57 mBrafV600E mice, we observe the opposite effect**.** More specifically, the Anxa1 gene is upregulated in all the cell populations of the NSG mBrafV600E groups (see **Appendix**). Anxa1 encodes for Annexin-1, known to be a strong regulator of inflammation in the tissues. Annexin-1 is cleaved for activation by neutrophil elastases, limits the recruitment of immune cells at the inflamed site and their pro-inflammatory functions, and positively regulates apoptosis and the elimination of apoptotic cells by macrophages (*Sugimoto et al., 2016*).

Moreover, Elane, coding for neutrophil elastase, is also upregulated, suggesting that Annexin-1, through cleavage, may play a role in the negative regulation against senescent cells that we observe in this model. Interestingly, we observe the opposite effect in C57 mBrafV600E mice, in which Anxa-1 is downregulated in both oncogene-expressing and bystander B cells, but not in myeloid cells (see **Appendix**). Elane is also either not significantly deregulated or downregulated in bystander B cells. Finally, among the upregulated transcription factors in NSG mBrafV600E mice, we observed Foxo3 in both oncogene-expressing and bystander myeloid cells (see **Appendix**), along with deregulation of the pro-apoptotic Bcl3 and Bcl10 genes in oncogene-expressing myeloid cells (data not shown). Foxo3 promotes apoptosis by regulating NFκB activation, since the knock-out of Foxo3 leads to hyperactivity of T cells because of aberrant NFκB signaling (*Su et al., 2004*). In C57 mice, we do not observe the deregulation of Foxo3, Bcl3, and Bcl10. Altogether, these results might suggest that in immune-competent mice the microenvironment around senescent cells, despite being immune-suppressive, does not induce apoptosis and is more prone to the recruitment of immune cells.

Other upregulated pathways in C57 mBrafV600E mice include G2/M checkpoint and E2F target hallmarks, as well as positive regulation of chromatin and chromosome organization, mitotic processes, and DNA repair and fidelity maintenance. In particular, B cells in C57 mice are showing upregulation of genes involved in the DNA replication machinery and in cell cycle checkpoint genes, which are fundamental to avoid the accumulation of DNA damage that is detrimental to B cell development. These results could potentially imply that B cells are escaping senescence in some way, by returning to the cell cycle and possibly having a role in the elimination of senescent cells that we observe in vivo. Another consideration could be that, in both NSG and C57 mice, we have performed RNA-sequencing on the few surviving B cells in a context in which this compartment is strongly impaired, albeit to a lesser extent in C57 mice. This could mean that the mitotic phenotype in B cells is one of the surviving cells, which are able to escape senescence. Overall, in our immune-competent model, it is not clear which immune cell population is responsible for the clearance of mBrafV600E-expressing cells. Further experiments on gene expression in T cells and in

vivo experiments selectively eliminating specific immune subsets (antigen presenting cells, NK cells, T cells, B cells) will elucidate this aspect in the future. Moreover, the contribution of the immunological competence of recipient mice in the clearance of oncogene-expressing cells could be elucidated by the use of different strains as recipient mice, for example NOD mice or $Rag1^{-/-}$ mice, which lack the capability of producing functional antigen presenting cells or B and T cells, respectively. Another aspect that could be addressed in the future is whether the dampening of inflammation in NSG recipients, for example with the use of senolytics and/or senomorphics, could favor the clearance of senescent cells. The reduction of inflammation, similarly with what happens in C57 recipients, could potentially give an advantage to immune cells.

We have observed the deregulation of genes encoding for immunoglobulin heavy and light chains in myeloid cells. This phenotype is more accentuated in NSG mice of the mBrafV600E group, followed by NSG mice of the mBraf trunc group, and mostly absent in C57 mice, although some genes are still deregulated. Spi1, encoding for PU.1, is also upregulated in NSG mice of the mBrafV600E group. PU.1 is a transcription factor that regulates immunoglobulin gene expression and rearrangement in B cells (*Eisenbeis et al., 1993; Batista et al., 2017*), even though PU.1 binding sites also comprise myeloid gene promoters (*Turkistany and DeKoter, 2011*). PU.1 is a target of NFκB signaling (*Bonadies et al., 2010*), one of the upregulated hallmarks in NSG mBrafV600E mice. PU.1 overexpression is associated with accelerated replication in AML cells, but also with the induction of senescence in primary hematopoietic cells through the DDR (*Rimmelé et al., 2017; Delestré et al., 2017*), and for this reason it is considered both a tumor promoter and a tumor suppressor. Regarding immunoglobulin production by myeloid cells, previous studies have reported that AML cells collected from patients express immunoglobulin heavy chain genes (*Qiu et al., 2013*). A following study of the same group highlighted that rearrangements of the variable portion of the heavy chain of immunoglobulins could be detected not only in cells collected from AML patients but also in 40% of monocytes samples and 15% of neutrophil samples collected from healthy donors (*Huang et al., 2014*). Interestingly, a rare form of histiocytosis named crystal-storing histiocytosis (CSH) is characterized by the

accumulation of immunoglobulins in a crystal form in the cytoplasm of histiocytes. 90% of CSH patients are affected by disorders in myeloid or lymphoid cells, the most recurrent ones being multiple myeloma or monoclonal gammopathy. (*Lebeau et al., 2002; Dogan et al., 2012: Thakral and Courville, 2014; Wiese-Hansen et al., 2021*). To our knowledge, the data from our study are the first to highlight immunoglobulin gene deregulation in senescent myeloid cells. These results are peculiar, given the previous literature connecting the expression of BRAFV600E in HSPCs and the onset of OIS with histiocytic disorders, such as LCH and ECD (*Biavasco, Lettera et al., 2021; Bigenwald et al., 2021; Molteni et al., 2021*). Histopathological analysis on our mice is currently ongoing. That analysis will eventually confirm not only the presence of histiocytic lesions in our model but also whether the deregulation of IgH and IgK genes results in the production and accumulation of immunoglobulins, similar to what happens in CSH patients.

With this PhD project, we have achieved characterization of oncogene-induced senescence in two different mouse models, an immune-deficient one and an immune-competent one. With further analysis and comparison of the two RNA-sequencing, we plan soon to identify a set of biomarkers of senescence and genotoxicity. These biomarkers will be fundamental to enhance the sensitivity of safety studies and identify early signs of genotoxicity and/or leukemia development in gene therapy patients. After this step, a set of biomarkers will be important to also develop novel senolytic approaches for the elimination of detrimental senescent cells.

5. Matherials and Methods

5.1 Cloning of lentiviral vectors constructs

We utilized the Snapgene software to design our constructs. We utilized the backbone of the 3rd generation lentiviral vector encoding for human BRAFV600E (named construct #3041 in our lab), reported in our previous work (Biavasco, Lettera, et al., 2021). The construct contains the following features:

pCCL.SIN.cPPT.SV40ployA.eGFP.minCMV.hPGK.hBRAFV600E.Wpre

Neutral marker Transgene

The vectors are constituted by a bidirectional construct, with the human PGK promoter controlling the transcription of the BRAFV600E transgene in one direction, while on the other a minimal CMV promoter controls the transcription of the GFP gene, as a neutral marker for transduced cells. Using Snapgene, we substituted the transgene portion with 3 different inserts: the coding sequence of mouse WT Braf for the #3044 (LV.mBrafWT) construct, the aberrant splicing product of truncated mouse Braf (characterized in *Montini et al., 2009; Cesana et al., 2012*) for the #3043 (LV.mBraftrunc) construct, and the mouse mBrafV600E sequence in the #3097 (LV.mBrafV600E) construct. For the last insert, we consulted the Materials and Methods of *Dankort et al., 2009* to perform mutagenesis on Snapgene and add the V600E mutation to the mBraf WT coding sequence. As a control vector, we used another 3rd generation lentiviral vector construct, coding only for eGFP. These constructs constituted our *transfer vector plasmids* for vector production.

5.2 Lentiviral vector production

We produced lentiviral vectors with the previous constructs by using the following protocol. We seeded 7.5 x 106 cells in a volume of 22 ml in a 15 cm dish. The medium used to culture cells is Iscove's Modified Dulbecco's Medium (IMDM), with 10% fetal bovine serum, Penstrep (100 U/ml), and glutamine (2 mM). Two hours before transfection, we changed the cell medium. Cells were left incubated at 37°C. We prepared the plasmid DNA mix with

ENV plasmid (VSV-G) (9 µg for 2 dishes), pMDLg/pRRE plasmid (III Gen Pack) (12.5µg for 2 dishes), REV plasmid 6.25 µg, pADVANTAGE (15 µg for 2 dishes), *transfer vector plasmid* (32µg for 2 dishes). The final volume of the plasmid solution was 1125 µl with 0.1X TE/dH2O (2:1). After incubation of the mix RT for 5 minutes, we added 125 ul of 2.5M CaCl2. We vortexed at full speed the plasmid DNA mix and added dropwise 1250 ul of HBS 2X for each 1250 ul of the mix, immediately adding the precipitate to the cells. After the addition of the precipitate, cells were incubated again at 37°C. The day after transfection, we quickly observed cells at the optical microscope the small calcium precipitates of plasmid DNA, accumulating on the bottom of the plate in the spaces between the cells. 16 hours after transfection we replaced the cell medium with fresh IMDM adding 1 uM Na butyrate. 30 hours after changing the media, we collected cell supernatant, containing our prepared lentiviral vectors. We did so by filtering cells with Stericup 0.22 µm and ultracentrifugation of the supernatant at the following conditions: 70,000 g, 2 hours, 4°C. Afterward, we discarded the supernatant and let the 38 ml collection tubes dry off completely. We resuspended the vector pellet in 70 ul of PBS for each tube. We aliquoted the vectors in 0.5 ml Eppendorf and stored them at -80°C until usage. We prepared two small aliquots (unconcentrated and concentrated) of each vector for their titration.

5.3 Lentiviral vector titration

In 2 6-well plates for each vector construct (1 plate for un-concentrated, 1 for concentrated), we seeded 5x104 HEK-293T cells in each well, in 1 ml of complete IMDM medium. 24 hours later, we performed dilutions of the concentrated vectors, by first adding 10 ul of the concentrated vector to 90 ul of PBS. Afterward, 20 ul of this first dilution were added in 980 ul of IMDM (dil -3). From this second dilution, we performed 5 other serial 1:10 dilutions (-4, -5, -6, -7, -8) using 100 ul of the previous one into 900 ul of IMDM. We discarded the previous medium of HEK-293T cells and added 500 ul of each of the dilutions into each well. Afterward, we added 500 ul IMDM supplemented with Polibrene 2X. Thus, we obtained vector dilutions ranging from 1x10-3 to 1x10-8. The remaining volume of vector dilutions will be used to quantify p24 and calculate infectivity. For the unconcentrated dilutions, we

firstly performed a 1:5 dilution using 200 ul of un-concentrated vector and 800 ul of IMDM (dil -1), and 5 following 1:10 dilutions (dil -2, -3, -4, -5, -6). Similarly to before, we added 500 ul of each dilution to the cells and 500 ul of medium + Polibrene to each well, thus obtaining dilutions ranging from 1x10-1 to 1x10-6. 24 hours post-transduction, we added 1 ml of complete IMDM to each well. After 10 days post-transduction, we assessed levels of transduction for each condition by Fluorescence Associated Cell Sorting (FACS), measuring the percentage of GFP+ cells. The percentage of marker-positive cells among the dilutions should decrease with a sigmoid shape. We calculated the vector titer by multiplying the GFP+ cells of the conditions in the linear range for its dilution factor (between 10% and 40% transduction) and the number of transduced cells (105). Titer will be expressed in transducing units per ml (TU/ml). After 2 weeks of culture, cells were collected for DNA extraction. Droplet digital PCR (ddPCR) probes against the LV LTR and a housekeeping gene (GAPDH) were used to quantify the relative amount of vector per genome in each dilution.

5.4 Mouse models

For in vivo experiments, we utilized 2 different strains of recipient CD45.1 mice: NOD.Cg-Prkdc^{scid} Il2rg^{tm1Wjl}/SzJ (NSG) mice to generate the immune-deficient model and C57BL/6 (C57) mice for the immune-competent model. Female 8-week-old mice were bought from Charles River Laboratories International, Inc., and irradiated with a sub-lethal dose (200 cGy) if NSG or lethal dose (800 cGy) if C57, 4 hours before transplantation. Antibiotics to prevent infections after irradiation was administered to the mice for two weeks post-transplant.

5.5 Mouse HSPCs purification and transduction

Mouse HSPCs were collected from the BM (tibia, femur, and humerus bone) of 8-week-old C57 CD45.2 mice, to distinguish donor (CD45.2) and recipient (CD45.1) cells in the following analyses. After bone collection, BM cells were flushed with a syringe with a 26G needle containing a solution of PBS + FBS 2% into a 50 ml falcon. Cells were passed through a syringe to have a single cell suspension and filtered with a 40 μm cell strainer to avoid aggregates. After centrifuging for 10 min at 1500 rpm, HSPCs were purified using the

Miltenyi Biotec Lineage Cell Depletion Kit, mouse. Cells were counted and resuspended in 40 ul of MACS buffer per 107 cells. 10 ul of Biotin-Antibody Cocktail per 107 cells were added for staining, and cells were incubated for 10 min at 40°C. Afterward, 30 ul of MACS buffer per 107 cells and 20 ul of Anti-Biotin Microbeads per 107 cells were added, with a 15 min incubation at 4°C. Cells were washed with MACS buffered and centrifuged for 10 min at 1500 rpm. Afterward, cells were resuspended with 500 ul of MACS Buffer every 108 cells and purified using LS columns (1 column up to 108 cells) on the magnetic MACS separator. Column washing was carried out 3 times, each time with 3 ml of MACS Buffer. Elute was collected with 15 ml tubes. After purification, cells were counted and resuspended in serum-free Stemspan medium, to which the following additions were made: Penstrep (100 U/ml), glutamine (2 mM), SCF (100 ng/ml), TPO (50 ng/ml), Flt3-Lig (100 ng/ml), and IL-3 (20 ng/ml). The final cell concentration was 1x106 cells/ml and cells were incubated at 37°C for at least 3 hours before transduction.

5.6 Cell transduction

For cell transduction, the following calculations were made:

$$Total\ TU = N°\ of\ cells \times Molteplicity\ Of\ Infection\ (MOI)$$

$$Vector\ ul\ to\ use = (Total\ TU / Vector\ titre) \times 1000$$

Vector number	*Vector titre (vg/ml)*	*MOI used*
3043	4×10^9	10
3044	3×10^9	10
3097	1×10^9	25
743	7×10^9	25

MOI represents the number of vector particles per cells, while Vector titre of each vector was previously calculated after production. The MOI of each vector was decided based on setting up experiments assessing the levels of transduction. Based on those experiments, we fixed the MOI in order to have at least 30% of GFP expressing cells. This percentage was decided

based on the previous humanized model, in which 30% of transduction was the standard transduction protocol for the induction of oncogene (hBRAFV600E) induced senescence in human HSPCs (*Biavasco, Lettera, et al., 2021*).

5.7 HSPCs transplantation

Mice were transplanted with donor HSPCs 24h after transduction. For conditioning, mice were irradiated with different doses based on the genotype. For NSG mice, we performed sub-lethal (200 cCy) irradiation 4 hours before transplantation. Afterward, we transplanted each mouse with 1.5x105 cells per mouse for the first mBraf trunc experiment (Results, **Figure 3.2**) or 2x105 cells for the mBrafV600E experiments. For C57 mice, we performed lethal (800 cGy) irradiation, dividing it into two equal doses separated 4 hours between each other. After 4 hours, we transplanted 3x105 cells per mouse. Cells were injected via the tail vein under BSL2 hoods, to preserve the sterile conditions of the cells and the mice.

5.8 Blood plasma collection, cytokine levels measurement, FACS staining of peripheral blood, BM, and spleen

We retrieved peripheral blood (PB) from experimental mice under anesthesia (isoflurane) by performing retro-orbital bleeding with heparin or EDTA-coated capillary tubes. To collect plasma, we centrifuged samples at 4000 rpm x 10 min at 4°C, collected the plasma, and stored it in -80°C freezers. Afterward, plasma samples were sent to Bioclarma – Research and Molecular Diagnostics, who performed cytokine levels measurements using the Bio-Plex Pro Mouse Cytokine 23-plex Assay #M60009RDPD.

The plasma-depleted PB samples were re-suspended in FBS, with the same amount of volume of plasma that was depleted, to reconstitute PB density. Afterward, we performed staining by adding antibodies and incubating samples for 20 min RT in the dark. Samples were lysed using the TQ-Prep Workstation instrument by Beckman Coulter in the FRACTAL facility in our institute, washed two times, and re-suspended in PBS + FBS 2%. BM and

spleen sample cells were lysed before staining using 1 ml of ACK (Ammonium-Chloride-Potassium) Lysing Buffer by Thermofisher. Cells were washed with PBS + FBS 2% and then stained for 20 min RT in the dark. After staining, cells were washed and re-suspended in PBS + FBS 2%. In each sample, 20 ul of Precision Count Beads™ by Biolegend (concentration: 1.03 x 106 beads/ml) was added for quantitative measurement of cellularity. Samples were then analyzed with BD FACSymphony™. After retrieving raw .fcs data, measurement of absolute counts was performed using the following formula provided by Biolegend:

$$\text{Absolute cell count } \left(\frac{\text{cells}}{\mu\text{l}}\right) = \frac{\text{cell count} \times \text{Precision Count Beads™ volume}}{\text{Precision Count Beads™ count} \times \text{cell volume}} \times \text{Precision Count Beads™ concentration } \left(\frac{\text{Beads}}{\text{ul}}\right)$$

BD antibodies used for staining are the following:

Code	*Surface molecule*	*Fluorophore*
560696	Anti-Mouse CD45.2	PE-Cy™7
560580	Anti-Mouse CD45.1	PerCP Cy5.5
562605	Anti-Mouse CD11b	BV421
561226	Anti-Mouse CD45R/B220	V500
565643	Anti-Mouse CD3 Molecular Complex	APC

5.9 Time-course experiment

For the time-course experiments, we characterized hematopoietic reconstitution at 6, 9, 15, and 24 days post-transplant. To do so, we transplanted 12 mice with mBraf WT-expressing HSPCs and 12 mice with mBraf trunc-expressing HSPCs. For each time point, we euthanized 3 mice and collected peripheral PB, BM, and spleen. Samples were analyzed with BD FACSymphony™. For PB samples, we processed them as described before. At the time of euthanasia, which corresponded to the late stage of pathology in the animals, we collected BM and spleen. For BM samples, we collected cells by flushing the bones as described before. For spleen samples, we smashed the tissue using a scalpel and generated a single-cell

suspension by filtering it with a syringe and a 40 μm nylon cell strainer. Afterward, we prepared the samples for FACS analysis as described before.

5.10 Cell sorting for RNA-sequencing experiments

For the gene expression experiments, donor HSPCs purified from C57 CD45.2 mice were transduced with #3043 mBraf trunc, #3097 mBrafV600E, or #743 PGK.GFP plasmid. After 24h they were transplanted into either NSG or C57 CD45.1 recipient mice after conditioning. One-month post-transplant, recipient mice were euthanized to collect cells from the BM for sorting. After collection, we lysed BM samples, and pooled together BM cells from 3 mice of the same group, in order to have the appropriate number of starting cells. For both experiments (NSG and C57), we had 3 samples for each group (mBrafV600E, mBraf trunc, PGK.GFP). Cells for each sample were counted in order to adjust the number of antibodies for staining. We stained cells using the same antibodies listed in the .7 paragraph, leaving samples for 20 min RT in the dark. We washed samples with PBS + FBS 2% twice and re-suspended them in cold PBS for cell sorting. Cell sorting was performed by Flow cytometry Resource, Advanced Cytometry Technical Applications Laboratory (FRACTAL), a core facility of IRCCS Ospedale San Raffaele. The instruments used were BD FACSAria™ Fusion Flow Cytometer and Beckman Coulter's Cell Sorter MoFlo Astrios. The gating strategy is specified in the Results section, in **Figure 3.8**. We sorted 4 different populations of donor cells: oncogene-expressing myeloid cells (CD11b+ GFP+), bystander myeloid cells (CD11b+ GFP-), oncogene-expressing B cells (B220+ GFP+), bystander B cells (B220+ GFP-). We added the appropriate amount of RLT + β-mercaptoethanol to the sorted samples and froze them at -80°C before RNA extraction.

5.11 Preparation of the RNA-sequencing cDNA library

RNA was extracted using QIAGEN RNeasy Micro Kit. RNA was quantified using Nanodrop and its quality was assessed with the High Sensitivity RNA ScreenTape Analysis kit, running the samples at the Agilent Tapestation. Retro-transcription and double-strand cDNA

formation was carried out according to Smart-seq2 protocols (*Picelli et al., 2013; Picelli et al., 2014*). Double strand cDNA was quantified with Qubit and its quality was evaluated using the D5000 DNA ScreenTape Analysis kit, running the samples at the Agilent Tapestation. Fragmentation and Illumina index primer ligation were carried out using the Illumina DNA Prep Kit and the Nextera DNA CD Indexes (96 Indexes, 96 Samples). DNA fragments that were correctly tagmented were quantified in each sample using the KAPA Library Quantification Kit, with the use of 6 standard samples for calibration, running the quantitative PCR on ViiA7 Real-Time PCR System. Equimolar sample quantities were pooled together to generate the final library for sequencing. Final samples were sequenced using Novaseq 6000, with a 150x150 coverage. Sequencing was performed by the Center for Omics Sciences at the IRCCS Ospedale San Raffaele (COSR).

5.11 Gene expression analysis

Gene expression analysis was performed in collaboration with Ivan Merelli from the Bioinformatics Core of San Raffaele Telethon Institute for Gene Therapy. The quality of the reads was determined by FastQC analysis, with low-quality sequences being trimmed with the trimmomatic tool. Afterward, reads were aligned to the mouse reference genome (GRCm38 - mm10) using STAR, with standard input parameters. Gene counts were generated using the software program Subread featureCounts, with Gencode M31 as gene annotation. Transcript counts were measured using the R/Bioconductor package DEseq, normalizing for library size using the trimmed mean of M-values, and correcting p values using false discovery rate (FDR). Enrichment and GSEA analysis were carried out with different public datasets, using the clusterProfiler package on Bioconductor. The utilized datasets are Mouse MSigDB Hallmark gene collections, KEGG Pathway Database, Gene Ontology, Reactome Pathway Database, and Molecular Signatures Database. Differentially expressed genes (DEGs) were classified as genes with a log(fold change) (logFC) value higher than 1 and an FDR lower than 0.05. Volcano plots display the gene expression results by plotting the statistical significance (-log10 adjusted p-value) against the logFC.

6. References

Abdel-Wahab O, Park CY (2014) BRAF-mutant hematopoietic malignancies. Oncotarget 5: 7980-7981

Acosta JC, Banito A, Wuestefeld T, Georgilis A, Janich P, Morton JP, Athineos D, Kang TW, Lasitschka F, Andrulis M et al (2013) A complex secretory program orchestrated by the inflammasome controls paracrine senescence. Nat Cell Biol 15: 978-990

Acosta JC, O'Loghlen A, Banito A, Guijarro MV, Augert A, Raguz S, Fumagalli M, Da Costa M, Brown C, Popov N et al (2008) Chemokine signaling via the CXCR2 receptor reinforces senescence. Cell 133: 1006-1018

Akira S, Uematsu S, Takeuchi O (2006) Pathogen recognition and innate immunity. Cell 124: 783-801

Amor C, Feucht J, Leibold J, Ho YJ, Zhu CY, Alonso-Curbelo D, Mansilla-Soto J, Boyer JA, Li X, Giavridis T et al (2020) Senolytic CAR T cells reverse senescence-associated pathologies. Nature 583: 127-+

Antelo-Iglesias L, Picallos-Rabina P, Estévez-Souto V, Da Silva-Álvarez S, Collado M (2021) The role of cellular senescence in tissue repair and regeneration. Mech Ageing Dev 198: 111528

Arnaud L, Gorochov G, Charlotte F, Lvovschi V, Parizot C, Larsen M, Ghillani-Dalbin P, Hervier B, Kahn J-E, Deback C et al (2011) Systemic perturbation of cytokine and chemokine networks in Erdheim-Chester disease: a single-center series of 37 patients. Blood 117: 2783-2790

Arons E, Roth L, Sapolsky J, Suntum T, Stetler-Stevenson M, Kreitman RJ (2011) Evidence of canonical somatic hypermutation in hairy cell leukemia. Blood 117: 4844-4851

Artandi SE, Chang S, Lee SL, Alson S, Gottlieb GJ, Chin L, DePinho RA (2000) Telomere dysfunction promotes non-reciprocal translocations and epithelial cancers in mice. Nature 406: 641-645

Arumugam PI, Higashimoto T, Urbinati F, Modlich U, Nestheide S, Xia P, Fox C, Corsinotti A, Baum C, Malik P (2009) Genotoxic Potential of Lineage-specific Lentivirus Vectors Carrying the β-Globin Locus Control Region. Mol Ther 17: 1929-1937

Badalian-Very G, Vergilio JA, Degar BA, MacConaill LE, Brandner B, Calicchio ML, Kuo FC, Ligon AH, Stevenson KE, Kehoe SM et al (2010) Recurrent BRAF mutations in Langerhans cell histiocytosis. Blood 116: 1919-1923

Bai F, Pei XH, Godfrey VL, Xiong Y (2003) Haploinsufficiency of p18(INK4c) sensitizes mice to carcinogen-induced tumorigenesis. Mol Cell Biol 23: 1269-1277

Baker DJ, Perez-Terzic C, Jin F, Pitel KS, Niederländer NJ, Jeganathan K, Yamada S, Reyes S, Rowe L, Hiddinga HJ et al (2008) Opposing roles for p16Ink4a and p19Arf in senescence and ageing caused by BubR1 insufficiency. Nat Cell Biol 10: 825-836

Baker DJ, Wijshake T, Tchkonia T, LeBrasseur NK, Childs BG, van de Sluis B, Kirkland JL, van Deursen JM (2011) Clearance of p16Ink4a-positive senescent cells delays ageing-associated disorders. Nature 479: 232-236

Ballesteros-Tato A, Stone SL, Lund FE (2014) Innate IFNγ-producing B cells. Cell Research 24: 135-136

Bantsimba-Malanda C, Marchal-Sommé J, Goven D, Freynet O, Michel L, Crestani B, Soler P (2010) A role for dendritic cells in bleomycin-induced pulmonary fibrosis in mice? Am J Respir Crit Care Med 182: 385-395

Bartkova J, Rezaei N, Liontos M, Karakaidos P, Kletsas D, Issaeva N, Vassiliou LV, Kolettas E, Niforou K, Zoumpourlis VC et al (2006) Oncogene-induced senescence is part of the tumorigenesis barrier imposed by DNA damage checkpoints. Nature 444: 633-637

Basu A, Ramamoorthi G, Albert G, Gallen C, Beyer A, Snyder C, Koski G, Disis ML, Czerniecki BJ, Kodumudi K (2021) Differentiation and Regulation of TH Cells: A Balancing Act for Cancer Immunotherapy. Frontiers in Immunology 12

Batista CR, Li SK, Xu LS, Solomon LA, DeKoter RP (2017) PU.1 Regulates Ig Light Chain Transcription and Rearrangement in Pre-B Cells during B Cell Development. J Immunol 198: 1565-1574

Baum C, Kustikova O, Modlich U, Li ZX, Fehse B (2006) Mutagenesis and oncogenesis by chromosomal insertion of gene transfer vectors. Hum Gene Ther 17: 253-263

Berres ML, Lim KP, Peters T, Price J, Takizawa H, Salmon H, Idoyaga J, Ruzo A, Lupo PJ, Hicks MJ et al (2014) BRAF-V600E expression in precursor versus differentiated dendritic cells defines clinically distinct LCH risk groups. J Exp Med 211: 669-683

Biavasco R, Lettera E, Giannetti K, Gilioli D, Beretta S, Conti A, Scala S, Cesana D, Gallina P, Norelli M et al (2021) Oncogene-induced senescence in hematopoietic progenitors features myeloid restricted hematopoiesis, chronic inflammation and histiocytosis. Nat Commun 12

Bigenwald C, Le Berichel J, Wilk CM, Chakraborty R, Chen ST, Tabachnikova A, Mancusi R, Abhyankar H, Casanova-Acebes M, Laface I et al (2021) BRAF(V600E)-induced senescence drives Langerhans cell histiocytosis pathophysiology. Nat Med 27: 851-+

Biran A, Perelmutter M, Gal H, Burton DG, Ovadya Y, Vadai E, Geiger T, Krizhanovsky V (2015) Senescent cells communicate via intercellular protein transfer. Genes Dev 29: 791-802

Black RA, Rauch CT, Kozlosky CJ, Peschon JJ, Slack JL, Wolfson MF, Castner BJ, Stocking KL, Reddy P, Srinivasan S et al (1997) A metalloproteinase disintegrin that releases tumour-necrosis factor-alpha from cells. Nature 385: 729-733

Blasi F, Carmeliet P (2002) uPAR: a versatile signalling orchestrator. Nat Rev Mol Cell Biol 3: 932-943

bluebird bio Receives FDA Accelerated Approval for SKYSONA® Gene Therapy for Early, Active Cerebral Adrenoleukodystrophy (CALD). News release. bluebird bio. September 16, 2022. https://finance.yahoo.com/news/bluebird-bio-receives-fda-accelerated-035100645.html

Bode-Böger SM, Scalera F, Martens-Lobenhoffer J (2005) Asymmetric dimethylarginine (ADMA) accelerates cell senescence. Vasc Med 10 Suppl 1: S65-71

Bodnar AG, Ouellette M, Frolkis M, Holt SE, Chiu CP, Morin GB, Harley CB, Shay JW, Lichtsteiner S, Wright WE (1998) Extension of life-span by introduction of telomerase into normal human cells. Science 279: 349-352

Boehm U, Klamp T, Groot M, Howard JC (1997) Cellular responses to interferon-gamma. Annu Rev Immunol 15: 749-795

Bonadies N, Neururer C, Steege A, Vallabhapurapu S, Pabst T, Mueller BU (2010) PU.1 is regulated by NF-kappaB through a novel binding site in a 17 kb upstream enhancer element. Oncogene 29: 1062-1072

Borghesan M, Fafián-Labora J, Eleftheriadou O, Carpintero-Fernández P, Paez-Ribes M, Vizcay-Barrena G, Swisa A, Kolodkin-Gal D, Ximénez-Embún P, Lowe R et al (2019) Small Extracellular Vesicles Are Key Regulators of Non-cell Autonomous Intercellular Communication in Senescence via the Interferon Protein IFITM3. Cell Rep 27: 3956-3971.e3956

Botton T, Talevich E, Mishra VK, Zhang TW, Shain AH, Berquet C, Gagnon A, Judson RL, Ballotti R, Ribas A et al (2019) Genetic Heterogeneity of BRAF Fusion Kinases in Melanoma Affects Drug Responses. Cell Rep 29: 573-+

Boztug K, Schmidt M, Schwarzer A, Banerjee PP, Díez IA, Dewey RA, Böhm M, Nowrouzi A, Ball CR, Glimm H et al (2010) Stem-cell gene therapy for the Wiskott-Aldrich syndrome. N Engl J Med 363: 1918-1927

Buj R, Leon KE, Anguelov MA, Aird KM (2021) Suppression of p16 alleviates the senescence-associated secretory phenotype. Aging-Us 13: 3290-3312

Burton DGA, Stolzing A (2018) Cellular senescence: Immunosurveillance and future immunotherapy. Ageing Res Rev 43: 17-25

Bushman FD (2020) Retroviral Insertional Mutagenesis in Humans: Evidence for Four Genetic Mechanisms Promoting Expansion of Cell Clones. Mol Ther 28: 352-356

Campisi J, d'Adda di Fagagna F (2007) Cellular senescence: when bad things happen to good cells. Nat Rev Mol Cell Biol 8: 729-740

Cánepa ET, Scassa ME, Ceruti JM, Marazita MC, Carcagno AL, Sirkin PF, Ogara MF (2007) INK4 proteins, a family of mammalian CDK inhibitors with novel biological functions. IUBMB Life 59: 419-426

Cangi MG, Biavasco R, Cavalli G, Grassini G, Dal-Cin E, Campochiaro C, Guglielmi B, Berti A, Lampasona V, von Deimling A et al (2015) BRAFV600E-mutation is invariably present and associated to oncogene-induced senescence in Erdheim-Chester disease. Ann Rheum Dis 74: 1596-1602

Cao X, Liang Y, Hu Z, Li H, Yang J, Hsu EJ, Zhu J, Zhou J, Fu Y-X (2021) Next generation of tumor-activating type I IFN enhances anti-tumor immune responses to overcome therapy resistance. Nat Commun 12: 5866

Carswell EA, Old LJ, Kassel RL, Green S, Fiore N, Williamson B (1975) An endotoxin-induced serum factor that causes necrosis of tumors. Proc Natl Acad Sci U S A 72: 3666-3670

Cavazzana-Calvo M, Hacein-Bey S, Basile CD, Gross F, Yvon E, Nusbaum P, Selz F, Hue C, Certain S, Casanova JL et al (2000) Gene therapy of human severe combined immunodeficiency (SCID)-X1 disease. Science 288: 669-672

Cavazzana-Calvo M, Payen E, Negre O, Wang G, Hehir K, Fusil F, Down J, Denaro M, Brady T, Westerman K et al (2010) Transfusion independence and HMGA2 activation after gene therapy of human β-thalassaemia. Nature 467: 318-322

Ceruti JM, Scassa ME, Fló JM, Varone CL, Cánepa ET (2005) Induction of p19INK4d in response to ultraviolet light improves DNA repair and confers resistance to apoptosis in neuroblastoma cells. Oncogene 24: 4065-4080

Cesana D, Ranzani M, Volpin M, Bartholomae C, Duros C, Artus A, Merella S, Benedicenti F, Sergi LS, Sanvito F et al (2014) Uncovering and Dissecting the Genotoxicity of Self-inactivating Lentiviral Vectors In Vivo. Mol Ther 22: 774-785

Cesana D, Santoni de Sio FR, Rudilosso L, Gallina P, Calabria A, Beretta S, Merelli I, Bruzzesi E, Passerini L, Nozza S et al (2017) HIV-1-mediated insertional activation of STAT5B and BACH2 trigger viral reservoir in T regulatory cells. Nat Commun 8

Cesana D, Sgualdino J, Rudilosso L, Merella S, Naldini L, Montini E (2012) Whole transcriptome characterization of aberrant splicing events induced by lentiviral vector integrations. J Clin Invest 122: 1667-1676

Cesana D, Calabria A, Rudilosso L, Gallina P, Benedicenti F, Spinozzi G, Schiroli G, Magnani A, Acquati S, Fumagalli F et al (2021) Retrieval of vector integration sites from cell-free DNA. Nat Med 27: 1458-1470

Chapman PB, Hauschild A, Robert C, Haanen JB, Ascierto P, Larkin J, Dummer R, Garbe C, Testori A, Maio M et al (2011) Improved survival with vemurafenib in melanoma with BRAF V600E mutation. N Engl J Med 364: 2507-2516

Chien Y, Scuoppo C, Wang X, Fang X, Balgley B, Bolden JE, Premsrirut P, Luo W, Chicas A, Lee CS et al (2011) Control of the senescence-associated secretory phenotype by NF-κB promotes senescence and enhances chemosensitivity. Genes Dev 25: 2125-2136

Chilosi M, Chiarle R, Lestani M, Menestrina F, Montagna L, Ambrosetti A, Prolla G, Pizzolo G, Doglioni C, Piva R et al (2000) Low expression of p27 and low proliferation index do not correlate in hairy cell leukaemia. Br J Haematol 111: 263-271

Chu T, D'Angio GJ, Favara BE, Ladisch S, Nesbit M, Pritchard J (1987) Histiocytosis syndromes in children. Lancet 2: 41-42

Chung SS, Kim E, Park JH, Chung YR, Lito P, Teruya-Feldstein J, Hu WH, Beguelin W, Monette S, Duy C et al (2014) Hematopoietic Stem Cell Origin of BRAFV600E Mutations in Hairy Cell Leukemia. Sci Transl Med 6

Cicalese MP, Migliavacca M, Cesana D, Caruso R, Calabria A, Barzaghi F, Dionisio F, Giannelli S, Spinozzi G, Benedicenti F, Rudilosso L, Ciolfi A, Bruselles A, Pizzi S, Casiraghi M, Fossati C, Zancan S, Gabaldo M, Tucci F, Strocchio L, Bernardo ME, Vinti L, Ferrua F, Calbi V, Gallo V, Carlucci F, Guerra A, Richardson A, Kudari M, Jones R, Cancrini C, Ciceri F, Naldini L, Tartaglia M, Montini E, Locatelli M, Aiuti A (2021) EHA Library 324666; S258

Cohen-Aubart F, Emile JF, Carrat F, Helias-Rodzewicz Z, Taly V, Charlotte F, Cluzel P, Donadieu J, Idbaih A, Barete S et al (2018) Phenotypes and survival in Erdheim-Chester disease: Results from a 165-patient cohort. Am J Hematol 93: E114-e117

Cohen-Aubart F, Emile JF, Maksud P, Galanaud D, Idbaih A, Chauvet D, Amar Y, Benameur N, Amoura Z, Haroche J (2014) Marked efficacy of vemurafenib in suprasellar Erdheim-Chester disease. Neurology 83: 1294-1296

Collier LS, Carlson CM, Ravimohan S, Dupuy AJ, Largaespada DA (2005) Cancer gene discovery in solid tumours using transposon-based somatic mutagenesis in the mouse. Nature 436: 272-276

Cope N, Candelora C, Wong K, Kumar S, Nan H, Grasso M, Novak B, Li Y, Marmorstein R, Wang Z (2018) Mechanism of BRAF Activation through Biochemical Characterization of the Recombinant Full-Length Protein. ChemBioChem 19: 1988-1997

Coppé J-P, Rodier F, Patil CK, Freund A, Desprez P-Y, Campisi J (2011) Tumor Suppressor and Aging Biomarker p16INK4a Induces Cellular Senescence without the Associated Inflammatory Secretory Phenotype. J Biol Chem 286: 36396-36403

Coppé JP, Patil CK, Rodier F, Krtolica A, Beauséjour CM, Parrinello S, Hodgson JG, Chin K, Desprez PY, Campisi J (2010) A human-like senescence-associated secretory phenotype is conserved in mouse cells dependent on physiological oxygen. Plos One 5: e9188

Coppé JP, Patil CK, Rodier F, Sun Y, Muñoz DP, Goldstein J, Nelson PS, Desprez PY, Campisi J (2008) Senescence-associated secretory phenotypes reveal cell-nonautonomous functions of oncogenic RAS and the p53 tumor suppressor. PLoS Biol 6: 2853-2868

Da Silva-Álvarez S, Guerra-Varela J, Sobrido-Cameán D, Quelle A, Barreiro-Iglesias A, Sánchez L, Collado M (2020) Cell senescence contributes to tissue regeneration in zebrafish. Aging Cell 19: e13052

Dankort D, Filenova E, Collado M, Serrano M, Jones K, McMahon M (2007) A new mouse model to explore the initiation, progression, and therapy of BRAF(V600E)-induced lung tumors. Gene Dev 21: 379-384

Das H, Kumar A, Lin Z, Patino WD, Hwang PM, Feinberg MW, Majumder PK, Jain MK (2006) Kruppel-Like Factor 2 (KLF2) Regulates Proinflammatory Activation of Monocytes. P Natl Acad Sci USA 103: 6653-6658

Davalos AR, Kawahara M, Malhotra GK, Schaum N, Huang J, Ved U, Beausejour CM, Coppe JP, Rodier F, Campisi J (2013) p53-dependent release of Alarmin HMGB1 is a central mediator of senescent phenotypes. J Cell Biol 201: 613-629

Davies H, Bignell GR, Cox C, Stephens P, Edkins S, Clegg S, Teague J, Woffendin H, Garnett MJ, Bottomley W et al (2002) Mutations of the BRAF gene in human cancer. Nature 417: 949-954

De Cecco M, Ito T, Petrashen AP, Elias AE, Skvir NJ, Criscione SW, Caligiana A, Brocculi G, Adney EM, Boeke JD et al (2019) L1 drives IFN in senescent cells and promotes age-associated inflammation. Nature 566: 73-78

Debyser Z, Christ F, De Rijck J, Gijsbers R (2015) Host factors for retroviral integration site selection. Trends Biochem Sci 40: 108-116

Deichmann A, Hacein-Bey-Abina S, Schmidt M, Garrigue A, Brugman MH, Hu J, Glimm H, Gyapay G, Prum B, Fraser CC et al (2007) Vector integration is nonrandom and clustered and influences the fate of lymphopoiesis in SCID-X1 gene therapy. J Clin Invest 117: 2225-2232

Delestré L, Cui H, Esposito M, Quiveron C, Mylonas E, Penard-Lacronique V, Bischof O, Guillouf C (2017) Senescence is a Spi1-induced anti-proliferative mechanism in primary hematopoietic cells. Haematologica 102: 1850-1860

Delfarah A, Parrish S, Junge JA, Yang J, Seo F, Li S, Mac J, Wang P, Fraser SE, Graham NA (2019) Inhibition of nucleotide synthesis promotes replicative senescence of human mammary epithelial cells. J Biol Chem 294: 10564-10578

Deichmann A, Hacein-Bey-Abina S, Schmidt M, Garrigue A, Brugman MH, Hu J, Glimm H, Gyapay G, Prum B, Fraser CC et al (2007) Vector integration is nonrandom and clustered and influences the fate of lymphopoiesis in SCID-X1 gene therapy. J Clin Invest 117: 2225-2232

Demaria M, Ohtani N, Youssef SA, Rodier F, Toussaint W, Mitchell JR, Laberge RM, Vijg J, Van Steeg H, Dollé ME et al (2014) An essential role for senescent cells in optimal wound healing through secretion of PDGF-AA. Dev Cell 31: 722-733

Di Micco R, Fumagalli M, Cicalese A, Piccinin S, Gasparini P, Luise C, Schurra C, Garre M, Nuciforo PG, Bensimon A et al (2006) Oncogene-induced senescence is a DNA damage response triggered by DNA hyper-replication. Nature 444: 638-642

Dietrich S, Hüllein J, Lee SC, Hutter B, Gonzalez D, Jayne S, Dyer MJ, Oleś M, Else M, Liu X et al (2015) Recurrent CDKN1B (p27) mutations in hairy cell leukemia. Blood 126: 1005-1008

Dogan S, Barnes L, Cruz-Vetrano WP (2012) Crystal-storing histiocytosis: report of a case, review of the literature (80 cases) and a proposed classification. Head Neck Pathol 6: 111-120

Donadieu J, Larabi IA, Tardieu M, Visser J, Hutter C, Sieni E, Kabbara N, Barkaoui M, Miron J, Chalard F et al (2019) Vemurafenib for Refractory Multisystem Langerhans Cell Histiocytosis in Children: An International Observational Study. J Clin Oncol 37: 2857-+

Dou Z, Ghosh K, Vizioli MG, Zhu J, Sen P, Wangensteen KJ, Simithy J, Lan Y, Lin Y, Zhou Z et al (2017) Cytoplasmic chromatin triggers inflammation in senescence and cancer. Nature 550: 402-406

Dougherty SC, Kapoor V, Uhlman AJ, Memon S, Cho M, Rose J, Swan GA, Hakim FT, Gress RE (2017) Accelerated T Cell Senescence after Allogeneic Hematopoeitic Stem Cell Transplantation. Blood 130: 4523-4523

Durham BH, Lopez Rodrigo E, Picarsic J, Abramson D, Rotemberg V, De Munck S, Pannecoucke E, Lu SX, Pastore A, Yoshimi A et al (2019) Activating mutations in CSF1R and additional receptor tyrosine kinases in histiocytic neoplasms. Nat Med 25: 1839-1842

Egashira M, Hirota Y, Shimizu-Hirota R, Saito-Fujita T, Haraguchi H, Matsumoto L, Matsuo M, Hiraoka T, Tanaka T, Akaeda S et al (2017) F4/80+ Macrophages Contribute to Clearance of Senescent Cells in the Mouse Postpartum Uterus. Endocrinology 158: 2344-2353

Eichler, F., Duncan, C., Musolino, P.L., Orchard, P.J., De Oliveira, S., Thrasher, A.J., Armant, M., Dansereau, C., Lund, T.C., Miller, W.P., et al. (2017). Hematopoietic Stem-Cell Gene Therapy for Cerebral Adrenoleukodystrophy. N Engl J Med 377, 1630-1638.

Eisenbeis CF, Singh H, Storb U (1993) PU.1 is a component of a multiprotein complex which binds an essential site in the murine immunoglobulin lambda 2-4 enhancer. Mol Cell Biol 13: 6452-6461

Eissner G, Kolch W, Scheurich P (2004) Ligands working as receptors: reverse signaling by members of the TNF superfamily enhance the plasticity of the immune system. Cytokine Growth Factor Rev 15: 353-366

Ellermann V, Bang O (1909) Experimentelle Leukämie bei Hühnern. II. 63: 231-272

Emery DW (2011) The Use of Chromatin Insulators to Improve the Expression and Safety of Integrating Gene Transfer Vectors. Hum Gene Ther 22: 761-774

Emile J-F, Cohen-Aubart F, Collin M, Fraitag S, Idbaih A, Abdel-Wahab O, Rollins BJ, Donadieu J, Haroche J (2021) Histiocytosis. The Lancet 398: 157-170

Emile JF, Diamond EL, Hélias-Rodzewicz Z, Cohen-Aubart F, Charlotte F, Hyman DM, Kim E, Rampal R, Patel M, Ganzel C et al (2014) Recurrent RAS and PIK3CA mutations in Erdheim-Chester disease. Blood 124: 3016-3019

Esteller M, Corn PG, Baylin SB, Herman JG (2001) A gene hypermethylation profile of human cancer. Cancer Res 61: 3225-3229

Euskirchen P, Haroche J, Emile JF, Buchert R, Vandersee S, Meisel A (2015) Complete remission of critical neurohistiocytosis by vemurafenib. Neurol Neuroimmunol Neuroinflamm 2: e78

Felgentreff K, Schuetz C, Baumann U, Klemann C, Viemann D, Ursu S, Jacobsen E-M, Debatin K-M, Schulz A, Hoenig M et al (2021) Differential DNA Damage Response of Peripheral Blood Lymphocyte Populations. Frontiers in Immunology 12

Ferrari G, Thrasher AJ, Aiuti A (2020) Gene therapy using haematopoietic stem and progenitor cells. Nat Rev Genet 22: 216-234

Ferrero E, Belloni D, Corti A, Doglioni C, Dagna L, Ferrarini M (2014) TNF-α in Erdheim–Chester disease pericardial effusion promotes endothelial leakage in vitro and is neutralized by infliximab. Rheumatology 53: 198-200

Forconi F, Sahota SS, Raspadori D, Mockridge CI, Lauria F, Stevenson FK (2001) Tumor cells of hairy cell leukemia express multiple clonally related immunoglobulin isotypes via RNA splicing. Blood 98: 1174-1181

Fraietta JA, Nobles CL, Sammons MA, Lundh S, Carty SA, Reich TJ, Cogdill AP, Morrissette JJD, DeNizio JE, Reddy S et al (2018) Disruption of TET2 promotes the therapeutic efficacy of CD19-targeted T cells. Nature 558: 307-312

Franceschi C, Bonafè M (2003) Centenarians as a model for healthy aging. Biochem Soc Trans 31: 457-461

Frankola KA, Greig NH, Luo W, Tweedie D (2011) Targeting TNF-α to elucidate and ameliorate neuroinflammation in neurodegenerative diseases. CNS Neurol Disord Drug Targets 10: 391-403

Freund A, Patil CK, Campisi J (2011) p38MAPK is a novel DNA damage response-independent regulator of the senescence-associated secretory phenotype. Embo J 30: 1536-1548

Fulop T, Le Page A, Garneau H, Azimi N, Baehl S, Dupuis G, Pawelec G, Larbi A (2012) Aging, immunosenescence and membrane rafts: the lipid connection. Longev Healthspan 1

Gabay C (2006) Interleukin-6 and chronic inflammation. Arthritis Res Ther 8 Suppl 2: S3

Gao P, Ascano M, Zillinger T, Wang W, Dai P, Serganov Artem A, Gaffney Barbara L, Shuman S, Jones Roger A, Deng L et al (2013) Structure-function analysis of STING activation by c[G(2',5')pA(3',5')p] and targeting by antiviral DMXAA. Cell 154: 748-762

Ghobadi A, Miller CA, Li T, O'Laughlin M, Lee YS, Ali M, Westervelt P, DiPersio JF, Wartman L (2019) Shared cell of origin in a patient with Erdheim-Chester disease and acute myeloid leukemia. Haematologica 104: e373-e375

Ghosh S, May MJ, Kopp EB (1998) NF-kappa B and Rel proteins: evolutionarily conserved mediators of immune responses. Annu Rev Immunol 16: 225-260

Glück S, Guey B, Gulen MF, Wolter K, Kang TW, Schmacke NA, Bridgeman A, Rehwinkel J, Zender L, Ablasser A (2017) Innate immune sensing of cytosolic chromatin fragments through cGAS promotes senescence. Nat Cell Biol 19: 1061-1070

Go H, Jeon YK, Huh J, Choi SJ, Choi YD, Cha HJ, Kim HJ, Park G, Min S, Kim JE (2014) Frequent detection of BRAF(V600E) mutations in histiocytic and dendritic cell neoplasms. Histopathology 65: 261-272

Gocher AM, Workman CJ, Vignali DAA (2022) Interferon-γ: teammate or opponent in the tumour microenvironment? Nature Reviews Immunology 22: 158-172

Goyal G, Shah MV, Hook CC, Wolanskyj AP, Call TG, Rech KL, Go RS (2018) Adult disseminated Langerhans cell histiocytosis: incidence, racial disparities and long-term outcomes. Br J Haematol 182: 579-581

Greaves WO, Verma S, Patel KP, Davies MA, Barkoh BA, Galbincea JM, Yao H, Lazar AJ, Aldape KD, Medeiros LJ et al (2013) Frequency and spectrum of BRAF mutations in a retrospective, single-institution study of 1112 cases of melanoma. J Mol Diagn 15: 220-226

Grillari J, Hohenwarter O, Grabherr RM, Katinger H (2000) Subtractive hybridization of mRNA from early passage and senescent endothelial cells. Exp Gerontol 35: 187-197

Grivennikov SI, Tumanov AV, Liepinsh DJ, Kruglov AA, Marakusha BI, Shakhov AN, Murakami T, Drutskaya LN, Förster I, Clausen BE et al (2005) Distinct and nonredundant in vivo functions of TNF produced by t cells and macrophages/neutrophils: protective and deleterious effects. Immunity 22: 93-104

Grosjean-Raillard J, Tailler M, Ades L, Perfettini JL, Fabre C, Braun T, De Botton S, Fenaux P, Kroemer G (2009) ATM mediates constitutive NF-kappa B activation in high-risk myelodysplastic syndrome and acute myeloid leukemia. Oncogene 28: 1099-1109

Gross L (1951) "Spontaneous" leukemia developing in C3H mice following inoculation in infancy, with AK-leukemic extracts, or AK-embrvos. Proc Soc Exp Biol Med 76: 27-32

Gullickson P, Xu YW, Niedernhofer LJ, Thompson EL, Yousefzadeh MJ (2022) The Role of DNA Repair in Immunological Diversity: From Molecular Mechanisms to Clinical Ramifications. Frontiers in Immunology 13

Guyot-Goubin A, Donadieu J, Barkaoui M, Bellec S, Thomas C, Clavel J (2008) Descriptive epidemiology of childhood Langerhans cell histiocytosis in France, 2000-2004. Pediatr Blood Cancer 51: 71-75

Haber DA (1997) Splicing into senescence: the curious case of p16 and p19ARF. Cell 91: 555-558

Hacein-Bey-Abina S, Von Kalle C, Schmidt M, McCormack MP, Wulffraat N, Leboulch P, Lim A, Osborne CS, Pawliuk R, Morillon E et al (2003) LMO2-associated clonal T cell proliferation in two patients after gene therapy for SCID-X1. Science 302: 415-419

Hacein-Bey-Abina S, Garrigue A, Wang GP, Soulier J, Lim A, Morillon E, Clappier E, Caccavelli L, Delabesse E, Beldjord K et al (2008) Insertional oncogenesis in 4 patients after retrovirus-mediated gene therapy of SCID-X1. J Clin Invest 118: 3132-3142

Hacein-Bey-Abina S, Le Deist F, Carlier F, Bouneaud C, Hue C, De Villartay JP, Thrasher AJ, Wulffraat N, Sorensen R, Dupuis-Girod S et al (2002) Sustained correction of X-linked severe combined immunodeficiency by ex vivo gene therapy. New Engl J Med 346: 1185-1193

Halbritter F, Farlik M, Schwentner R, Jug G, Fortelny N, Schnöller T, Pisa H, Schuster LC, Reinprecht A, Czech T et al (2019) Epigenomics and Single-Cell Sequencing Define a Developmental Hierarchy in Langerhans Cell Histiocytosis. Cancer Discov 9: 1406-1421

Hall BM, Balan V, Gleiberman AS, Strom E, Krasnov P, Virtuoso LP, Rydkina E, Vujcic S, Balan K, Gitlin, II et al (2017) p16(Ink4a) and senescence-associated β-galactosidase can be induced in macrophages as part of a reversible response to physiological stimuli. Aging (Albany NY) 9: 1867-1884

Hall BM, Balan V, Gleiberman AS, Strom E, Krasnov P, Virtuoso LP, Rydkina E, Vujcic S, Balan K, Gitlin I et al (2016) Aging of mice is associated with p16(Ink4a)- and β-galactosidase-positive macrophage accumulation that can be induced in young mice by senescent cells. Aging (Albany NY) 8: 1294-1315

Hamsanathan S, Gurkar AU (2022) Lipids as Regulators of Cellular Senescence. Frontiers in Physiology 13

Haroche J, Charlotte F, Arnaud L, von Deimling A, Hélias-Rodzewicz Z, Hervier B, Cohen-Aubart F, Launay D, Lesot A, Mokhtari K et al (2012) High prevalence of BRAF V600E mutations in Erdheim-Chester disease but not in other non-Langerhans cell histiocytoses. Blood 120: 2700-2703

Hart PH, Vitti GF, Burgess DR, Whitty GA, Piccoli DS, Hamilton JA (1989) Potential antiinflammatory effects of interleukin 4: suppression of human monocyte tumor necrosis factor alpha, interleukin 1, and prostaglandin E2. Proc Natl Acad Sci U S A 86: 3803-3807

Hayflick L, Moorhead PS (1961) The serial cultivation of human diploid cell strains. Exp Cell Res 25: 585-621

Hemann MT, Greider CW (2000) Wild-derived inbred mouse strains have short telomeres. Nucleic Acids Res 28: 4474-4478

Herbein G, O'Brien WA (2000) Tumor necrosis factor (TNF)-alpha and TNF receptors in viral pathogenesis. Proc Soc Exp Biol Med 223: 241-257

Hernández-Mercado E, Prieto-Chávez JL, Arriaga-Pizano LA, Hernández-Gutierrez S, Mendlovic F, Königsberg M, López-Díazguerrero NE (2021) Increased CD47 and MHC Class I Inhibitory Signals Expression in Senescent CD1 Primary Mouse Lung Fibroblasts. Int J Mol Sci 22

Hernandez-Segura A, de Jong TV, Melov S, Guryev V, Campisi J, Demaria M (2017) Unmasking Transcriptional Heterogeneity in Senescent Cells. Curr Biol 27: 2652-2660.e2654

Herranz N, Gil J (2018) Mechanisms and functions of cellular senescence. J Clin Invest 128: 1238-1246

Hesse M, Modolell M, La Flamme AC, Schito M, Fuentes JM, Cheever AW, Pearce EJ, Wynn TA (2001) Differential regulation of nitric oxide synthase-2 and arginase-1 by type 1/type 2 cytokines in vivo: granulomatous pathology is shaped by the pattern of L-arginine metabolism. J Immunol 167: 6533-6544

Hilpert M, Legrand C, Bluteau D, Balayn N, Betems A, Bluteau O, Villeval JL, Louache F, Gonin P, Debili N et al (2014) p19 INK4d controls hematopoietic stem cells in a cell-autonomous manner during genotoxic stress and through the microenvironment during aging. Stem Cell Reports 3: 1085-1102

Hoare M, Ito Y, Kang T-W, Weekes MP, Matheson NJ, Patten DA, Shetty S, Parry AJ, Menon S, Salama R et al (2016) NOTCH1 mediates a switch between two distinct secretomes during senescence. Nat Cell Biol 18: 979-992

Hornebeck W, Maquart FX (2003) Proteolyzed matrix as a template for the regulation of tumor progression. Biomed Pharmacother 57: 223-230

Howe SJ, Mansour MR, Schwarzwaelder K, Bartholomae C, Hubank M, Kempski H, Brugman MH, Pike-Overzet K, Chatters SJ, de Ridder D et al (2008) Insertional mutagenesis combined with acquired somatic mutations causes leukemogenesis following gene therapy of SCID-X1 patients. The Journal of Clinical Investigation 118: 3143-3150

Huang J, Sun X, Gong X, He Z, Chen L, Qiu X, Yin CC (2014) Rearrangement and expression of the immunoglobulin μ-chain gene in human myeloid cells. Cell Mol Immunol 11: 94-104

Hwang B, McCool K, Wan J, Wuerzberger-Davis SM, Young EWK, Choi EY, Cingolani G, Weaver BA, Miyamoto S (2015) IPO3-mediated Nonclassical Nuclear Import of NF-κB Essential Modulator (NEMO) Drives DNA Damage-dependent NF-κB Activation. J Biol Chem 290: 17967-17984

Iannello A, Thompson TW, Ardolino M, Lowe SW, Raulet DH (2013) p53-dependent chemokine production by senescent tumor cells supports NKG2D-dependent tumor elimination by natural killer cells. J Exp Med 210: 2057-2069

Ishihara K, Hirano T (2002) IL-6 in autoimmune disease and chronic inflammatory proliferative disease. Cytokine Growth Factor Rev 13: 357-368

Ishikawa H, Barber GN (2008) STING is an endoplasmic reticulum adaptor that facilitates innate immune signalling. Nature 455: 674-678

Ito Y, Hoare M, Narita M (2017) Spatial and Temporal Control of Senescence. Trends Cell Biol 27: 820-832

Ivanov A, Pawlikowski J, Manoharan I, van Tuyn J, Nelson DM, Rai TS, Shah PP, Hewitt G, Korolchuk VI, Passos JF et al (2013) Lysosome-mediated processing of chromatin in senescence. J Cell Biol 202: 129-143

Jang DI, Lee AH, Shin HY, Song HR, Park JH, Kang TB, Lee SR, Yang SH (2021) The Role of Tumor Necrosis Factor Alpha (TNF-α) in Autoimmune Disease and Current TNF-α Inhibitors in Therapeutics. Int J Mol Sci 22

Janik JE (2011) Tumor markers in hairy cell leukemia. Leuk Lymphoma 52 Suppl 2: 69-71

Jin L, Waterman Paul M, Jonscher Karen R, Short Cindy M, Reisdorph Nichole A, Cambier John C (2008) MPYS, a Novel Membrane Tetraspanner, Is Associated with Major Histocompatibility Complex Class II and Mediates Transduction of Apoptotic Signals. Mol Cell Biol 28: 5014-5026

Juliusson G, Lenkei R, Liliemark J (1994) Flow cytometry of blood and bone marrow cells from patients with hairy cell leukemia: phenotype of hairy cells and lymphocyte subsets after treatment with 2-chlorodeoxyadenosine. Blood 83: 3672-3681

Jun JI, Lau LF (2010) The matricellular protein CCN1 induces fibroblast senescence and restricts fibrosis in cutaneous wound healing (vol 12, pg 676, 2010). Nat Cell Biol 12: 1249-1249

Kamijo T, Zindy F, Roussel MF, Quelle DE, Downing JR, Ashmun RA, Grosveld G, Sherr CJ (1997) Tumor suppression at the mouse INK4a locus mediated by the alternative reading frame product p19ARF. Cell 91: 649-659

Kang C, Xu Q, Martin TD, Li MZ, Demaria M, Aron L, Lu T, Yankner BA, Campisi J, Elledge SJ (2015) The DNA damage response induces inflammation and senescence by inhibiting autophagy of GATA4. Science 349: aaa5612

Kang T-W, Yevsa T, Woller N, Hoenicke L, Wuestefeld T, Dauch D, Hohmeyer A, Gereke M, Rudalska R, Potapova A et al (2011) Senescence surveillance of pre-malignant hepatocytes limits liver cancer development. Nature 479: 547-551

Kannourakis G, Abbas A (1994) The role of cytokines in the pathogenesis of Langerhans cell histiocytosis. Br J Cancer Suppl 23: S37-40

Khan SH, Moritsugu J, Wahl GM (2000) Differential requirement for p19ARF in the p53-dependent arrest induced by DNA damage, microtubule disruption, and ribonucleotide depletion. Proc Natl Acad Sci U S A 97: 3266-3271

Khandelwal S, Van Rooijen N, Saxena RK (2007) Reduced expression of CD47 during murine red blood cell (RBC) senescence and its role in RBC clearance from the circulation. Transfusion 47: 1725-1732

Kidd P (2003) Th1/Th2 balance: the hypothesis, its limitations, and implications for health and disease. Altern Med Rev 8: 223-246

Krimpenfort P, Quon KC, Mooi WJ, Loonstra A, Berns A (2001) Loss of p16(Ink4a) confers susceptibility to metastatic melanoma in mice. Nature 413: 83-86

Krizhanovsky V, Yon M, Dickins RA, Hearn S, Simon J, Miething C, Yee H, Zender L, Lowe SW (2008) Senescence of activated stellate cells limits liver fibrosis. Cell 134: 657-667

Krtolica A, Parrinello S, Lockett S, Desprez PY, Campisi J (2001) Senescent fibroblasts promote epithelial cell growth and tumorigenesis: A link between cancer and aging. P Natl Acad Sci USA 98: 12072-12077

Kuilman T, Michaloglou C, Vredeveld LC, Douma S, van Doorn R, Desmet CJ, Aarden LA, Mooi WJ, Peeper DS (2008) Oncogene-induced senescence relayed by an interleukin-dependent inflammatory network. Cell 133: 1019-1031

Kushwah R, Hu J (2011) Role of dendritic cells in the induction of regulatory T cells. Cell & Bioscience 1: 20

Lanna A, Vaz B, D'Ambra C, Valvo S, Vuotto C, Chiurchiù V, Devine O, Sanchez M, Borsellino G, Akbar AN et al (2022) An intercellular transfer of telomeres rescues T cells from senescence and promotes long-term immunological memory. Nat Cell Biol 24: 1461-1474

Lau L, David G (2019) Pro- and anti-tumorigenic functions of the senescence-associated secretory phenotype. Expert Opinion on Therapeutic Targets 23: 1041-1051

Lau L, Porciuncula A, Yu A, Iwakura Y, David G (2019) Uncoupling the Senescence-Associated Secretory Phenotype from Cell Cycle Exit via Interleukin-1 Inactivation Unveils Its Protumorigenic Role. Mol Cell Biol 39

Lavoie H, Thevakumaran N, Gavory G, Li JJ, Padeganeh A, Guiral S, Duchaine J, Mao DY, Bouvier M, Sicheri F et al (2013) Inhibitors that stabilize a closed RAF kinase domain conformation induce dimerization. Nat Chem Biol 9: 428-436

Lebeau A, Zeindl-Eberhart E, Müller E-C, Müller-Höcker J, Jungblut PR, Emmerich B, Löhrs U (2002) Generalized crystal-storing histiocytosis associated with monoclonal gammopathy: molecular analysis of a disorder with rapid clinical course and review of the literature. Blood 100: 1817-1827

Leevers SJ, Paterson HF, Marshall CJ (1994) Requirement for Ras in Raf activation is overcome by targeting Raf to the plasma membrane. Nature 369: 411-414

Lessard F, Igelmann S, Trahan C, Huot G, Saint-Germain E, Mignacca L, Del Toro N, Lopes-Paciencia S, Le Calvé B, Montero M et al (2018) Senescence-associated ribosome biogenesis defects contributes to cell cycle arrest through the Rb pathway. Nat Cell Biol 20: 789-799

Li T, Chen ZJ (2018) The cGAS-cGAMP-STING pathway connects DNA damage to inflammation, senescence, and cancer. J Exp Med 215: 1287-1299

Liu D, Hornsby PJ (2007) Senescent human fibroblasts increase the early growth of xenograft tumors via matrix metalloproteinase secretion. Cancer Res 67: 3117-3126

Liu S, Cai X, Wu J, Cong Q, Chen X, Li T, Du F, Ren J, Wu Y-T, Grishin NV et al (2015) Phosphorylation of innate immune adaptor proteins MAVS, STING, and TRIF induces IRF3 activation. Science 347: aaa2630

Liu JY, Souroullas GP, Diekman BO, Krishnamurthy J, Hall BM, Sorrentino JA, Parker JS, Sessions GA, Gudkov AV, Sharpless NE (2019) Cells exhibiting strong p16(INK4a)

promoter activation in vivo display features of senescence. Proc Natl Acad Sci U S A 116: 2603-2611

Liu T, Zhang L, Joo D, Sun S-C (2017) NF-κB signaling in inflammation. Signal Transduction and Targeted Therapy 2: 17023

Lopes-Paciencia S, Saint-Germain E, Rowell MC, Ruiz AF, Kalegari P, Ferbeyre G (2019) The senescence-associated secretory phenotype and its regulation. Cytokine 117: 15-22

Lowe SW, Sherr CJ (2003) Tumor suppression by Ink4a-Arf: progress and puzzles. Current Opinion in Genetics & Development 13: 77-83

Lu SY, Chang KW, Liu CJ, Tseng YH, Lu HH, Lee SY, Lin SC (2006) Ripe areca nut extract induces G1 phase arrests and senescence-associated phenotypes in normal human oral keratinocyte. Carcinogenesis 27: 1273-1284

Lujambio A, Akkari L, Simon J, Grace D, Tschaharganeh DF, Bolden JE, Zhao Z, Thapar V, Joyce JA, Krizhanovsky V et al (2013) Non-cell-autonomous tumor suppression by p53. Cell 153: 449-460

Lund AH, Turner G, Trubetskoy A, Verhoeven E, Wientjens E, Hulsman D, Russell R, DePinho RA, Lenz J, van Lohuizen M (2002) Genome-wide retroviral insertional tagging of genes involved in cancer in Cdkn2a-deficient mice. Nature Genetics 32: 160-165

Luo G, Niesel DW, Shaban RA, Grimm EA, Klimpel GR (1993) Tumor necrosis factor alpha binding to bacteria: evidence for a high-affinity receptor and alteration of bacterial virulence properties. Infect Immun 61: 830-835

Lv Z, Bian Z, Shi L, Niu S, Ha B, Tremblay A, Li L, Zhang X, Paluszynski J, Liu M et al (2015) Loss of Cell Surface CD47 Clustering Formation and Binding Avidity to SIRPα Facilitate Apoptotic Cell Clearance by Macrophages. The Journal of Immunology 195: 661-671

MacMicking J, Xie QW, Nathan C (1997) Nitric oxide and macrophage function. Annu Rev Immunol 15: 323-350

MacRae SL, Croken MM, Calder RB, Aliper A, Milholland B, White RR, Zhavoronkov A, Gladyshev VN, Seluanov A, Gorbunova V et al (2015) DNA repair in species with extreme lifespan differences. Aging (Albany NY) 7: 1171-1184

Maggio M, Guralnik JM, Longo DL, Ferrucci L (2006) Interleukin-6 in aging and chronic disease: a magnificent pathway. J Gerontol A Biol Sci Med Sci 61: 575-584

Maitre E, Cornet E, Troussard X (2019) Hairy cell leukemia: 2020 update on diagnosis, risk stratification, and treatment. Am J Hematol 94: 1413-1422

Maloum K, Magnac C, Azgui Z, Cau C, Charlotte F, Binet JL, Merle-Béral H, Dighiero G (1998) VH gene expression in hairy cell leukaemia. Br J Haematol 101: 171-178

Marini B, Kertesz-Farkas A, Ali H, Lucic B, Lisek K, Manganaro L, Pongor S, Luzzati R, Recchia A, Mavilio F et al (2015) Nuclear architecture dictates HIV-1 integration site selection. Nature 521: 227-231

Martens JW, Sieuwerts AM, Bolt-deVries J, Bosma PT, Swiggers SJ, Klijn JG, Foekens JA (2003) Aging of stromal-derived human breast fibroblasts might contribute to breast cancer progression. Thromb Haemost 89: 393-404

Martínez-Cué C, Rueda N (2020) Cellular Senescence in Neurodegenerative Diseases. Front Cell Neurosci 14: 16

Martínez-Zamudio RI, Robinson L, Roux PF, Bischof O (2017) SnapShot: Cellular Senescence Pathways. Cell 170: 816-816.e811

Martini H, Passos JF (2022) Cellular senescence: all roads lead to mitochondria. Febs j

Mauro CD, Pesapane A, Formisano L, Rosa R, D'Amato V, Ciciola P, Servetto A, Marciano R, Orsini RC, Monteleone F et al (2017) Urokinase-type plasminogen activator receptor (uPAR) expression enhances invasion and metastasis in RAS mutated tumors. Sci Rep-Uk 7: 9388

McCain J (2013) The MAPK (ERK) Pathway: Investigational Combinations for the Treatment Of BRAF-Mutated Metastatic Melanoma. P t 38: 96-108

Meng A, Wang Y, Van Zant G, Zhou D (2003) Ionizing radiation and busulfan induce premature senescence in murine bone marrow hematopoietic cells. Cancer Res 63: 5414-5419

Mercogliano MF, Bruni S, Elizalde PV, Schillaci R (2020) Tumor Necrosis Factor α Blockade: An Opportunity to Tackle Breast Cancer. Frontiers in Oncology 10

Michaloglou C, Vredeveld LCW, Soengas MS, Denoyelle C, Kuilman T, van der Horst CMAM, Majoor DM, Shay JW, Mooi WJ, Peeper DS (2005) BRAFE600-associated senescence-like cell cycle arrest of human naevi. Nature 436: 720-724

Mills CD, Kincaid K, Alt JM, Heilman MJ, Hill AM (2017) Pillars Article: M-1/M-2 Macrophages and the Th1/Th2 Paradigm. J. Immunol. 2000. 164: 6166-6173. J Immunol 199: 2194-2201

Mitchell RS, Beitzel BF, Schroder AR, Shinn P, Chen H, Berry CC, Ecker JR, Bushman FD (2004) Retroviral DNA integration: ASLV, HIV, and MLV show distinct target site preferences. PLoS Biol 2: E234

Modlich U, Navarro S, Zychlinski D, Maetzig T, Knoess S, Brugman MH, Schambach A, Charrier S, Galy A, Thrasher AJ et al (2009) Insertional Transformation of Hematopoietic Cells by Self-inactivating Lentiviral and Gammaretroviral Vectors. Mol Ther 17: 1919-1928

Molteni R, Biavasco R, Stefanoni D, Nemkov T, Dominguez-Andres J, Arts RJ, Merelli I, Mazza D, Zambrano S, Panigada M et al (2021) Oncogene-induced maladaptive activation of trained immunity in the pathogenesis and treatment of Erdheim-Chester disease. Blood 138: 1554-1569

Montini E, Cesana D, Schmidt M, Sanvito F, Ponzoni M, Bartholomae C, Sergi Sergi L, Benedicenti F, Ambrosi A, Di Serio C et al (2006) Hematopoietic stem cell gene transfer in a tumor-prone mouse model uncovers low genotoxicity of lentiviral vector integration. Nat Biotechnol 24: 687-696

Montini E, Cesana D, Schmidt M, Sanvito F, Bartholomae CC, Ranzani M, Benedicenti F, Sergi LS, Ambrosi A, Ponzoni M et al (2009) The genotoxic potential of retroviral vectors is

strongly modulated by vector design and integration site selection in a mouse model of HSC gene therapy. J Clin Invest 119: 964-975

Mu XC, Higgins PJ (1995) Differential growth state-dependent regulation of plasminogen activator inhibitor type-1 expression in senescent IMR-90 human diploid fibroblasts. J Cell Physiol 165: 647-657

Mu XC, Staiano-Coico L, Higgins PJ (1998) Increased transcription and modified growth state-dependent expression of the plasminogen activator inhibitor type-1 gene characterize the senescent phenotype in human diploid fibroblasts. J Cell Physiol 174: 90-98

Muñoz-Lorente MA, Cano-Martin AC, Blasco MA (2019) Mice with hyper-long telomeres show less metabolic aging and longer lifespans. Nat Commun 10: 4723

Nagel S, Ehrentraut S, Meyer C, Kaufmann M, Drexler HG, MacLeod RA (2015) NFκB is activated by multiple mechanisms in hairy cell leukemia. Genes Chromosomes Cancer 54: 418-432

Naldini L, Cicalese MP, Bernardo ME, Gentner B, Gabaldo M, Ferrari G, Aiuti A (2022) The EHA Research Roadmap: Hematopoietic Stem Cell Gene Therapy. HemaSphere 6

Nelson DS, Marano RL, Joo Y, Tian SY, Patel B, Kaplan DH, Shlomchik MJ, Stevenson K, Bronson RT, Rollins BJ (2019) BRAF V600E and Pten deletion in mice produces a histiocytic disorder with features of Langerhans cell histiocytosis. Plos One 14: e0222400

Nelson G, Kucheryavenko O, Wordsworth J, von Zglinicki T (2018) The senescent bystander effect is caused by ROS-activated NF-κB signalling. Mech Ageing Dev 170: 30-36

Orjalo AV, Bhaumik D, Gengler BK, Scott GK, Campisi J (2009) Cell surface-bound IL-1α is an upstream regulator of the senescence-associated IL-6/IL-8 cytokine network. Proceedings of the National Academy of Sciences 106: 17031-17036

Ortega S, Malumbres M, Barbacid M (2002) Cyclin D-dependent kinases, INK4 inhibitors and cancer. Biochim Biophys Acta 1602: 73-87

Ott MG, Schmidt M, Schwarzwaelder K, Stein S, Siler U, Koehl U, Glimm H, Kühlcke K, Schilz A, Kunkel H et al (2006) Correction of X-linked chronic granulomatous disease by gene therapy, augmented by insertional activation of MDS1-EVI1, PRDM16 or SETBP1. Nat Med 12: 401-409

Palanisamy N, Ateeq B, Kalyana-Sundaram S, Pflueger D, Ramnarayanan K, Shankar S, Han B, Cao Q, Cao XH, Suleman K et al (2010) Rearrangements of the RAF kinase pathway in prostate cancer, gastric cancer and melanoma. Nat Med 16: 793-U794

Panda AC, Abdelmohsen K, Gorospe M (2017) SASP regulation by noncoding RNA. Mech Ageing Dev 168: 37-43

Papo M, Diamond EL, Cohen-Aubart F, Emile JF, Roos-Weil D, Gupta N, Durham BH, Ozkaya N, Dogan A, Ulaner GA et al (2017) High prevalence of myeloid neoplasms in adults with non-Langerhans cell histiocytosis. Blood 130: 1007-1013

Parrinello S, Samper E, Krtolica A, Goldstein J, Melov S, Campisi J (2003) Oxygen sensitivity severely limits the replicative lifespan of murine fibroblasts. Nat Cell Biol 5: 741-747

Passos JF, Nelson G, Wang C, Richter T, Simillion C, Proctor CJ, Miwa S, Olijslagers S, Hallinan J, Wipat A et al (2010) Feedback between p21 and reactive oxygen production is necessary for cell senescence. Mol Syst Biol 6: 347

Patriotis C, Makris A, Bear SE, Tsichlis PN (1993) Tumor Progression Locus-2 (Tpl-2) Encodes a Protein-Kinase Involved in the Progression of Rodent T-Cell Lymphomas and in T-Cell Activation. P Natl Acad Sci USA 90: 2251-2255

Patriotis C, Makris A, Chernoff J, Tsichlis PN (1994) Tpl-2 Acts in Concert with Ras and Raf-1 to Activate Mitogen-Activated Protein-Kinase. P Natl Acad Sci USA 91: 9755-9759

Pereira BI, Devine OP, Vukmanovic-Stejic M, Chambers ES, Subramanian P, Patel N, Virasami A, Sebire NJ, Kinsler V, Valdovinos A et al (2019) Senescent cells evade immune clearance via HLA-E-mediated NK and CD8+ T cell inhibition. Nat Commun 10: 2387

Perkins ND, Gilmore TD (2006) Good cop, bad cop: the different faces of NF-kappaB. Cell Death Differ 13: 759-772

Pimentel-Muiños FX, Seed B (1999) Regulated commitment of TNF receptor signaling: a molecular switch for death or activation. Immunity 11: 783-793

Pini M, Czibik G, Sawaki D, Mezdari Z, Braud L, Delmont T, Mercedes R, Martel C, Buron N, Marcelin G et al (2021) Adipose tissue senescence is mediated by increased ATP content after a short-term high-fat diet exposure. Aging Cell 20: e13421

Polliack A (2002) Hairy cell leukemia: biology, clinical diagnosis, unusual manifestations and associated disorders. Rev Clin Exp Hematol 6: 366-388; discussion 449-350

Poulikakos PI, Persaud Y, Janakiraman M, Kong XJ, Ng C, Moriceau G, Shi HB, Atefi M, Titz B, Gabay MT et al (2011) RAF inhibitor resistance is mediated by dimerization of aberrantly spliced BRAF(V600E). Nature 480: 387-U144

Pratilas CA, Xing F, Solit DB (2012) Targeting oncogenic BRAF in human cancer. Curr Top Microbiol Immunol 355: 83-98

Pruss D, Bushman FD, Wolffe AP (1994a) Human immunodeficiency virus integrase directs integration to sites of severe DNA distortion within the nucleosome core. Proc Natl Acad Sci U S A 91: 5913-5917

Pruss D, Reeves R, Bushman FD, Wolffe AP (1994b) The influence of DNA and nucleosome structure on integration events directed by HIV integrase. J Biol Chem 269: 25031-25041

Qi Y, Gregory MA, Li Z, Brousal JP, West K, Hann SR (2004) p19ARF directly and differentially controls the functions of c-Myc independently of p53. Nature 431: 712-717

Qiu X, Sun X, He Z, Huang J, Hu F, Chen L, Lin P, You MJ, Medeiros LJ, Yin CC (2013) Immunoglobulin gamma heavy chain gene with somatic hypermutation is frequently expressed in acute myeloid leukemia. Leukemia 27: 92-99

Rahman AH, Aloman C (2013) Dendritic cells and liver fibrosis. Biochimica et Biophysica Acta (BBA) - Molecular Basis of Disease 1832: 998-1004

Rajagopalan S, Long EO (2012) Cellular senescence induced by CD158d reprograms natural killer cells to promote vascular remodeling. Proc Natl Acad Sci U S A 109: 20596-20601

Rangarajan A, Weinberg RA (2003) Opinion: Comparative biology of mouse versus human cells: modelling human cancer in mice. Nat Rev Cancer 3: 952-959

Raskov H, Orhan A, Christensen JP, Gögenur I (2021) Cytotoxic CD8+ T cells in cancer and cancer immunotherapy. British Journal of Cancer 124: 359-367

Reinhard J, Wagner N, Krämer MM, Jarocki M, Joachim SC, Dick HB, Faissner A, Kakkassery V (2020) Expression Changes and Impact of the Extracellular Matrix on Etoposide Resistant Human Retinoblastoma Cell Lines. Int J Mol Sci 21

Rimmelé P, Esposito M, Delestré L, Guervilly J-H, Ridinger-Saison M, Despras E, Moreau-Gachelin F, Rosselli F, Guillouf C (2017) The Spi1/PU.1 transcription factor accelerates replication fork progression by increasing PP1 phosphatase in leukemia. Oncotarget 8

Rocco JW, Sidransky D (2001) p16(MTS-1/CDKN2/INK4a) in cancer progression. Exp Cell Res 264: 42-55

Rodier F, Coppé J-P, Patil CK, Hoeijmakers WAM, Muñoz DP, Raza SR, Freund A, Campeau E, Davalos AR, Campisi J (2009) Persistent DNA damage signalling triggers senescence-associated inflammatory cytokine secretion. Nat Cell Biol 11: 973-979

Rous P (1910) A TRANSMISSIBLE AVIAN NEOPLASM. (SARCOMA OF THE COMMON FOWL.). J Exp Med 12: 696-705

Rovillain E, Mansfield L, Caetano C, Alvarez-Fernandez M, Caballero OL, Medema RH, Hummerich H, Jat PS (2011) Activation of nuclear factor-kappa B signalling promotes cellular senescence. Oncogene 30: 2356-2366

Sagiv A, Biran A, Yon M, Simon J, Lowe SW, Krizhanovsky V (2013) Granule exocytosis mediates immune surveillance of senescent cells. Oncogene 32: 1971-1977

Saitoh T, Fujita N, Hayashi T, Takahara K, Satoh T, Lee H, Matsunaga K, Kageyama S, Omori H, Noda T et al (2009) Atg9a controls dsDNA-driven dynamic translocation of

STING and the innate immune response. Proceedings of the National Academy of Sciences 106: 20842-20846

Sarkar D, Lebedeva IV, Emdad L, Kang DC, Baldwin AS, Jr., Fisher PB (2004) Human polynucleotide phosphorylase (hPNPaseold-35): a potential link between aging and inflammation. Cancer Res 64: 7473-7478

Satoh T, Smith A, Sarde A, Lu HC, Mian S, Trouillet C, Mufti G, Emile JF, Fraternali F, Donadieu J et al (2012) B-RAF mutant alleles associated with Langerhans cell histiocytosis, a granulomatous pediatric disease. Plos One 7: e33891

Scassa ME, Marazita MC, Ceruti JM, Carcagno AL, Sirkin PF, González-Cid M, Pignataro OP, Cánepa ET (2007) Cell cycle inhibitor, p19INK4d, promotes cell survival and decreases chromosomal aberrations after genotoxic insult due to enhanced DNA repair. DNA Repair (Amst) 6: 626-638

Schröder AR, Shinn P, Chen H, Berry C, Ecker JR, Bushman F (2002) HIV-1 integration in the human genome favors active genes and local hotspots. Cell 110: 521-529

Schwarzwaelder K, Howe SJ, Schmidt M, Brugman MH, Deichmann A, Glimm H, Schmidt S, Prinz C, Wissler M, King DJ et al (2007) Gammaretrovirus-mediated correction of SCID-X1 is associated with skewed vector integration site distribution in vivo. J Clin Invest 117: 2241-2249

Sedelnikova OA, Horikawa I, Zimonjic DB, Popescu NC, Bonner WM, Barrett JC (2004) Senescing human cells and ageing mice accumulate DNA lesions with unrepairable double-strand breaks. Nat Cell Biol 6: 168-170

Sen R, Baltimore D (1986) Inducibility of kappa immunoglobulin enhancer-binding protein Nf-kappa B by a posttranslational mechanism. Cell 47: 921-928

Serrano M, Lee H, Chin L, Cordon-Cardo C, Beach D, DePinho RA (1996) Role of the INK4a locus in tumor suppression and cell mortality. Cell 85: 27-37

Serrano M, Lin AW, McCurrach ME, Beach D, Lowe SW (1997) Oncogenic ras provokes premature cell senescence associated with accumulation of p53 and p16INK4a. Cell 88: 593-602

Shah, N.N., Qin, H., Yates, B., Su, L., Shalabi, H., Raffeld, M., Ahlman, M.A., Stetler-Stevenson, M., Yuan, C., Guo, S., et al. (2019). Clonal expansion of CAR T cells harboring lentivector integration in the CBL gene following anti-CD22 CAR T-cell therapy. Blood Adv 3, 2317-2322.

Sharpless NE, Bardeesy N Fau - Lee KH, Lee Kh Fau - Carrasco D, Carrasco D Fau - Castrillon DH, Castrillon Dh Fau - Aguirre AJ, Aguirre Aj Fau - Wu EA, Wu Ea Fau - Horner JW, Horner Jw Fau - DePinho RA, DePinho RA Loss of p16Ink4a with retention of p19Arf predisposes mice to tumorigenesis.

Shaw AC, Panda A, Joshi SR, Qian F, Allore HG, Montgomery RR (2011) Dysregulation of human Toll-like receptor function in aging. Ageing Res Rev 10: 346-353

Shultz LD, Ishikawa F, Greiner DL (2007) Humanized mice in translational biomedical research. Nat Rev Immunol 7: 118-130

Sithanandam G, Kolch W, Duh FM, Rapp UR (1990) Complete coding sequence of a human B-raf cDNA and detection of B-raf protein kinase with isozyme specific antibodies. Oncogene 5: 1775-1780

Sivori S, Carlomagno S, Pesce S, Moretta A, Vitale M, Marcenaro E (2014) TLR/NCR/KIR: Which One to Use and When? Frontiers in Immunology 5

Six E, Gandemer v, Magnani A , Nobles C, Everett J, Male F, Plantier C, Hmitou I, Semeraro M, Magrin E, Caccavelli L, Trinquand A, Asnafi V, Lapierre JM, Tuchmann-Durand C, André-Schmutz I, Hacein-Bey-Abina S, Romana S, Macintyre E, Bushman FD, Fischer A, Cavazzana M (2017) ASGCT Annual Meeting Abstracts. Mol Ther 25: 1-363

Smogorzewska A, de Lange T (2002) Different telomere damage signaling pathways in human and mouse cells. Embo J 21: 4338-4348

Stein S, Ott MG, Schultze-Strasser S, Jauch A, Burwinkel B, Kinner A, Schmidt M, Krämer A, Schwäble J, Glimm H et al (2010) Genomic instability and myelodysplasia with monosomy 7 consequent to EVI1 activation after gene therapy for chronic granulomatous disease. Nat Med 16: 198-204

Storer M, Mas A, Robert-Moreno A, Pecoraro M, Ortells MC, Di Giacomo V, Yosef R, Pilpel N, Krizhanovsky V, Sharpe J et al (2013) Senescence is a developmental mechanism that contributes to embryonic growth and patterning. Cell 155: 1119-1130

Su H, Bidere N, Lenardo M (2004) Another fork in the road: Foxo3a regulates NF-kappaB activation. Immunity 21: 133-134

Sugimoto MA, Vago JP, Teixeira MM, Sousa LP (2016) Annexin A1 and the Resolution of Inflammation: Modulation of Neutrophil Recruitment, Apoptosis, and Clearance. Journal of Immunology Research 2016: 8239258

Sun W, Li Y, Chen L, Chen H, You F, Zhou X, Zhou Y, Zhai Z, Chen D, Jiang Z (2009) ERIS, an endoplasmic reticulum IFN stimulator, activates innate immune signaling through dimerization. Proceedings of the National Academy of Sciences 106: 8653-8658

Sun L, Wu J, Du F, Chen X, Chen ZJ (2013) Cyclic GMP-AMP Synthase Is a Cytosolic DNA Sensor That Activates the Type I Interferon Pathway. Science 339: 786-791

Takimoto CH, Chao MP, Gibbs C, McCamish MA, Liu J, Chen JY, Majeti R, Weissman IL (2019) The Macrophage 'Do not eat me' signal, CD47, is a clinically validated cancer immunotherapy target. Annals of Oncology 30: 486-489

Tanaka Y, Chen ZJ (2012) STING Specifies IRF3 Phosphorylation by TBK1 in the Cytosolic DNA Signaling Pathway. Science Signaling 5: ra20-ra20

Taniguchi H, Jacinto FV, Villanueva A, Fernandez AF, Yamamoto H, Carmona FJ, Puertas S, Marquez VE, Shinomura Y, Imai K et al (2012) Silencing of Kruppel-like factor 2 by the histone methyltransferase EZH2 in human cancer. Oncogene 31: 1988-1994

Tao W, Levine AJ (1999) P19(ARF) stabilizes p53 by blocking nucleo-cytoplasmic shuttling of Mdm2. Proc Natl Acad Sci U S A 96: 6937-6941

Tasdemir N, Banito A, Roe JS, Alonso-Curbelo D, Camiolo M, Tschaharganeh DF, Huang CH, Aksoy O, Bolden JE, Chen CC et al (2016) BRD4 Connects Enhancer Remodeling to Senescence Immune Surveillance. Cancer Discov 6: 612-629

Tavera-Mendoza LE, Wang TT, White JH (2006) p19INK4D and cell death. Cell Cycle 5: 596-598

Teo YV, Rattanavirotkul N, Olova N, Salzano A, Quintanilla A, Tarrats N, Kiourtis C, Müller M, Green AR, Adams PD et al (2019) Notch Signaling Mediates Secondary Senescence. Cell Rep 27: 997-1007.e1005

Thakral B, Courville E (2014) Crystal-storing histiocytosis with IgD κ–associated plasma cell neoplasm. Blood 123: 3540-3540

Tham M, Stark HJ, Jauch A, Harwood C, Lorie EP, Boukamp P (2022) Adverse Effects of Vemurafenib on Skin Integrity: Hyperkeratosis and Skin Cancer Initiation Due to Altered MEK/ERK-Signaling and MMP Activity. Frontiers in Oncology 12

Tiacci E, De Carolis L, Simonetti E, Capponi M, Ambrosetti A, Lucia E, Antolino A, Pulsoni A, Ferrari S, Zinzani PL et al (2021) Vemurafenib plus Rituximab in Refractory or Relapsed Hairy-Cell Leukemia. New Engl J Med 384: 1810-1823

Tiacci E, Park JH, De Carolis L, Chung SS, Broccoli A, Scott S, Zaja F, Devlin S, Pulsoni A, Chung YR et al (2015) Targeting Mutant BRAF in Relapsed or Refractory Hairy-Cell Leukemia. New Engl J Med 373: 1733-1747

Tiacci E, Pettirossi V, Schiavoni G, Falini B (2017) Genomics of Hairy Cell Leukemia. J Clin Oncol 35: 1002-1010

Tiacci E, Trifonov V, Schiavoni G, Holmes A, Kern W, Martelli MP, Pucciarini A, Bigerna B, Pacini R, Wells VA et al (2011) BRAF mutations in hairy-cell leukemia. N Engl J Med 364: 2305-2315

Toso A, Revandkar A, Di Mitri D, Guccini I, Proietti M, Sarti M, Pinton S, Zhang J, Kalathur M, Civenni G et al (2014) Enhancing chemotherapy efficacy in Pten-deficient prostate tumors by activating the senescence-associated antitumor immunity. Cell Rep 9: 75-89

Tschan MP, Peters UR, Cajot JF, Betticher DC, Fey MF, Tobler A (1999) The cyclin-dependent kinase inhibitors p18INK4c and p19INK4d are highly expressed in CD34+ progenitor and acute myeloid leukaemic cells but not in normal differentiated myeloid cells. British Journal of Haematology 106: 644-651

Turkistany SA, DeKoter RP (2011) The transcription factor PU.1 is a critical regulator of cellular communication in the immune system. Arch Immunol Ther Exp (Warsz) 59: 431-440

Vallabhapurapu S, Karin M (2009) Regulation and function of NF-kappaB transcription factors in the immune system. Annu Rev Immunol 27: 693-733

Van Den Steen PE, Wuyts A, Husson SJ, Proost P, Van Damme J, Opdenakker G (2003) Gelatinase B/MMP-9 and neutrophil collagenase/MMP-8 process the chemokines human GCP-2/CXCL6, ENA-78/CXCL5 and mouse GCP-2/LIX and modulate their physiological activities. Eur J Biochem 270: 3739-3749

van Deursen JM (2014) The role of senescent cells in ageing. Nature 509: 439-446

van Tuyn J, Jaber-Hijazi F, MacKenzie D, Cole JJ, Mann E, Pawlikowski JS, Rai TS, Nelson DM, McBryan T, Ivanov A et al (2017) Oncogene-Expressing Senescent Melanocytes Up-Regulate MHC Class II, a Candidate Melanoma Suppressor Function. J Invest Dermatol 137: 2197-2207

von Zglinicki T (2002) Oxidative stress shortens telomeres. Trends Biochem Sci 27: 339-344

Wahl GM, Carr AM (2001) The evolution of diverse biological responses to DNA damage: insights from yeast and p53. Nat Cell Biol 3: E277-E286

Wajapeyee N, Serra RW, Zhu X, Mahalingam M, Green MR (2008) Oncogenic BRAF induces senescence and apoptosis through pathways mediated by the secreted protein IGFBP7. Cell 132: 363-374

Wan PT, Garnett MJ, Roe SM, Lee S, Niculescu-Duvaz D, Good VM, Jones CM, Marshall CJ, Springer CJ, Barford D et al (2004) Mechanism of activation of the RAF-ERK signaling pathway by oncogenic mutations of B-RAF. Cell 116: 855-867

Wang B, Li Q, Qin L, Zhao S, Wang J, Chen X (2011) Transition of tumor-associated macrophages from MHC class IIhi to MHC class IIlow mediates tumor progression in mice. BMC Immunology 12: 43

Wang B, Varela-Eirin M, Brandenburg SM, Hernandez-Segura A, van Vliet T, Jongbloed EM, Wilting SM, Ohtani N, Jager A, Demaria M (2022) Pharmacological CDK4/6 inhibition reveals a p53-dependent senescent state with restricted toxicity. The EMBO Journal 41

Wang S, Moerman EJ, Jones RA, Thweatt R, Goldstein S (1996) Characterization of IGFBP-3, PAI-1 and SPARC mRNA expression in senescent fibroblasts. Mech Ageing Dev 92: 121-132

Weber CK, Slupsky JR, Kalmes HA, Rapp UR (2001) Active Ras induces heterodimerization of cRaf and BRaf. Cancer Res 61: 3595-3598

Weiss RA (1982) Viral mechanisms of carcinogenesis. IARC Sci Publ: 307-316

Wiese-Hansen H, Leh F, Lodvir Hemsing A, Reikvam H (2021) Immunoglobulin-Storing Histiocytosis: A Case Based Systemic Review. J Clin Med 10

Wiggins KA, Parry AJ, Cassidy LD, Humphry M, Webster SJ, Goodall JC, Narita M, Clarke MCH (2019) IL-1α cleavage by inflammatory caspases of the noncanonical inflammasome controls the senescence-associated secretory phenotype. Aging Cell 18: e12946

Williams DA, Bledsoe JR, Duncan CN, et al. Myelodysplastic syndromes after eli-cel gene therapy for cerebral adrenoleukodystrophy (CALD). Presented at: ASGCT 25th Annual Meeting; May 16-19, 2022. Washington DC.

Wright WE, Shay JW (2000) Telomere dynamics in cancer progression and prevention: fundamental differences in human and mouse telomere biology. Nat Med 6: 849-851

Wu J, Lingrel JB (2004) KLF2 inhibits Jurkat T leukemia cell growth via upregulation of cyclin-dependent kinase inhibitor p21WAF1/CIP1. Oncogene 23: 8088-8096

Wu ZH, Miyamoto S (2008) Induction of a pro-apoptotic ATM-NF-kappaB pathway and its repression by ATR in response to replication stress. Embo J 27: 1963-1973

Wu ZH, Shi Y, Tibbetts RS, Miyamoto S (2006) Molecular linkage between the kinase ATM and NF-kappaB signaling in response to genotoxic stimuli. Science 311: 1141-1146

Wu X, Li Y, Crise B, Burgess SM (2003) Transcription start regions in the human genome are favored targets for MLV integration. Science 300: 1749-1751

Wu J, Sun L, Chen X, Du F, Shi H, Chen C, Chen ZJ (2013) Cyclic GMP-AMP Is an Endogenous Second Messenger in Innate Immune Signaling by Cytosolic DNA. Science 339: 826-830

Xue W, Zender L, Miething C, Dickins RA, Hernando E, Krizhanovsky V, Cordon-Cardo C, Lowe SW (2007) Senescence and tumour clearance is triggered by p53 restoration in murine liver carcinomas. Nature 445: 656-660

Yang H, Wang H, Ren J, Chen Q, Chen ZJ (2017) cGAS is essential for cellular senescence. Proc Natl Acad Sci U S A 114: E4612-e4620

Ye J, Huang X, Hsueh EC, Zhang Q, Ma C, Zhang Y, Varvares MA, Hoft DF, Peng G (2012) Human regulatory T cells induce T-lymphocyte senescence. Blood 120: 2021-2031

Yaswen P, Campisi J (2007) Oncogene-induced senescence pathways weave an intricate tapestry. Cell 128: 233-234

Yu RC, Chu C, Buluwela L, Chu AC (1994) Clonal proliferation of Langerhans cells in Langerhans cell histiocytosis. Lancet 343: 767-768

Zaman A, Wu W, Bivona TG (2019) Targeting Oncogenic BRAF: Past, Present, and Future. Cancers (Basel) 11

Zhang X, Shi H, Wu J, Zhang X, Sun L, Chen C, Chen Zhijian J (2013) Cyclic GMP-AMP Containing Mixed Phosphodiester Linkages Is An Endogenous High-Affinity Ligand for STING. Mol Cell 51: 226-235

Zhong B, Yang Y, Li S, Wang Y-Y, Li Y, Diao F, Lei C, He X, Zhang L, Tien P et al (2008) The Adaptor Protein MITA Links Virus-Sensing Receptors to IRF3 Transcription Factor Activation. Immunity 29: 538-550

Zhuang L, Fulton RJ, Rettman P, Sayan AE, Coad J, Al-Shamkhani A, Khakoo SI (2019) Activity of IL-12/15/18 primed natural killer cells against hepatocellular carcinoma. Hepatology International 13: 75-83

Zufferey R, Dull T, Mandel RJ, Bukovsky A, Quiroz D, Naldini L, Trono D (1998) Self-inactivating lentivirus vector for safe and efficient in vivo gene delivery. J Virol 72: 9873-9880

zur Hausen H (1991) Viruses in human cancers. Science 254: 1167-1173

Zychlinski D, Schambach A, Modlich U, Maetzig T, Meyer J, Grassman E, Mishra A, Baum C (2008) Physiological Promoters Reduce the Genotoxic Risk of Integrating Gene Vectors. Mol Ther 16: 718-725

Signature of the student

7. Appendix

	mBrafV600E							
	NSG							
Gene	CD11b+ GFP+		CD11b+ GFP-		B220+ GFP+		B220+ GFP-	
Tap1	-1.13	*1.1E-03*	-2.09	*1.1E-12*	-1.35	*0.001*	-2.30550831	*5.8E-15*
CD47	1.66	*3.6E-05*	1.07	*1.7E-02*	1.07	*ns*	0.057526921	*ns*
Anxa1	4.87	*6.7E-06*	5.17	*1.4E-06*	3.20	*0.091*	4.05765501	*5.5E-04*
Elane	2.68	*5.4E-02*	2.65	*4.4E-02*	3.14	*ns*	4.998420122	*9.2E-06*
Foxo3	2.72	*1.1E-03*	1.70	*6.1E-02*	-0.16	*ns*	-0.47409182	*ns*
Spi1	2.29	*1.6E-02*	2.28	*1.3E-02*	1.26	*ns*	0.823377547	*ns*

	C57							
Gene	CD11b+ GFP+		CD11b+ GFP-		B220+ GFP+		B220+ GFP-	
Tap1	-1.02	*ns*	-1.589947085	*ns*	-2.11	*9.94E-04*	-2.03	*1.49E-03*
CD47	-0.31	*ns*	-1.257228856	*ns*	0.44	*ns*	0.15	*ns*
Anxa1	-0.39	*ns*	-1.84205903	*ns*	-3.08	*8.48E-03*	-2.64	*2.55E-02*
Elane	2.24	*ns*	0.164556564	*ns*	-0.34	*ns*	-4.97	*3.15E-03*
Foxo3	0.85	*ns*	1.942854727	*ns*	1.28	*ns*	-5.59	*1.56E-06*
Spi1	-0.01	*ns*	-1.183839067	*ns*	0.88	*ns*	-0.30	*ns*

	mBraf trunc							
	NSG							
Gene	CD11b+ GFP+		CD11b+ GFP-		B220+ GFP+		B220+ GFP-	
Tap1	0.63	*ns*	-0.80	*ns*	0.11	*ns*	-0.77	*ns*
CD47	0.81	*9.0E-02*	-0.82	*ns*	0.76	*ns*	0.13	*ns*
Anxa1	2.62	*3.3E-02*	0.22	*ns*	3.27	*7.6E-02*	3.36	*1.8E-02*
Elane	0.10	*ns*	-0.38	*ns*	3.45	*5.7E-02*	4.87	*6.6E-05*
Foxo3	0.82	*ns*	-0.68	*ns*	0.86	*ns*	-1.22	*ns*
Spi1	0.99	*ns*	-0.59	*ns*	1.07	*ns*	1.29	*ns*

	C57							
Gene	CD11b+ GFP+		CD11b+ GFP-		B220+ GFP+		B220+ GFP-	
Tap1	-0.15	*ns*	-0.23	*ns*	-0.02	*ns*	0.30	*ns*
CD47	0.05	*ns*	-0.29	*ns*	-0.25	*ns*	-1.62	*3.2E-02*
Anxa1	-0.45	*ns*	-0.92	*ns*	-3.66	*3.5E-02*	-1.73	*ns*
Elane	1.10	*ns*	0.76	*ns*	-5.56	*2.8E-02*	-3.42	*ns*
Foxo3	-0.48	*ns*	0.25	*ns*	0.73	*ns*	0.99	*ns*
Spi1	1.65	*ns*	1.46	*ns*	0.72	*ns*	-0.21	*ns*

Table 7.1. Differentially expressed genes mentioned in the discussion. *Left column for each population represents logFC, while the right column in Italic represents FDR. FDR in blue are the ones between 0.05 and 0.10.*